Robbin Bastiaansen
robbin.bastiaansen@gmail.com

Bending and Buckling in Elastic Patterned Sheets

Bachelorscriptie, 25 juli 2013

Scriptiebegeleiders:
prof.dr. M. van Hecke (LION)
dr. V. Rottschäfer (MI)

Leids Instituut voor Onderzoek in de Natuurkunde (LION)
Mathematisch Instituut (MI)
Universiteit Leiden

Abstract

In this bachelor thesis we study models for the elastic deformations of patterned quasi 2D sheets. The main ingredients for these models are elastic beams and we focus on four different models for elastic beams in this study. We start from the theory of elasticity and derive four beam models for both inextensible and extensible beams, by using the Euler Lagrangian equations. One of these models is the classic Euler-Bernoulli beam model, which is valid for elastic beams that are not compressible and have only small, weakly non-linear deflections. The other models are extensions of this model and are valid for strong non-linear behaviour and/or compressible beams. With these models we analyze the compression and buckling of beams with various boundary conditions such as a pinned-pinned beam and a beam attached to two circular, freely rotary nodes. Finally we also present some simulations for both a single beam between two circular, freely rotary nodes and the elastic patterned sheets.

Contents

1 Introduction **6**

2 Background on strains and elastic energy **12**
2.1 Introduction 13
2.2 Elastic Strain 15
2.3 Elastic Stress 18
2.3.1 Hooke's law 18
2.3.2 Twisting energy 19
2.3.3 Stretching and bending energy 19
2.4 Wrap-up 22

3 Beam Models **24**
3.1 Inextensible small deflection model (Euler Bernoulli model) . . . 25
3.1.1 Introduction to the model 25
3.1.2 Energy in the model 26
3.1.3 Boundary conditions and solutions 30
3.1.4 A pinned-pinned beam 31
3.1.5 Other simple boundary conditions 38
3.1.6 Beam between two, freely rotary nodes 42
3.2 Inextensible model for large deflections 49
3.2.1 Introduction to the model 49
3.2.2 Energy in the model 49
3.2.3 Boundary conditions and solution 50
3.2.4 A pinned-pinned beam 50
3.3 Extensible beam model for small deflections 56
3.3.1 Introduction to the model 56
3.3.2 Energy in the model 57
3.3.3 A pinned-pinned beam 60
3.3.4 Beam between two, freely rotary nodes 64
3.4 Extensible beam model for large deflections 67
3.4.1 Introduction to model 67
3.4.2 Energy in the model 67
3.4.3 A pinned-pinned beam 72

4 Simulations on Elastic Sheets **84**
4.1 Assumption in the simulations 84
4.2 Simulations on a single beam 87
4.2.1 Explanation of numeric simulation 87

4.2.2 Numeric study of a single beam 93
4.3 Simulations on elastic patterned sheets 102
4.3.1 Explanation of numeric simulation 102
4.3.2 Simulations on the elastic patterned sheets 102

5 Conclusion + Outlook **106**

6 Acknowledgments **109**

7 List of Notations **112**

Chapter 1

Introduction

When we try to compress a material, we see that it deforms. There are many ways in which a material can deform. For instance steel breaks when we load it with too much force. Clearly this kind of deformation is irreversible. However there are many reversible ways in which a material can react to being compressed. A spring, for example, returns to its original state when we remove the compressing loads. These reversible deformations are called elastic deformations.

These elastic deformations are mathematically described with so-called elastic moduli. They measure how a specific object deforms elastically when it is compressed. Hence the elastic moduli are material properties. The most well-known is the Bulk modulus (denoted with either a K or a B). This elastic modulus specifies the material's resistance to uniform compression: the higher the Bulk modulus of a material, the less easy we can compress it (see figure 1.1).

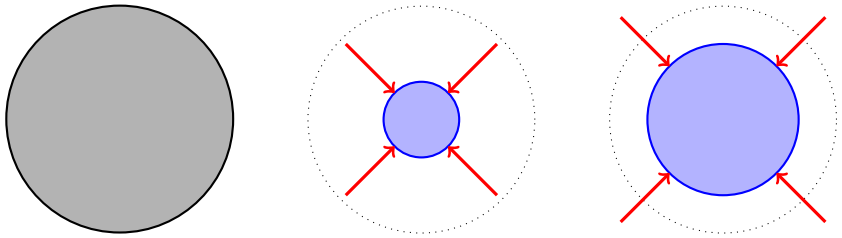

Figure 1.1 – Schematic 2D illustration of the Bulk modulus. In figure (a) the original state of the sphere is shown. In figure (b) a material with a low Bulk modulus is shown, while in figure (c) we see a material with a high Bulk modulus. The original sphere is shown in both figures with dots.

The Bulk modulus measures what happens to an object when an uniform load is applied. Instead of compressing a material in all directions, we could also compress it in only one direction (see figure 1.2). Leonhard Euler (1707-1783) first studied this sort of elastic deformations in 1727. He found that there is - in

good approximation - a linear response between the stresses σ (i.e. the force per unit area) on an elastic solid and the strain ϵ (i.e. the relative compression) of it. Later Thomas Young (1773-1783) described this behaviour again in 1807. He then introduced the Young's modulus E which accounts for this proportionality of the stress and strain in an elastic solid:

$$\sigma = E\epsilon \tag{1.1}$$

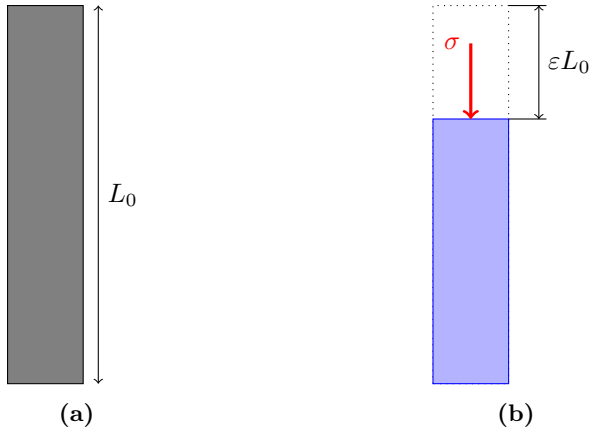

Figure 1.2 – Schematic 2D illustration of compression in only one direction. In figure (a) the original state of an elastic solid (in this case an elastic beam) is shown. In figure (b) this solid is undergoing a certain stress σ. As a result the beam has a strain ε. The dotted lines show the original beam which has a length L_0.

But this does not describe everything that happens when we compress an elastic solid. The previous description thus far only accounts for the deformation of the solid in the direction in which we apply a force on it (so-called axial deformation). However, besides this, there is also a lateral expansion of the elastic material (see figure 1.3a). This phenomenon is called the Poisson effect, after Siméon Poisson (1781-1840). The amount of this effect is expressed with the Poisson's ratio (denoted as ν). It is defined as the ratio between the strain in the transversal direction and the strain in the axial direction. That is,

$$\nu = -\frac{\varepsilon_{\text{transversal}}}{\varepsilon_{\text{axial}}} \tag{1.2}$$

Normal materials that expand when compressed have positive Poisson's ratios up to a ratio of 0.5. There are however materials that have a negative Poisson's ratio, meaning that they are in fact shrinking in all directions when they are being compressed (see figure 1.3b). For instance Rod Lakes published an example of a synthetic material with a negative Poisson's ratio (see Lakes [1987]). These kind of materials with a negative Poisson's ratio are called auxetic.

This Poisson effect is clearly visible when we compress slender elastic rods (also called 'elastic beams'). They however have yet another interesting feature, since they exhibit an instability under a large enough load. When we compress elastic

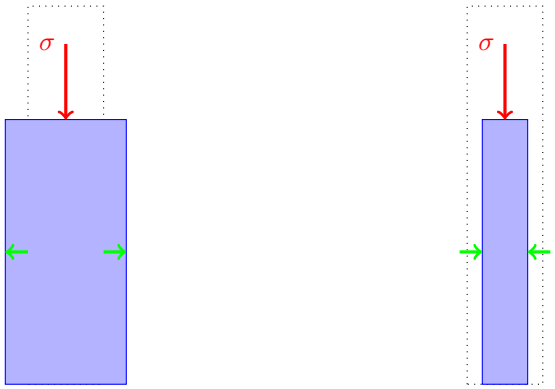

(a) 2D material with a positive Poisson's ratio.

(b) 2D material with a negative Poisson's ratio.

Figure 1.3 – 2D illustration of both a material with a positive (a) and a negative Poisson's ratio (b). Both samples are compressed with a force (red). The dotted black rectangle is the original form of the material, while the blue rectangles are the new form when they are compressed. The green arrows show what happens in the direction perpendicular to the direction in which the material is compressed.

rods with a great enough force, they suddenly buckle. The point at which this buckling starts, is a bifurcation point at which a pitchfork bifurcation occurs (see Bazant and Cendolin [2009]).

Though there is a linear response between the local stress and strain, as we have seen in equation (1.1), there is not a linear relation between the global stress and strain in an elastic rod. The global stress strain relation exhibits some non-linear behaviour (see figure 1.4). This non-linearity is however purely due to the changed geometry of the elastic beams when they are buckled.

Recently a new material has been found that has both a negative Poisson's ratio and a negative slope in the force strain curve (see Mullin et al. [2007] and Bertoldi et al. [2010]). This material is an elastic sheet, in which circular holes are made in a regular way (see figure 1.5). These so-called monoholar

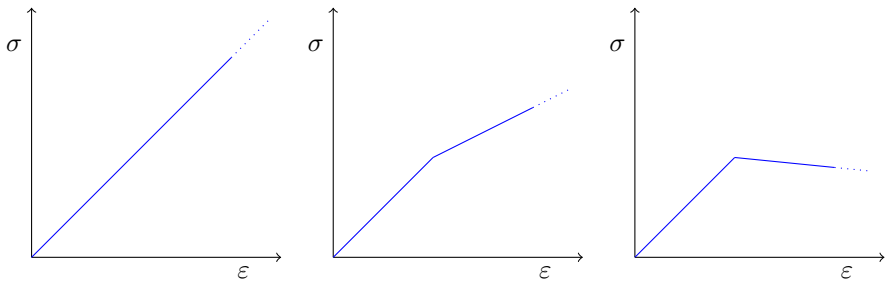

(a) **(b)** **(c)**

Figure 1.4 – Sketches of possible stress strain curves for a normal elastic material (a) and two possible stress strain curves for an elastic beam that buckles (b and c). The kink in these curves indicate the buckling bifurcation point.

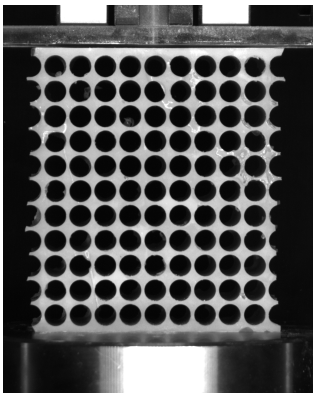

(a) Photo of monoholar elastic patterned sheet when not compressed

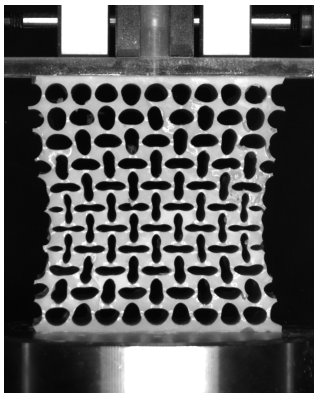

(b) Photo of monoholar elastic patterned sheet when compressed

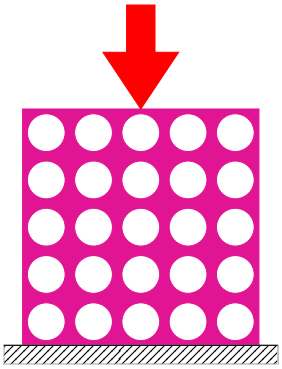

(c) Sketch of a monoholar elastic patterned sheet which is loaded from above

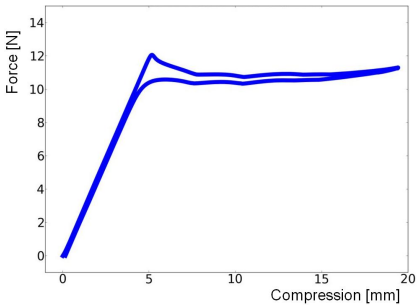

(d) Force extension curve for a monoholar elastic patterned sheet for both compression (upper line) and relaxation (experimental data).

Figure 1.5 – Monoholar elastic sheets in which circular holes are made in a regular way (elastic patterned sheets). Photos of this kind of elastic sheets are shown in (a) and (b). We can clearly see the negative Poisson's ratio in figure (b). In figure (c) the set-up for a loading experiment is sketched. The resulting force extension curve is shown in figure (d). There is a clear negative slope visible in this curve, which normal materials don't have.

elastic patterned networks also exhibit a particular peak in their force extension curves (see figure 1.5d), which for now is not fully comprehended.

The behaviour of these new materials is purely due to the geometry of the holes in the sheet. We see this clearly when we inspect another sort of elastic sheets. Instead of punching out circles of constant radii, this material has holes of two radii (in a regular way). These elastic sheets are called biholar elastic patterned sheets. In contrary to the monoholar sheets, they don't have the particular peak or a negative slope in their force extension curves (see figure 1.6), though they have a negative Poisson's ratio.

We believe it is possible to model both the monoholar and the biholar networks in a numerical simulation. To do this, we first observe that there is a relatively

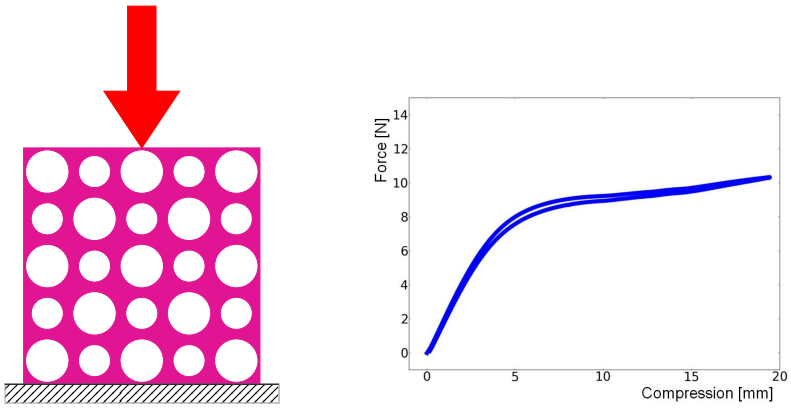

(a) **(b)**

Figure 1.6 – Biholar elastic patterned sheet. In figure (a) the set-up for a loading experiment is sketched. In figure (b) the force extension curve is shown. Clearly the strange behaviour (i.e. the peak) from figure 1.5d is gone

large portion of the elastic sheet between the holes. We can think of these portions as an undeformable, circular 'nodes'. We can then model the elastic material that is left between the nodes as elastic 'beams' (i.e. slender elastic rods). This idea is illustrated in figure 1.7.

To understand this model of the elastic networks, we first need to understand the behaviour of the (single) beams themselves. In general there are three things that a beam can do when it is being deformed. First, the length of the beam may change. This is called stretching. Second, the beam can rotate in a direction perpendicular to its main axis (i.e. the axis in which the beam is the longest). When this happens, we say that the beam is bending. At last, the beam can rotate around its main axis. If that happens, the beam is said to be twisting. These three possibilities are drawn in figure 1.8.

The theory of the elastic beams was first described by Leonhard Euler and Daniel Bernoulli in the 17th century. Since then many additional beam models and theories have been developed. These various models differ in how realistic they describe the elastic rods. For instance most neglect the twisting of the beams completely, since this effect is generally the least important one. Further differences between the models arise because the stretching of the beam is sometimes neglected. The original Euler-Bernoulli beam model is an example that models the beams as inextensible, not-stretchable beams. Finally there are great differences in the detail of the beam's shape between beam theories. Generally, less detail means a model that is easier to work with, but less realistic.

In this bachelor thesis we will heavily investigate various beam models. The starting point for this study is the energy that the beams have, which we will derive in chapter 2 from the theory of elasticity. In chapter 3 we will then acquire four beam models, which are increasingly more realistic. Moreover, we will also study various possible configurations of the beams with these models in that chapter. At last, we will use the model explained above to simulate both a single beam between two nodes and the elastic patterned sheets in chapter 4.

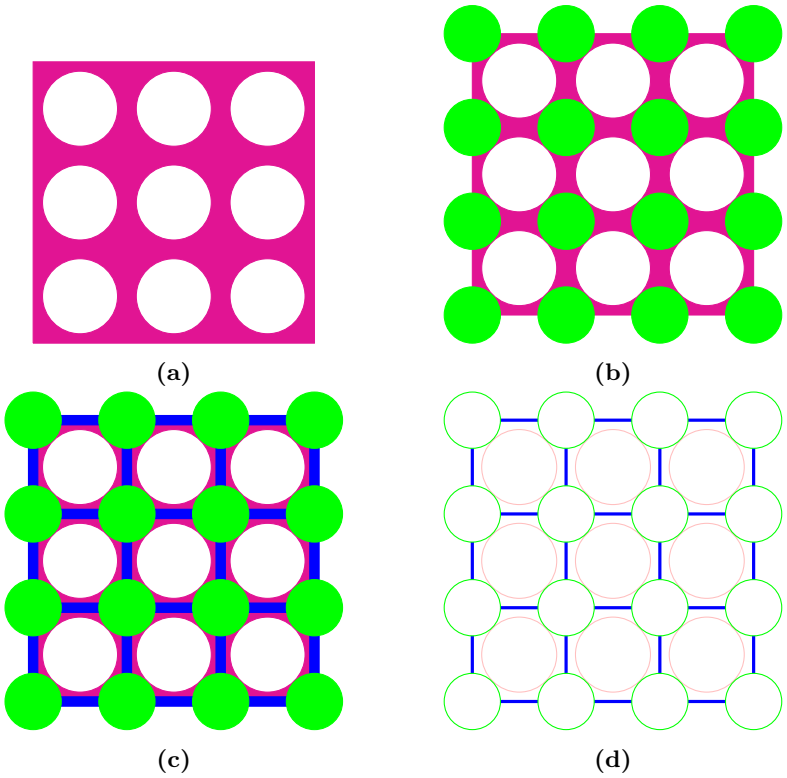

Figure 1.7 – Illustration of the model of a elastic patterned sheet (pink) as combination of nodes (green) and beams (blue). In figure (a) a piece of the elastic patterned sheet is shown. The white circles are the holes in the network. In figure (b) the nodes (green) are drawn. These are placed at the positions between the holes where there are large portions of elastic material. Then in figure (c) the beams (blue) are also shown. These represent the remaining elastic material between the nodes. In figure (d) the resulting model is shown. In this last picture the elastic sheet in pink is erased. The original holes in the elastic patterned sheets are drawn as a reminder of the elastic patterned sheet. In the simulations these circles are not shown anymore.

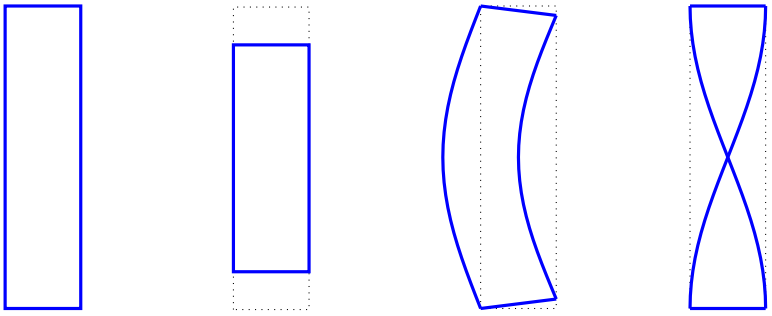

(a) Original elastic beam

(b) Stretching of an elastic beam

(c) Bending of an elastic beam

(d) Twisting of an elastic beam

Figure 1.8 – Illustration of the various modes possible in the beam. In each figure the original position (a) is shown with dotted lines.

Chapter 2

Background on strains and elastic energy

In this chapter we discuss the general behaviour of the elastic beams that we use to model the elastic patterned sheets. Since these elastic beams are far much longer than wide, we can see them as slender solid rods (see figure 2.1). When these rods are being deformed (for instance by the application of external loads as we will do in Chapter 3), initial properties of the elastic beam like the stress and the strain are changed. The theory behind these changing properties is called elasticity (a field in continuum mechanics).

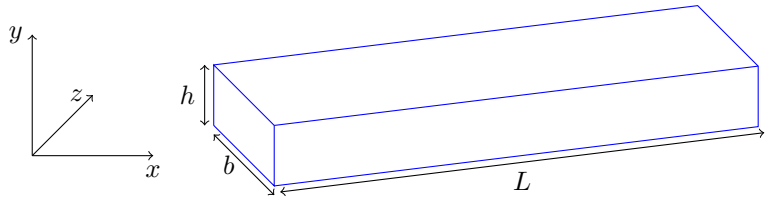

Figure 2.1 – General set up for the three dimensional beam (blue). The elastic beam is much longer than wide (i.e. $L \gg b, h$), so it can be seen as a slender rod.

Central in the theory of elasticity are the stresses and strains inside the beam. These properties measure the internal forces per unit area and the relative changes in shape or size of parts of the beam respectively. For instance when the beam is deformed by the application of a load, the beam is being squeezed (see figure 2.2). Since the beam wants to restore its initial position (i.e. when not deformed), the beam exerts internal forces opposite to the applied load. These internal forces are called the stresses in the beam.

In essence these processes are the same as what's happening when you squeeze a normal spring. The theory of elasticity can be seen as a generalization of the theory on elastic springs to three dimensional objects. It deals with how solid elastic objects, like our elastic beams, deform and become internally stressed due to external loads. A simplification of the general elasticity is the linear elasticity. In this simplification it is assumed that the resulting internal strains

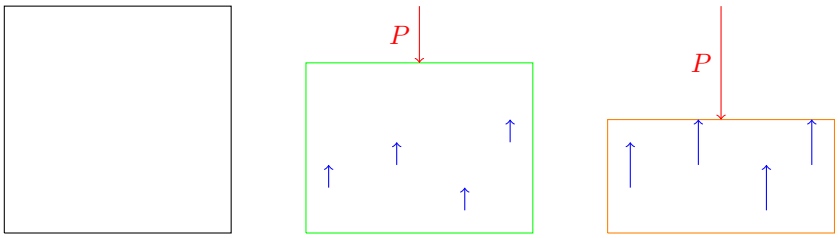

Figure 2.2 – Graphical illustration of the effect of an external force P (red) on the internal stresses (blue) in an elastic solid. The first picture (black) illustrates the original state of the elastic solid. The two other pictures (green and orange) show the effect of an increasing external load P on the elastic solid. When this load P increases, the stresses (blue) inside the elastic solid also increase. The strain in these cases also increases, since the solid is squeezed.

are relatively small and that there is a linear relation between the original displacements of the elastic solid and the resulting strains.

In this chapter we start from the general, three dimensional, linear elasticity theory and apply it to our case of the slender elastic beams. Since we are dealing with slender rods, we reduce this elastic theory to a quasi one dimensional problem. At the end of this chapter we find an expression for the (potential) elastic energy in our elastic beams. This expression will be our starting point to derive the various beam models in Chapter 3.

2.1 Introduction

Let's now inspect the three dimensional elastic rod from figure 2.1. This elastic rod has a cross-sectional area Ω_0 (see figure 2.3). Note that this cross-section can be dependent on the x position. We choose the origin of the coordinates y and z as the centroid of this cross-sectional area Ω_0. This is done to ensure the model is symmetric in the y and z directions, which makes the resulting expressions in section 2.3.3 more simple and helps us reduce the dimensions that we need to take into account. Mathematically formulated this choice ensures that we have per construction

$$\iint_{\Omega_0} z \; dzdy = \iint_{\Omega_0} y \; dzdy = 0 \tag{2.1}$$

Each point (x, y, z) on this elastic rod experiences, under load, a three dimensional displacement which we denote by u_x, u_y and u_z for displacements in respectively the x, y and z directions (see figure 2.4). From these displacements we find the strains and stresses inside the beam in the following sections, which we will use to express the elastic energy of elastic beams.

Both the strain and the stress are second-rank tensors. That means they both

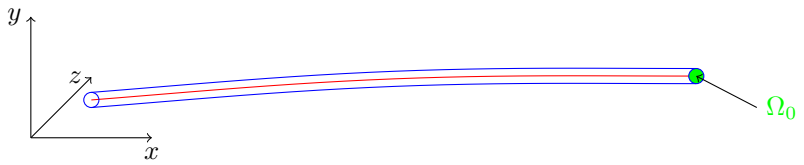

Figure 2.3 – General set up of the three dimensional rod problem. The green part, Ω_0, is the cross-section (at a certain point z) of the elastic rod. The red line is centroid of the cross-section Ω_0 at a position z.

can be expressed as matrices

$$\sigma = \begin{pmatrix} \sigma_{xx} & \sigma_{xy} & \sigma_{xz} \\ \sigma_{yx} & \sigma_{yy} & \sigma_{yz} \\ \sigma_{zx} & \sigma_{zy} & \sigma_{zz} \end{pmatrix}, \ \epsilon = \begin{pmatrix} \epsilon_{xx} & \epsilon_{xy} & \epsilon_{xz} \\ \epsilon_{yx} & \epsilon_{yy} & \epsilon_{yz} \\ \epsilon_{zx} & \epsilon_{zy} & \epsilon_{zz} \end{pmatrix} \tag{2.2}$$

Each element of these matrices corresponds to a different geometrical interpretation. For instance σ_{yy} is the stress in the y-direction that is working on the y-face of the inspected solid and σ_{yx} is the stress in the x-direction that is working on the y-face of the solid (see figure 2.5).

The potential elastic energy can be found with the stress and strains inside the elastic solid (see Barber [2010])

$$E_{el} = \sum_{i,j} \frac{1}{2} \int_{x_s}^{x_e} \iint_{\Omega_0} \sigma_{ij}\epsilon_{ij} \, dz \, dy \, dx \tag{2.3}$$

(in which $i, j \in \{x, y, z\}$ and x_s and x_e denote respectively the beginning and end of the beam on the x-axis.)

In the following sections we find expressions for the strain tensor ϵ and the stress tensor σ so we can find an explicit expression for this elastic energy, which we then will use in chapter 3 to acquire various beam models.

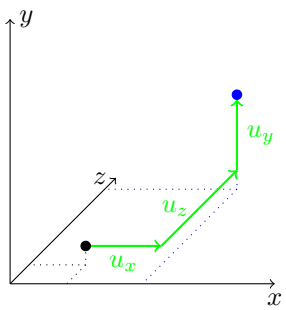

Figure 2.4 – The three kinds of displacements of a infinitesimal piece of the elastic rod. The black dot is the original position of this point and the blue dot is the new position. The arrows (green) denote the displacements u_x, u_y and u_z in the x, y and z-directions.

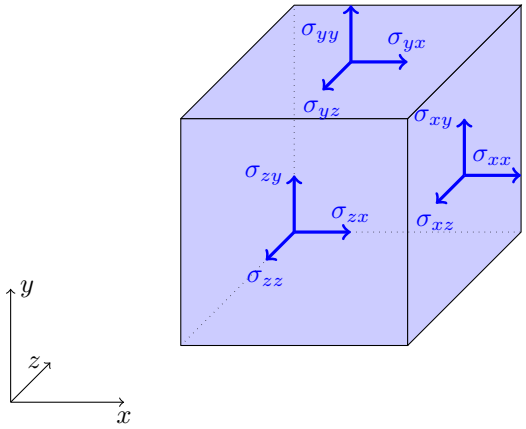

Figure 2.5 – The various components of the second-rank tensor for the stress σ (blue) inside an elastic solid (a cube in this case).

2.2 Elastic Strain

From the displacements u_x, u_y and u_z we can determine the strain tensors in the elastic rod (see Landau and Lifshitz) with

$$\epsilon_{ij} = \frac{1}{2}(u_{i,j} + u_{j,i} + u_{k,i}u_{k,j}) \tag{2.4}$$

(in which $u_{a,b} \equiv \frac{\partial u_a}{\partial b}$ and $i, j \in \{x, y, z\}$)

In linear elasticity the gradient of displacements is assumed to be small and hence the last term disappear. Hence there is a linearized strain tensor whose elements can be calculated with (see Emam [2002] and Landau and Lifshitz):

$$\epsilon_{ij} = \frac{1}{2}(u_{i,j} + u_{j,i}) \tag{2.5}$$

In elasticity it is more common to work with the strain ϵ than it is to work with the original displacements u_x, u_y and u_z. If we work with this strain ϵ however, we must remember the form of the strain in equation (2.5). Saint Venant postulated a *geometric compatibility condition* for the strain ϵ to ensure that the tensor has this desired form of equation (2.5). This constraint is (see Emam [2002]):

$$\epsilon_{ij,kl} + \epsilon_{kl,ij} - \epsilon_{ik,jl} - \epsilon_{jl,ik} = 0 \tag{2.6}$$

In this expression we use the notation $\epsilon_{ij,kl}$ for the second derivative of ϵ_{ij} with respect to k and l. That is,

$$\epsilon_{ij,kl} \equiv \frac{\partial^2 \epsilon_{ij}}{\partial k \partial l} \tag{2.7}$$

(for $i, j, k, l \in \{x, y, z\}$.)

This geometric compatibility must hold for all $i, j, k, l \in \{x, y, z\}$. If we write out all of the geometric compatibility conditions we end up with 81 conditions.

Luckily most of these are either trivial or duplicates (since the strain tensor is symmetric as seen in equation (2.5)). We hence end up with the following six geometric compatibility conditions:

$$\epsilon_{xx,yy} + \epsilon_{yy,xx} - 2\epsilon_{xy,xy} = 0 \tag{2.8}$$
$$\epsilon_{yy,zz} + \epsilon_{zz,yy} - 2\epsilon_{yz,yz} = 0 \tag{2.9}$$
$$\epsilon_{xx,zz} + \epsilon_{zz,xx} - 2\epsilon_{xz,xz} = 0 \tag{2.10}$$
$$\epsilon_{zz,xy} + \epsilon_{xy,zz} - \epsilon_{xz,yz} - \epsilon_{yz,xz} = 0 \tag{2.11}$$
$$\epsilon_{xx,yz} + \epsilon_{yz,xx} - \epsilon_{xy,xz} - \epsilon_{xz,xy} = 0 \tag{2.12}$$
$$\epsilon_{yy,xz} + \epsilon_{xz,yy} - \epsilon_{xy,yz} - \epsilon_{yz,xy} = 0 \tag{2.13}$$

Since we are studying slender elastic rods (i.e. $L \gg h, d$), we may assume that the strain does not change much for small variations of x for the microscopic solutions that we are studying in this chapter. This means that constants in this chapter do depend slowly on the variable x. Hence when we are inspecting the macroscopic behaviour of the beams in subsequent chapters, we will see that these 'constants' are in fact depending on x. Hence the assumption we make for the microscopic strain in this chapter is

$$\epsilon_{ij,x} = 0 \tag{2.14}$$

for $i, j \in \{x, y, z\}$. In this $\epsilon_{ij,x} \equiv \frac{\partial \epsilon_{ij}}{\partial x}$.

With his assumption the geometric compatibility conditions (equations (2.8)-(2.13)) reduce to the following set of constraints:

$$\epsilon_{zz,yy} + \epsilon_{yy,zz} - 2\epsilon_{zy,zy} = 0 \tag{2.15}$$
$$\epsilon_{xx,yy} = 0 \tag{2.16}$$
$$\epsilon_{xx,zz} = 0 \tag{2.17}$$
$$\epsilon_{xx,zy} = 0 \tag{2.18}$$
$$\epsilon_{yx,zz} - \epsilon_{zx,zy} = 0 \tag{2.19}$$
$$\epsilon_{xz,yy} - \epsilon_{yx,zy} = 0 \tag{2.20}$$

These six conditions form the starting point of our search for the microscopic strain elements ϵ_{ij} ($i, j \in \{x, y, z\}$). In the rest of this section we use them and try to find the strains.

Acquiring ϵ_{xx}

Thus, it follows from (2.16), (2.17) and (2.18) that the second derivatives of ϵ_{xx} with respect y and z are always zero. Moreover, from equation (2.14) it follows that ϵ_{xx} is not linear in x. This means the ϵ_{xx} is of the form

$$\epsilon_{xx} = \varepsilon + \kappa_z y + \kappa_y z \tag{2.21}$$

Here ε, κ_z and κ_y are constants, which correspond to either the stretching mode (ε) or the bending mode (κ_z and κ_y) of the beam (see figure 1.8).

Acquiring ϵ_{xy} and ϵ_{xz}

Then we try to find the strains ϵ_{yx} and ϵ_{zx}. For this end, we now use the geometric compatibility conditions (2.19) and (2.20). If we add these two expression we get

$$0 = \epsilon_{yx,zz} - \epsilon_{yx,zy} - (\epsilon_{zx,yz} - \epsilon_{zx,yy}) = \left(\frac{\partial}{\partial z} - \frac{\partial}{\partial y}\right)(\epsilon_{yx,z} - \epsilon_{zx,y}) \tag{2.22}$$

If we subtract the same conditions (2.19) and (2.20) we get:

$$0 = \epsilon_{yx,zz} + \epsilon_{yx,zy} - (\epsilon_{zx,yz} + \epsilon_{zx,yy}) = \left(\frac{\partial}{\partial z} + \frac{\partial}{\partial y}\right)(\epsilon_{yx,z} - \epsilon_{zx,y}) \tag{2.23}$$

These two expressions imply that

$$\frac{\partial}{\partial x}(\epsilon_{yx,z} - \epsilon_{zx,y}) = \frac{\partial}{\partial y}(\epsilon_{yx,z} - \epsilon_{zx,y}) \tag{2.24}$$

and

$$\frac{\partial}{\partial x}(\epsilon_{yx,z} - \epsilon_{zx,y}) = -\frac{\partial}{\partial y}(\epsilon_{yx,z} - \epsilon_{zx,y}) \tag{2.25}$$

From this and equation (2.14) we obtain that $\epsilon_{yx,z} - \epsilon_{zx,y}$ must be constant. Hence this implies

$$\epsilon_{yx,z} - \epsilon_{zx,y} = \kappa_x \tag{2.26}$$

Here we have κ_x as a constant which corresponds to the twisting mode of the beam (see figure 1.8).

We now have an expression for $\epsilon_{yx,z} - \epsilon_{zx,y}$. To separate these two strain elements we need to apply some trick. To do this we rewrite equation (2.26) to

$$\frac{\partial}{\partial z}\left(\frac{2}{\kappa_x}\epsilon_{yx} - z\right) = \frac{\partial}{\partial y}\left(\frac{2}{\kappa_x}\epsilon_{zx} + y\right) \tag{2.27}$$

By using Schwarz's theorem about the equality of mixed partial derivatives (see Feldman), we know that the form of this equation suggests that there exists some potential function Φ such that

$$\frac{\partial}{\partial z}\Phi = \frac{2}{\kappa_x}\epsilon_{zx} + y \tag{2.28}$$

and

$$\frac{\partial}{\partial y}\Phi = \frac{2}{\kappa_x}\epsilon_{yx} - z \tag{2.29}$$

If we rewrite these two equations we end up with

$$\epsilon_{zx} = \frac{\kappa_x}{2}(\Phi_z - y) \tag{2.30}$$

$$\epsilon_{yx} = \frac{\kappa_x}{2}(\Phi_y + z) \tag{2.31}$$

(in this notation $\Phi_i \equiv \frac{\partial}{\partial i}\Phi$ for $i \in \{z, y\}$.)

The remaining strain elements

For now, we will not try to find the remaining four strain elements. Later on in section 2.3.3 we will use the last geometric compatibility condition (equation (2.15)) to acquire these.

2.3 Elastic Stress

In the previous section we have found five strain elements. However, to actually calculate the elastic energy via equation (2.3) these strain elements are not enough. We also need the corresponding stress elements. In this section we will try to find these. The main ingredient in this search is Hooke's law, which we will first inspect. Moreover, we also find the remaining strain elements. Finally we find the various energy contributions at the end of this section.

2.3.1 Hooke's law

Since we are working with linear elasticity, we can use Hooke's law (see Landau et al. [1995]). This law gives us the following relation between the stress tensor σ and the strain tensor ϵ:

$$\sigma = \lambda I \mathrm{Tr}(\epsilon) + 2\mu\epsilon \tag{2.32}$$

Here λ is the first Lamé parameter and $\mu = G$ is the shear modulus. Moreover, I is the (three dimensional) identity matrix and Tr denotes the trace of the matrix (i.e. the sum of the elements on the main diagonal of the matrix).

We can invert Hooke's law. To do this, we observe that

$$\mathrm{Tr}(\sigma) = \mathrm{Tr}(\lambda \mathrm{Tr}(\epsilon)\ I + 2\mu\epsilon) = (3\lambda + 2\mu)\mathrm{Tr}(\epsilon) \tag{2.33}$$

If we substitute this into the original Hooke's law we obtain

$$\sigma = \frac{\lambda}{3\lambda + 2\mu} I \mathrm{Tr}(\sigma) + 2\mu\epsilon \tag{2.34}$$

If we change the elastic moduli from λ and $\mu = G$ (the Lamé parameter and the shear modulus) to $E = \frac{(3\lambda+2\mu)\mu}{\lambda+\mu}$ and $\nu = \frac{\lambda}{2(\lambda+\mu)}$ (respectively the Young's modulus and the Poisson's ratio), we find the inverse of Hooke's law,

$$\epsilon = \frac{1}{E}((1+\nu)\sigma - \nu I \mathrm{Tr}(\sigma)) \tag{2.35}$$

In this relation we have used the elastic moduli E, the Young's modulus, and ν, the Poisson's ratio.

2.3.2 Twisting energy

From equation (2.32) (Hooke's law) and the equations for the strain associated with the twisting mode (equations (2.30) and (2.31)) we obtain the stresses σ_{xz} and σ_{yz}:

$$\sigma_{xz} = \mu\kappa_x(\Phi_z - y) \tag{2.36}$$

$$\sigma_{yz} = \mu\kappa_x(\Phi_y + z) \tag{2.37}$$

Now that we have found both the stresses σ_{xz} and σ_{yz} and the strains ϵ_{xz} and ϵ_{yz}, we obtain the elastic energy that is coming from the twisting of the beam. This elastic energy follows by substituting these strains and stresses in the equation for the elastic energy (equation (2.3)). The summation in this expression is however replaced with a new summation over only the stresses and strains that are associated with the twisting of the beam. That is,

$$E_{twisting} = \frac{1}{2}\int_{x_s}^{x_e}\iint_{\Omega_0}(\sigma_{xz}\epsilon_{xz} + \sigma_{zx}\epsilon_{zx} + \sigma_{yz}\epsilon_{yz} + \sigma_{zy}\epsilon_{zy})\ dz\ dy\ dx \tag{2.38}$$

Since we have both ϵ_{zx} and ϵ_{xz} and they are the same as we have seen in equation (2.5) (and the same for ϵ_{yx} and the stresses), the factor $\frac{1}{2}$ in front of the integral for the elastic energy disappears. Hence we get for the twisting energy:

$$E_{twisting} = \frac{1}{2}\int_{x_s}^{x_a}\iint_{\Omega_0}\mu\kappa_z^2\Big((\Phi_{,z} - y)^2 + (\Phi_{,z} + x)^2\Big)\ dz\ dy\ dx \tag{2.39}$$

A part of this integral can be identified as the torsion constant J. This constant only depends on the geometry of the cross-sectional area Ω_0 and is defined as:

$$J \equiv \iint_{\Omega_0}\Big((\Phi_{,z} - y)^2 + (\Phi_{,y} + z)^2\Big)\ dz\ dy \tag{2.40}$$

Hence we can rewrite the twisting energy in a shorter way as

$$E_{twisting} = \frac{1}{2}\int_{x_s}^{x_e}\mu\kappa_x^2 J\ dx = \frac{1}{2}\mu\int_{x_s}^{x_e} J\kappa_x^2 dx \tag{2.41}$$

Thus at this point we have found the contribution to the elastic (potential) energy that is due to bending. As can be seen, this contribution is depending on a geometrical property of the materials cross-section (i.e. J), a material property (μ) and a geometric property, which is related to the twisting of a beam (i.e. κ_x).

2.3.3 Stretching and bending energy

In section 2.2 we have found five of the nine strain elements. To find the four remaining strains, we use the inverse of Hooke's law (equation (2.35)) to express

these in terms of the stresses in the following way:

$$\epsilon_{zz} = \frac{1}{E}(\sigma_{zz} - \nu\sigma_{yy} - \nu\sigma_{xx}) \tag{2.42}$$

$$\epsilon_{yy} = \frac{1}{E}(-\nu\sigma_{zz} + \sigma_{yy} - \nu\sigma_{xx}) \tag{2.43}$$

$$\epsilon_{xx} = \frac{1}{E}(-\nu\sigma_{zz} - \nu\sigma_{yy} + \sigma_{xx}) \tag{2.44}$$

$$\epsilon_{zy} = \frac{1+\nu}{E}\sigma_{zy} \tag{2.45}$$

Since we have already found an expression for the strain ϵ_{xx} (see equation (2.21)), we would like to use this to obtain the other strains. To do this, we can substitute equation (2.44) in equations (2.42) and (2.43) to eliminate σ_{xx}. Thus we acquire

$$\epsilon_{zz} = \frac{1}{E}\big(\sigma_{zz}\big(1-\nu^2\big) + \sigma_{yy}\big(-\nu-\nu^2\big)\big) - \nu\epsilon_{xx} \tag{2.46}$$

$$\epsilon_{yy} = \frac{1}{E}\big(\sigma_{zz}\big(-\nu-\nu^2\big) + \sigma_{yy}\big(1-\nu^2\big)\big) - \nu\epsilon_{xx} \tag{2.47}$$

$$\epsilon_{zy} = \frac{1+\nu}{E}\sigma_{zy} \tag{2.48}$$

At this point we return to the remaining compatibility condition, equation (2.15). By substituting the above equations into this condition and noting that ϵ_{xx} has only constant and linear terms (i.e. the second derivatives are zero), we get a condition for the stresses:

$$\begin{aligned} 0 = (\sigma_{zz,yy} + \sigma_{yy,zz} - 2\sigma_{zy,zy}) - \nu(\sigma_{yy,yy} + \sigma_{zz,zz} + 2\sigma_{zy,zy}) \\ - \nu^2(\sigma_{zz,yy} + \sigma_{yy,zz} + \sigma_{zz,zz} + \sigma_{yy,yy}) \end{aligned} \tag{2.49}$$

Since this must be zero in general, for all possible values for ν, the three terms in the parentheses are zero. If we manipulate these constraints, we find the following condition for the stresses:

$$\sigma_{zz,yy} + \sigma_{yy,zz} = -\sigma_{zz,zz} - \sigma_{yy,yy} = 2\sigma_{xy,xy} \tag{2.50}$$

This can only be true if σ_{zz}, σ_{yy} and σ_{zy} have no non-linear terms, but only terms that are constant of linearly depending on y or z.

Now we need to additionally assume that the external forces are only applied at infinity (i.e. the length of the beam is assumed to be very large compared to the width of the beam). This ensures that we have an equilibrium state inside at each point in the beam. Thus we need to have no net force at each point in the beam. That means that the divergence of the stresses in the interior must be zero (see Emam [2002]). That is,

$$\sigma_{iz,z} + \sigma_{iy,y} + \sigma_{ix,x} = 0 \tag{2.51}$$

(for $i \in \{x, y, z\}$.)

Moreover, from this assumption of an internal equilibrium state we also know that there is no force at the lateral boundaries of the elastic rod. Thus the assumption yields us another set of constraints

$$(\sigma_{ij} N_j)_{\partial\Omega_0} = 0 \tag{2.52}$$

(with $i, j \in \{z, y\}$ and N_j the vector that is normal to the boundary.)

By applying these boundary conditions to our stresses σ_{zz}, σ_{zy} and σ_{yy}, we find that they need to be identically zero. Hence

$$\sigma_{zz} = 0 \tag{2.53}$$
$$\sigma_{yy} = 0 \tag{2.54}$$
$$\sigma_{zy} = 0 \tag{2.55}$$

So, now that we have the stresses σ_{zz}, σ_{yy} and σ_{zy} it is straightforward to also find the strains. From equations (2.42)-(2.44) we obtain:

$$\epsilon_{zz} = -\nu\epsilon_{xx} \tag{2.56}$$
$$\epsilon_{yy} = -\nu\epsilon_{xx} \tag{2.57}$$
$$\epsilon_{zy} = 0 \tag{2.58}$$

We still need to find the last unknown stress element, σ_{xx}. To do this, we start with the inverted Hooke's law (equation (2.35)). Since $\sigma_{xx} = \sigma_{yy} = 0$ we find

$$E\epsilon_{xx} = \sigma_{xx} \tag{2.59}$$

Now we use the expression for the elastic energy (equation (2.3)) again to find the remainder of the potential elastic energy, which is due to the bending and the stretching of the beam (see figure 1.8). As we did before in section 2.3.2 we now change the summation again, this time to sum over the stresses σ_{xx}, σ_{xy}, σ_{yx}, σ_{yy} and σ_{zz}. From the equations for the strain ϵ_{xx} (equation (2.21)), the equations for the other strains (equations (3.174), (3.175) and (2.58)) and the fact that $\sigma_{zz} = \sigma_{yy} = \sigma_{zy} = 0$ the combination of the stretching and bending energy in the beam follows

$$E_{bending} + E_{stretching} = \frac{1}{2} \int \iint_{\Omega_0} \epsilon_{xx}\sigma_{xx} \; dx \; dy \; dz \tag{2.60}$$
$$= \int \frac{E}{2} \iint_{\Omega_0} (\varepsilon + \kappa_z y - \kappa_y x)^2 \; dx \; dy \; dz \tag{2.61}$$

And by expanding this, we get:

$$E_{bending} + E_{stretching} = \int_{x_s}^{x_e} \frac{E}{2} \left(\iint_{\Omega_0} \varepsilon^2 \; dz \; dy + \right.$$
$$\left. \iint_{\Omega_0} \left(\kappa_z^2 y^2 + \kappa_y z^2 - 2\kappa_z\kappa_y zy\right) \; dz \; dy + \iint_{\Omega_0} (2\varepsilon\kappa_z y - 2\varepsilon\kappa_y z) \; dz \; dy \right) \; dx \tag{2.62}$$

Since we have chosen the origin of the axis in a smart way such that it is the centroid of the axis (see section 2.1 and equation (2.1)), we now have that $\iint_{\Omega_0} z\ dz\ dy = \iint_{\Omega_0} y\ dz\ dy = 0$. Moreover we observe that $\iint_{\Omega_0} dz\ dy = A$, the area of the cross-section. Furthermore we have $\iint_{\Omega_0} z^2\ dx\ dy \equiv I_{yy}$, $\iint_{\Omega_0} y^2\ dz\ dy \equiv I_{yy}$ and $\iint_{\Omega_0} xy\ dz\ dy \equiv -I_{zy}$. These are the second (geometric) moments of inertia of the cross-section. All of the other variables don't depend on z or y, so we can rewrite the energy again to find the expression:

$$E_{bending}+E_{stretching} = \int_{x_s}^{x_e} \frac{1}{2}EA\varepsilon^2\ dx+\int_{x_s}^{x_e} \frac{1}{2}E\big(I_{zz}\kappa_z^2 + I_{yy}\kappa_y^2 + 2I_{zy}\kappa_z\kappa_y\big)\ dx \tag{2.63}$$

We now have two separated integrals. One of them depends only on ε, so we can identify this part as the stretching energy of the beam. The other integral is a function of the bending constants κ_x and κ_y. This one can be seen as the bending energy of the beam. So we define:

$$E_{stretching} = \frac{1}{2}E\int_{x_s}^{x_e} A\varepsilon^2 dz \tag{2.64}$$

$$E_{bending} = \frac{1}{2}E\int_{x_s}^{x_e} \big(I_{zz}\kappa_z^2 + I_{yy}\kappa_y^2 + 2I_{zy}\kappa_z\kappa_y\big)dx \tag{2.65}$$

As with the twisting energy, in both of these energy contributions we find a constant that depends on the geometry of the beam's cross-sectional area (i.e. A and I), a material property (i.e. E) and a variable that depends on the geometry of the whole beam (i.e. κ_z, κ_y and ε).

2.4 Wrap-up

In this chapter we have derived the potential elastic energy for an elastic rod. To do this, we needed to assume the following things:

- The rod obeys linear elasticity (i.e. we can use Hooke's law and we can ignore the gradient of displacements in the strain expression, equation (2.4)).
- The strain does not change much for small variations of x (i.e. $\frac{\partial}{\partial x}\epsilon_{ij} = 0$ for all $i, j \in \{x, y, z\}$).
- External forces are applied only at infinity (i.e. the length of the beam is much larger than its other dimensions are).

The (potential) elastic energy that we have calculated in this chapter can be expressed as a sum of the stretching energy, the bending energy and the twisting energy of a beam. The total elastic energy can be expressed as

$$\begin{aligned} E_{el} &= E_{stretching} + E_{bending} + E_{twisting} \\ &= \int_{x_s}^{x_e} \frac{1}{2}EA\varepsilon^2\ dx + \int_{x_s}^{x_e} \frac{1}{2}E\big(I_{zz}\kappa_z^2 + I_{yy}\kappa_y^2 + 2I_{zy}\kappa_z\kappa_y\big)dx + \int_{x_s}^{x_e} \frac{1}{2}\mu J\kappa_x^2\ dx \end{aligned} \tag{2.66}$$

Note that if we have a beam that only bends in one direction, perpendicular to the x-axis, and we choose our coordinates in such a way that one of our axis coincides with this direction, we can get rid of some of the term in the bending energy. In that case the energy looks like

$$E_{el} = \int_{x_s}^{x_e} \frac{1}{2} EA\varepsilon^2 \, dx + \int_{x_s}^{x_e} \frac{1}{2} EI_{\alpha\alpha}\kappa_\alpha^2 \, dx + \int_{x_s}^{x_e} \frac{1}{2} \mu J \kappa_x^2 \, dx \tag{2.67}$$

In this α is the direction in which the beam is bending.

The variables ε (associated with the stretching mode in the beam), κ_α (associated with the bending mode) and κ_x (associated with the twisting mode) are properties of the deformation of the beam. In this chapter we have assumed they were constants, since we were interested in the microscopic solutions in the beam. In the next chapters we will however inspect the macroscopic behaviour of the elastic beams. This means (as stated in section 2.2) that the 'constants' can in fact be depending on x.

Chapter 3

Beam Models

In Chapter 2 we have found the elastic energy in equation (2.66). In this chapter we will inspect some of the various beam models that exists. Throughout this chapter we will assume that the elastic beams only bend in one direction (i.e. the y-direction). We hence have the following (potential) elastic energy:

$$E_{el} = \int \left(\frac{1}{2} EA\varepsilon^2 + \frac{1}{2} EI_{yy} k_y^2 + \frac{1}{2} \mu J \kappa_x^2 \right) dx \tag{3.1}$$

We will use this expression in this chapter to find equations for the equilibria configurations of the beam by means of Euler-Lagrangian optimalization. To do this, however, we must assume various things on ε (i.e. stretching of the beam), κ_y (bending of the beam) and κ_z (twisting of the beam). Depending on these assumptions we will derive the different beam models in this chapter.

The most important distinction between the various beam models that we will inspect in this chapter is whether or not the model takes the extensibility of the beam into account. If a model ignores this extensibility, the beams are said to be inextensible. This means that in this model the beam always has the same arc length as it initially had. If a model however accounts for the extensibility the beams are called extensible. In this case the beam can be compressed when a load is applied to it (see figure 3.1).

In this chapter we will derive and study the following beam models:

- The Euler Bernoulli beam model for inextensible beams when the deflections of the beam stay small (see section 3.1).
- A variant of the previous model, for inextensible beams which allows for large deflections (see section 3.2).
- An extensible beam model when the deflections of the beam stay small (see section 3.3).
- A model for extensible beams which allows for large deflections (see section 3.4).

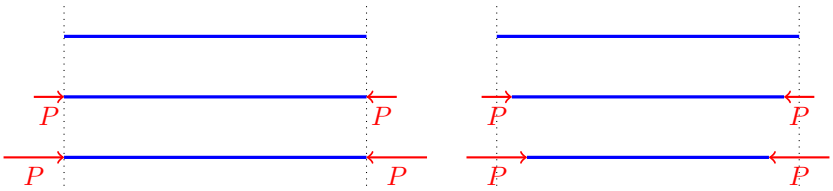

(a) Example of an inextensible beam **(b)** Example of an extensible beam

Figure 3.1 – Examples of both an inextensible (a) and an extensible (b) beam (blue) with various loads P applied to it (before buckling). The uppermost picture is the initial configuration of the beam, the other two are the configurations when an increasing load P is applied to the beams. The inextensible beam remains to have the same length as it had initially, while the extensible beam is compressed for the same loads P.

3.1 Inextensible small deflection model (Euler Bernoulli model)

In this section we will study a beam model that models the beams as inextensible. Moreover, in this model we assume that the beams deflections stay small. We start this chapter with an introduction about the model. Then we derive the governing differential equation starting from the elastic energy in section 3.1.2. After we have acquired this equation, we use the model to study various beam configurations. In this study we focus on both the force-strain relationship and the actual configuration of the beam (i.e. the deflections of the beam).

3.1.1 Introduction to the model

We inspect a beam as in figure 3.2 that is loaded from both sides with a force P. From experiments it is known that at a certain load P, the beam will buckle and will be in a bended position. We denote this deflection of (the centroid) of the beam in the y-direction at time t of a point x on the beam with $w(x,t)$ as shown in the figure. At this point we need to be careful and very precisely about what we mean by 'a point x on the beam': what we mean is *not* the position x the point we are observing had on the initial, straight, beam. Instead we mean the x-coordinate of the current position of a point on the beam.

To stress this even more we will define the initial length of the beam as L_0. This is the length the beam has when there is no force P acting on it. When there is a force working on it, the beam may span a shorter length in the x-direction. We will denote this length by L. In the bended configuration there is also a real length of the beam, which is the length of the beam measured over the beam itself (i.e. the arc length). We will denote this length as ℓ. By assuming the beam is inextensible (the assumption of the Euler Bernoulli beam model), what we will do in this section, we will essentially assume that this length is the same as the initial length (i.e. $\ell = L_0$).

Throughout this section we will assume that the deflections $w(x,t)$ of the beam

are relatively small. More precisely we will assume that the slope is small (i.e. $\frac{\partial}{\partial x}w(x,t)$ is small). This approximation seems not good when we compare this to experimental results, since the slope $\frac{\partial}{\partial x}w(x,t)$ is generally not small when the beam is buckled. In contrary, when the beam is bended the slope is too large to justify this approximation.

The results in this sections however are still insightful. These can serve as a first order approximation for the deflections $w(x,t)$ and the general behaviour of the elastic beam. Especially the results on the critical Euler loads (i.e. the load P at which the beam will buckle) are in good agreement with experiments (see for instance Bazant and Cendolin [2009]).

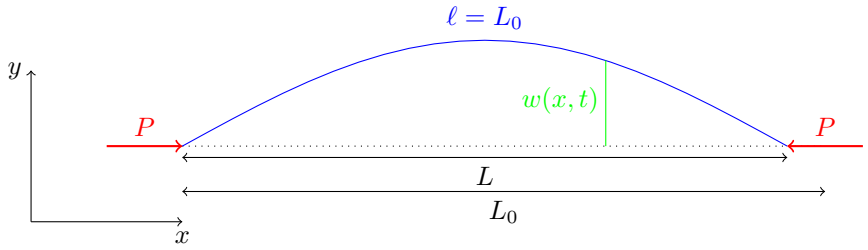

Figure 3.2 – General set-up for the beam. The load P is applied in the x-direction, while the deflection, $w(x)$ is in the y-direction. The blue line represent the beam (bended in this case). L_0 is the initial length of the beam, L is the current span in the x-direction of the beam and ℓ is the real length of the beam.

3.1.2 Energy in the model

In this set up of the beam, we have different kinds of energy that we need to take into account. Foremost we of course have the elastic energy, equation (3.1). But besides that, we also have the work that is done by the load P that we apply on the beam, $W = P\Delta L$. In this $\Delta L \equiv L_0 - L$, which is called the strain. Moreover, if we are interested into the kinematics of the beam and not only the equilibrium of the beam, we also have the kinetic energy of the beam that is important. To summarize we have the following energies in our system:

- Elastic Energy E_{el} (see equation (3.1));
- Kinetic Energy $E_{kin} = \int \frac{1}{2}\mu w_t^2 dx$. In this μ is the mass density in the cross-section of the beam and $w_t \equiv \frac{\partial}{\partial t}w(x,t)$;
- The work of the applied load $W = P\Delta L$, with $\Delta L = L_0 - L$.

In the remainder of this subsection we inspect these energy contributions. More specifically, we find expressions for the various used quantities, like κ_y and ΔL. When we have acquired these, we will use the Lagrangian and the Euler Lagrangian variation theorem to acquire the differential equation for this beam model.

Let's start with inspecting the elastic energy in the Euler Bernoulli beam model. This model assumes that beams aren't stretching or turning at all and hence assumes that $\varepsilon = 0$ and $\kappa_x = 0$. By using these assumption on equation (3.1),

the energy of a beam, we get the expression for the elastic energy in the Euler Bernoulli beam model:

$$E_{el,EB} = \int \frac{1}{2} EI_{yy} k_y^2 dx \tag{3.2}$$

The previously mentioned energies in this Euler Bernoulli rod can be combined. We can make the Lagrangian for this model, which as it turns out will be:

$$\mathcal{L} = \int \left(\frac{1}{2} \mu w_t^2 - \frac{1}{2} EI_{yy} \kappa_y^2 \right) dx + P\Delta L \tag{3.3}$$

We would like to use the Euler Lagrangian optimization to find kinematic expressions for the behavior of the (deflection of the) beam. To do this we however must first start with finding out what those constants κ_y and ΔL are. This is what we will do in the next subsections.

The curvature κ_y associated with the bending of the beam

The term κ_y is something that we first have used in equation (2.21). We introduced it as being associated with the bending of the beam in the y direction. To be more precise, we find that κ_y can be identified as the local curvature of the beam at a position x (see Audoly). This curvature is defined as the rate of change of the direction of the tangent line θ (at a point x) with respect to the arc length change s (at the same point x). See figure 3.3 for a graphical illustration. The mathematical formulation of this is

$$\kappa_y = \frac{d\theta}{ds} \tag{3.4}$$

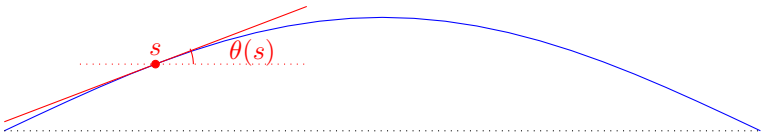

Figure 3.3 – Definiton of θ and a point s on the beams arc. $\theta(s)$ is the angle between the tangent line to the beam at a position s and a line parallel to the x-axis.

This formulation, however, is not useful in this form for us. We need to find another way to describe it (we will do this following Bourne). We know that $\frac{d\theta}{ds} = \frac{d\theta}{dx}\frac{dx}{ds}$, so we can also calculate these to find the curvature. Per definition of θ we know that $\tan(\theta) = \frac{dw}{dx}$. This means that $\theta = \arctan(\frac{dw}{dx})$. If we use this, we find the derivative with respect to x as

$$\frac{d\theta}{dx} = \frac{\frac{d^2w}{dx^2}}{1 + \left(\frac{dw}{dx}\right)^2} = \frac{w_{xx}}{1 + (w_x)^2} \tag{3.5}$$

In this the notation the subscript x means a derivation with respect to the variable x (i.e. $w_x \equiv \frac{\partial}{\partial x} w(x,t)$ and $w_{xx} \equiv \frac{\partial^2}{\partial x^2} w(x,t)$).

Moreover, since we know that $ds = \sqrt{(dx)^2 + (dw)^2}$ (Pythagoreans theorem on a infinitesimal piece of the beam), we know that $\frac{ds}{dx} = \sqrt{1 + (w_x)^2}$. This thus implies

$$\frac{dx}{ds} = \frac{1}{\sqrt{1 + (w_x)^2}} \tag{3.6}$$

If we now combine both of these equations (equation (3.5) and (3.6)), we acquire the expression for the curvature that we wanted to get.

$$\kappa_y = \frac{w_{xx}}{\left(1 + (w_x)^2\right)^{3/2}} \tag{3.7}$$

Since we are inspecting only the cases when the slope of the deflection stays small (i.e. $w_x(x,t)$ is small) as stated in section 3.1.1, we can use a Taylor expansion to find an approximate expression for the curvature κ_y:

$$\kappa_y = \frac{w_{xx}}{\left(1 + (w_x)^2\right)^{3/2}} \approx w_{xx}\left(1 - \frac{3}{2}(w_x)^2 + \frac{15}{8}(w_x)^4 + \dots\right) \approx w_{xx} + \mathcal{O}(w_x^2) \tag{3.8}$$

The strain ΔL in an inextensible beam

Per definition of the strain, we know that $\Delta L = L_0 - L$. Moreover, in this section we have assumed that the beam is inextensible. As a consequence of this, the length of the beam stays the same. This means that at a given configuration, $\ell = L_0$, as we have stated in the introduction in section 3.1.1. If we use this information, we know that $\Delta L = \ell - L$. That is the same as the difference between the real length of a (curved) beam and the distance between both end points of it. Both can be calculated via an integral, and it is even possible to write ds as $\sqrt{1 + w_x^2}\, dx$ as we have seen previously. By assuming again that $w_x(x)$ is small, we can use another Taylor expansion to find a good approximation for the strain ΔL:

$$\Delta L = \int (ds - dx) = \int \left(\sqrt{1 + (w_x)^2} - 1\right) dx \approx \frac{1}{2} \int (w_x)^2 dx \tag{3.9}$$

Derivation of the beam model using Euler Lagrange variation method

In the previous subsections we found expressions for both the strain ΔL (equation (3.9)) and the curvature κ_y (equation (3.8)). If we use these equations

and substitute them into equation (3.10), the Lagrangian for this model, we get another way to express this Lagrangian:

$$\int \left(\frac{1}{2}\mu w_t^2 - \frac{1}{2}EI_{yy}w_{xx}^2 + \frac{1}{2}P(w_x)^2 \right) dx \tag{3.10}$$

We can now finally use the Euler Lagrange variation method (see Sochi [2013]) to find this model's kinematics. To do this we will define Π as the integrand of the Langrangian. That is,

$$\Pi = \frac{1}{2}\mu w_t^2 - \frac{1}{2}EI_{yy}(w_{xx})^2 + \frac{1}{2}P(w_x)^2 \tag{3.11}$$

The Euler Langrange variation method tells us that for optimal energy the following equation must be satisfied. This equation will be the kinematics of the model, that we were looking for.

$$0 = \frac{\partial \Pi}{\partial w} - \frac{\partial}{\partial t}\frac{\partial \Pi}{\partial w_t} - \frac{\partial}{\partial x}\frac{\partial \Pi}{\partial w_x} + \frac{\partial^2}{\partial t^2}\frac{\partial \Pi}{\partial w_{tt}} + \frac{\partial^2}{\partial x^2}\frac{\partial \Pi}{\partial w_{xx}} + \frac{\partial^2}{\partial x \partial t}\frac{\partial \Pi}{\partial w_{xt}} \tag{3.12}$$

Since we have a particular Π, we can substitute this into this condition. From this point we will simply write $I = I_{yy}$ for notational simplicity. This yields the kinematics :

$$(EIw_{xx})_{xx} + (Pw_x)_x + \mu w_{tt} = 0 \tag{3.13}$$

According to Emam [2002] we could have added a damping term to the Lagrangian. By doing so this energy optimization yields the dynamic buckling equation (which can be found op page 144 of Bazant and Cendolin [2009]):

$$(EIw_{xx})_{xx} + (Pw_x)_x + \mu w_{tt} + cw_t = 0 \tag{3.14}$$

(here c is the damping coefficient.)

Most of the times we are not interested in the kinematics however, but only in the equilibrium deflections; beams generally quickly get to their equilibrium positions, especially in the set-ups we will be looking at. This means we generally can forget about the time derivatives, since these will be zero in equilibriums. If we do this we get the following equation:

$$(EIw_{xx})_{xx} + (Pw_x)_x = 0 \tag{3.15}$$

This doesn't look that nice, since the derivatives need to be taken over the whole EIw_{xx} and Pw_x. But luckily, most of the times the Young's modulus E, the second moment of inertia I and the load P do not depend on x. That is, most beams are homogeneous and their attributes are the same everywhere inside the beam. Hence it is pretty safe to assume that E, I and P don't depend on the position x. Hence we obtain what is known as the Euler Bernoulli beam model:

$$EIw_{xxxx} + Pw_{xx} = 0 \tag{3.16}$$

This is the equation for a beam that was initially straight. If we, however, inspect a beam that has some (place dependent) initial deflections $z_0(x)$, this equation is not useful and a modification is needed (see figure 3.4) When we go back to the energies, we see that the kinetic and potential energies of the beam remain unchanged. The work done by the applied load P is however different, since the length is different. By the same logic as before we now have:

$$\Delta L = \int \left(\sqrt{1 + (w_x + (z_0)_x)^2} - 1 \right) dx \approx \frac{1}{2} \int (w_x + (z_0)_x)^2 dx \tag{3.17}$$

If we apply the same Euler Lagrange variation principle to the new Lagrangian, we acquire the differential equation for the equilibrium of an inextensible beam with initial curvature $z_0(x)$:

$$EIw_{xxxx} + P(w_{xx} + (z_0)_{xx}) = 0 \tag{3.18}$$

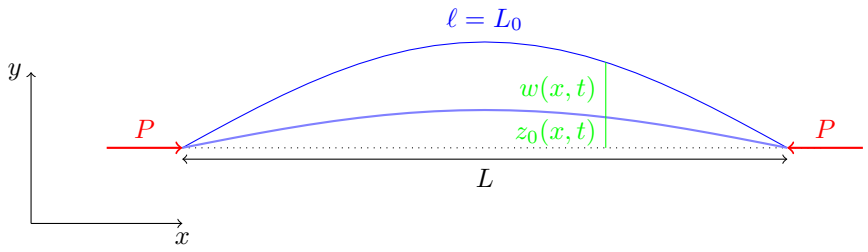

Figure 3.4 – General set-up for a beam with initial curvature $z_0(x)$. The load P is applied in the x-direction, while the deflection, $w(x)$, i sin the y-direction. The blue line represents the beam, the light blue line is the original position of the beam.

3.1.3 Boundary conditions and solutions

In the previous section we have found the differential equation for an inextensible beam model (for small deflections w). In this section we find the general solution to this equation. Furthermore we briefly summarize some of the possible boundary for elastic beams. For notational simplicity we define the constant $k^2 = \frac{P}{EI}$. By doing so, we get the following differential equation for the inextensible beam:

$$w_{xxxx} + k^2 w_{xx} + k^2 (z_0)_{xx} = 0 \tag{3.19}$$

It is quite easy for us to solve this equation and we find that the general solution as:

$$w(x) = A\sin(kx) + B\cos(kx) + Cx + D + \phi(x) \tag{3.20}$$

In this expression the term $\phi(x)$ is a particular solution to the non-homogeneous differential equation. This term is dependent on $z_0(x)$ and will only be in our solution if there is an initial bending in the beam we are studying. Besides this

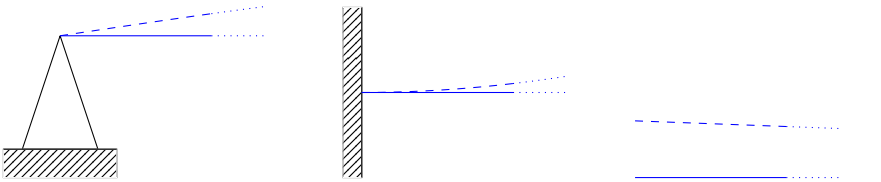

(a) A pinned boundary. At the pinned boundary the beam can freely rotate and hence the torque of the beam on the boundary is zero.

(b) A fixed boundary. At a fixed boundary the beam's slope is fixed.

(c) A free boundary. Neither the deflection nor the slope of the deflection is fixed, but the torque and the shear forces are zero.

Figure 3.5 – Graphical illustration of various boundary conditions possible for beam attachments. In each picture two possible configurations of an beam attached to this boundary condition are shown in blue.

particular solution, there are four constants. The values of these constant are depending on the boundary conditions of the beam. We need four of them to find all the constants.

In most buckling problems there are two boundary conditions at the left end of the beam and two at the right end of the beam. What these boundary conditions are, is implied by how the beam is attached to its surroundings. In table 3.1 and figure 3.5 some of the most frequent boundary conditions are summarized. When referring to a specific configuration of an elastic beam it is convenient to address them by the two boundary conditions the configuration has. So a beam that has one free boundary and one fixed boundary is referred to as a free-fixed beam (or a fixed-free beam).

Table 3.1 – Summary of the most frequently occuring boundary conditions at the end x of a beam. If a beam is pinned at one end it is free to rotate and hence the torque of the beam must be zero (i.e. $w''(x) = 0$). If a beam is fixed at an end point, its starting angle is fixed. When a beam is free at an end point, this means it is free to rotate and its shear forces must be zero. In the table M is the torque and Q is the shear force that is being acted on the beam at the point x.

Name	w	$w_x\ (=\theta)$	$w_{xx}\ (=\frac{M}{EI})$	$w_{xxx}(=\frac{Q}{EI})$	w_{xxxx}
pinned	$w(x)=0$		$w_{xx}(x)=0$		
fixed	$w(x)=0$	$w_x(x)=0$			
free			$w_{xx}(x)=0$	$w_{xxx}(x)=0$	

3.1.4 A pinned-pinned beam

Let's turn our attention to a specific configuration of a beam. We will be inspecting a pinned-pinned beam with no initial curvature (see figure 3.6). The beam is of length L (its initial length is L_0) and we apply a load P at both end points (as we did in figure 3.2). Because both end points are pinned, this means that the beam is free to rotate at both its end point and hence that the torques at these points are zero. Since the beam has no initial curvature, we will

lose the particular solution $\phi(x)$ in our general solution in equation (3.20). By looking up the boundary conditions in this case we get the following conditions:

$$w(0) = 0 \tag{3.21}$$
$$w_{xx}(0) = 0 \tag{3.22}$$
$$w(L) = 0 \tag{3.23}$$
$$w_{xx}(L) = 0 \tag{3.24}$$

In this section we will start with the general solution in equation (3.20) and apply the boundary conditions of the pinned-pinned beam. Hence we acquire knowledge about the behaviour of a pinned-pinned beam. In this section we will focus on both the force strain relationship for this configuration as on the actual deflection w of the beam.

We start by substutiting the boundary conditions in the general solution we had. We hence acquire the following constraints for this configuration:

$$B + D = 0 \tag{3.25}$$
$$B = 0 \tag{3.26}$$
$$A\sin(kL) + B\cos(kL) + CL + D = 0 \tag{3.27}$$
$$-k^2 A\sin(kL) - k^2 B\cos(kL) = 0 \tag{3.28}$$

From the first two of these we can already conclude that $-D = B = 0$. Hence this implies by use of (3.28) that $A\sin(kL) = 0$ If we substitute this into the other remaining constraint, equation (3.27), we get $C = 0$.

So at this point we have found the solution for this particular case (which is plotted in figure 3.7):

$$w(x) = A\sin(kx) \tag{3.29}$$

There is the additional constraint that either $A = 0$ or $\sin(kL) = 0$. If we have that $A = 0$ then the deflection is $w = 0$ and we must conclude that there is no bending of the beam at all. So this corresponds to the non-buckled phase of the beam.

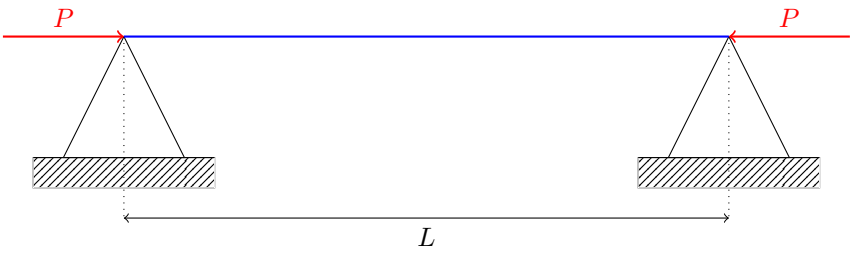

Figure 3.6 – The configuration of a pinned-pinned beam in its non-buckled state. Both end points of the beam are pinned. Thus the torque (EIw_{xx}) and the deflection w are zero at these points. A non-buckled straight state of the beam is shown in blue. The distance between both ends of the beams is L.

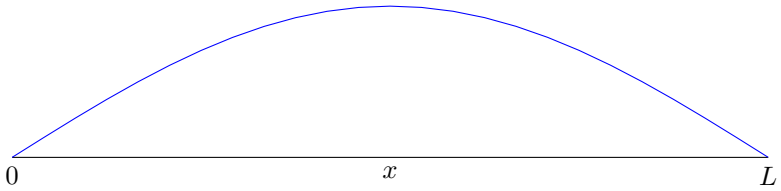

Figure 3.7 – The solution for the pinned-pinned beam configuration is plotted (i.e. $w(x) = A\sin(kx)$). We have used equation (3.29) with $A = 2$, $k = \pi$ and $L = 1$.

If, however, $A \neq 0$ but rather $\sin(kL) = 0$, then we have a non-zero deflection w. This situation corresponds to the buckled phase of the beam. The constraint $\sin(kL) = 0$ can be formulated in another way, since this constraint is equivalent to requiring that $kL = n\pi$ (with $n \in \mathbb{Z}$). If we now use the definition of k, we can also write this constraint as a constraint in terms of P. Doing so we get the following constraint:

$$P = EI\left(\frac{n\pi}{L}\right)^2 \tag{3.30}$$

Thus the above derivations imply that non-zero deflections are possible whenever this constraint (equation (3.30)) is satisfied. If we hence inspect a beam which end points are kept a fixed distance L apart and apply different kind of loads P there are only a few loads when the beam can have a non-zero deflection w. This is graphically illustrated in figure 3.8.

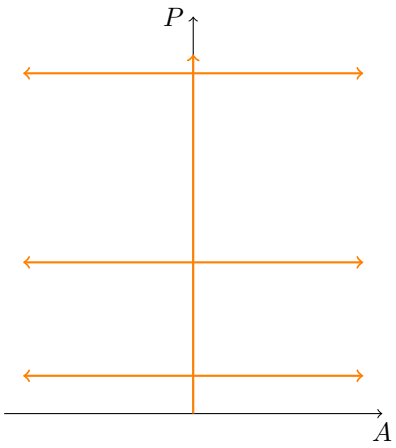

Figure 3.8 – Graphical illustration of the possible values of the constant A in equation (3.29) as function of a varying load P (when L is kept fixed). It is shown that from above considerations A could take on any value at some of the values for P, but for most values of the load P the constant A should be zero.

This is however not what is observed in experiments. Hence we conclude that there needs to be another constraint that we haven't used up to now. This additional constraint will tell us what the amplitude A of the beam is at a certain,

specified moment. However we first inspect the constraint in equation (3.30) and find a relation between the force and the strain in the pinned-pinned configuration.

Force strain relation

In equation (3.30) we got a requirement for the load P to make a non-zero deflection possible. In most experimental cases it is more convenient to find a relationship between the force P and the (relative) strain $\frac{\Delta L}{L_0}$. Since $\Delta L = L_0 - L$ this essentially is quite easy since we can substitute $L = L_0 - \Delta L$ into equation (3.30). If we do this we get the force strain relationship we wanted:

$$P = EI\left(\frac{n\pi}{L_0}\right)^2 \left(\frac{1}{1-\frac{\Delta L}{L_0}}\right)^2 \tag{3.31}$$

In buckling experiments however generally the only value for n that is relevant is when $n = 1$ (since higher values won't be achieved and negative values would physically not agree with pressing on the beam). So for the strain curve of a typical beam we can set $n = 1$. Moreover, the constant term $EI\left(\frac{\pi}{L_0}\right)^2$ is defined as the so-called 'Euler load' and is denoted by $P_e = EI\left(\frac{\pi}{L_0}\right)^2$. We can apply this to the force strain relationship to find:

$$P = P_e \left(\frac{1}{1-\frac{\Delta L}{L_0}}\right)^2 \tag{3.32}$$

If we are interested in the force strain relationship just after the beam has buckled, we could suffice by looking at only small deflections ΔL. We could use a Taylor expansion to find this force strain curve (just) after buckling:

$$P = P_c\left(1 + 2\frac{\Delta L}{L_0}\right) + \mathcal{O}\left(\left(\frac{\Delta L}{L_0}\right)^2\right) \tag{3.33}$$

So based on this argument we would expect a slope of 2 just after the buckling of a beam[1]. This kind of force strain relation is displayed in figure 3.9.

The amplitude A of the deflection w

In the previous we have found a requirement for the load P to allow non-zero deflections $w(x)$ and found a force strain relationship. However, if the requirement for the load P is met, one of the boundary conditions (namely (3.28)) becomes degenerate and there is no way to find the amplitude A of the

[1] In experiments we don't see this slope of 2. The experimental slopes generally are less than 0.5. Moreover they depend on the geometry of the beams, a thing that we only will start to take into account from section 3.3 onwards.

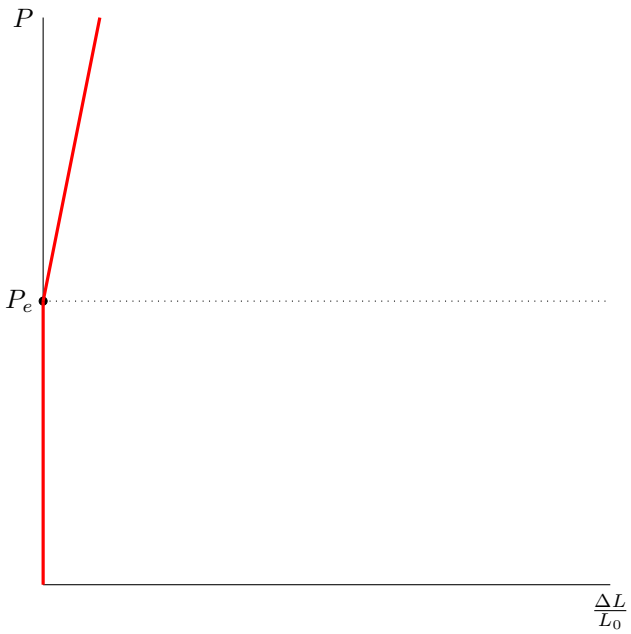

Figure 3.9 – The force strain relationship for an (inextensible) Euler Bernoulli beam before buckling and (just) after buckling. The slope of the after buckling part is 2 times the Euler Load P_e.

sine deflection $w(x)$. Thus we need to imply another condition to the beam to actually find the deflection $w(x)$.

Luckily there is a natural one. Since we are dealing with inextensible cases we have already assumed that the length of the beam must stay the same for all time. That is, we assume that $\ell = L_0$. The value ℓ can be calculated with an integral as we have seen before (in the derivation of equation (3.9)). So the additional condition for the beam is

$$L_0 = \int_0^L \sqrt{1 + (w_x)^2}\, dx \tag{3.34}$$

We now use the expression for the deflection $w(x)$ that we have found in the case that the beam is buckled ($w(x) = A\sin(kx)$). We substitute this equation into equation (3.34). If we then manipulate the expression a bit by using some trigonometric identities we express this condition in a different way:

$$L_0 = \int_0^L \sqrt{1 + (Ak)^2 \cos^2(kx)}\, dx \tag{3.35}$$

$$= \int_0^L \sqrt{(1 + (Ak)^2) - (Ak)^2 \sin^2(kx)}\, dx \tag{3.36}$$

$$= \sqrt{1 + k^2A^2} \int_0^L \sqrt{1 - \frac{A^2k^2}{1 + A^2k^2} \sin^2(kx)}\, dx \tag{3.37}$$

If we now substitute $q = kx$, we get as our last condition on the amplitude A:

$$L_0 = \frac{\sqrt{1 + A^2k^2}}{k} \int_0^{kL} \sqrt{1 - \frac{A^2k^2}{1 + A^2k^2} \sin^2(q)}\ dq \tag{3.38}$$

The integral that we thus have created is the incomplete elliptic integral of the second kind. By definition this integral is:

$$E(z|\lambda) = \int_0^z \sqrt{1 - \lambda \sin^2(x)}\ dx \tag{3.39}$$

So by using this definition on our condition for the amplitude A we can express it shortly as:

$$L_0 = \frac{\sqrt{1 + A^2k^2}}{k} E\left(kL \left| \frac{A^2k^2}{1 + k^2A^2} \right.\right) \tag{3.40}$$

This equation we got is the general condition for the amplitude A in terms of the initial length L_0. We can derive some limit behavior of this condition if we exploit some of the properties of the (in)complete elliptic integral of the second kind (see Wolfram).

When $A = 0$

Let's first assume that our amplitude $A = 0$ to make sure that this condition is in agreement with what we already know about the non-buckled state of our beam. If $A = 0$ the elliptic integral reduces to $E(kL|0)$. This is one of the special cases when this integral can be explicitly found and it turns out that $E(kL|0) = kL$. If we substitute this into equation (3.40) and fill in the rest of the amplitudes, we get the requirement

$$L_0 = L \tag{3.41}$$

So this means that the beam must be as large as it initial was, when the beam is perfectly straight. This makes perfectly sense in this model, since we have assumed that the beam is inextensible. So this condition is indeed in agreement with all the previous things we derived.

When $A \neq 0$

When the amplitude is not zero, we know that $kL = n\pi$ (since the boundary condition in equation (3.28) must be satisfied). We now can use another exciting property of the elliptic integral: $E(\lambda\pi|m) = 2\lambda E(m)$ for all integers λ. In this we have $E(m) \equiv \int_0^{\pi/2} \sqrt{1 - m \sin^2(x)}\ dx$, the *complete* elliptic integral of the second kind. There is also a property of this complete elliptic integral that we

can exploit: $E(1-\frac{1}{z}) = \frac{E(1-z)}{\sqrt{z}}$ for all z. So with this knowledge we can rewrite the condition in equation (3.40) to acquire

$$L_0 = \frac{\sqrt{1+A^2k^2}}{k} 2nE\left(1 - \frac{1}{1+A^2k^2}\right) \tag{3.42}$$

$$= \frac{2n}{k} E\big(-A^2k^2\big) \tag{3.43}$$

This is the condition that we additionally need to impose on the amplitude A to find the deflection of the pinned-pinned beam we were inspecting. We now will study the limit behaviour of this expression.

When $A \to 0$

When the amplitude becomes very small (i.e. $A \to 0$) we can use the Taylor expansion of the elliptic integral around zero. This approximation is $E(x) = \frac{\pi}{2}(1-\frac{x}{4}) + \mathcal{O}(x^2)$ when $|x| \ll 1$. If we use this approximation on equation (3.43) we get an approximation for small amplitudes:

$$L_0 \approx \frac{n\pi}{k}(1 + \frac{1}{4}A^2k^2) + \mathcal{O}(A^4) \tag{3.44}$$

Since we are inspecting the case of non-zero deflections, we know that the amplitude can't be zero and hence that $kL = n\pi$ as stated before. We can substitute this into the equation to get rid of some terms and regain our length L:

$$L_0 \approx L(1 + \frac{1}{4}A^2k^2) + \mathcal{O}(A^4) \tag{3.45}$$

We now have the condition on the amplitude A. By rewriting this condition we get an expression for the amplitude A for the sine deflection $w(x) = A\sin(kx)$ of the pinned-pinned beam:

$$A = \pm\frac{2}{k}\sqrt{\frac{L_0}{L} - 1} \tag{3.46}$$

This expression makes sense. From it we find $A = 0$ when $\frac{L_0}{L} = 1$. That is, the beam is not buckled, when the beam has remained its initial length. Since the beam is modeled inextensible, this is precisely what we would have expected.

If we use the information about the applied load (i.e. $kL = n\pi$) and rewrite everything again in terms of the strain we end up with the condition for A as function of the strain ΔL (we once more assume that $n = 1$ since this is the physical relevant value for n):

$$A = \pm\frac{2}{\pi}\sqrt{\Delta L(L_0 - \Delta L)} \tag{3.47}$$

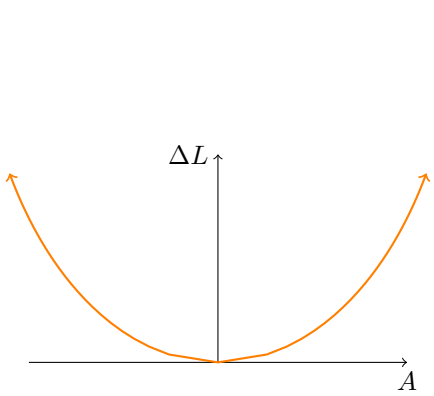

(a) Amplitude A for various strains ΔL. This is a plot of the function $A = \pm\frac{2}{\pi}\sqrt{\Delta L(L_0 - \Delta L)}$.

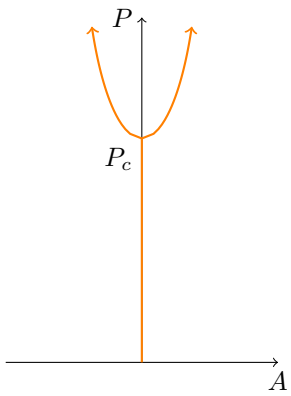

(b) Amplitude A for various loads P. This is a plot of the function $A = \pm\frac{L_0^3}{\pi^3}\sqrt{(P - \frac{\pi^2}{L_0^2})(3\frac{\pi^2}{L_0^2} - P)}$, which is obtained by combining equations (3.47) and (3.32).

Figure 3.10 – This figure shows the various possible amplitudes A for different strains (a) or loads (b). The values used for these plots are $L_0 = 2$ and $EI = 1$. The figure now shows that at a given P there is a certain amplitude A, which figure 3.8 did not show.

When $A \to \infty$

If we now assume that the amplitude becomes very large, we can use another Taylor expansion for the elliptic integral. In this case we have $E(z) \to \sqrt{-z}$ (if $|z| \to \infty$). Thus by this approximation we acquire the condition on the amplitude as

$$L_0 = 2n|A| \tag{3.48}$$

In this relation we once again use the fact that $kL = n\pi$.

$$|A| = \frac{\pi}{2k}\frac{L_0}{L} \tag{3.49}$$

This result on the amplitude A makes sense, since the amplitude A can only be great when the beam length L is small. So this is also in agreement with the expectations we had.

3.1.5 Other simple boundary conditions

In the previous section we have inspected a pinned-pinned beam. In section 3.1.3 however we have found that there are plenty more boundary conditions possible. Since a pinned-pinned beam has the most simple boundary conditions for the problem, we have started by inspecting that configuration. In this section we will start inspecting some other relatively simple boundary conditions, such as a pinned-fixed beam and a fixed-fixed beam.

A pinned-fixed beam

As we did in the pinned-pinned case, we inspect in this section a beam which has no initial curvature. This time however the boundary conditions at one end of the beam change, since one of the end points of the beam is now fixed (instead of pinned). The beam is fixed at the end point $x = L$ and hence we get a pinned-fixed beam (see figure 3.11). We could also fix the other boundary point, but this doesn't matter for the physics of this configuration.

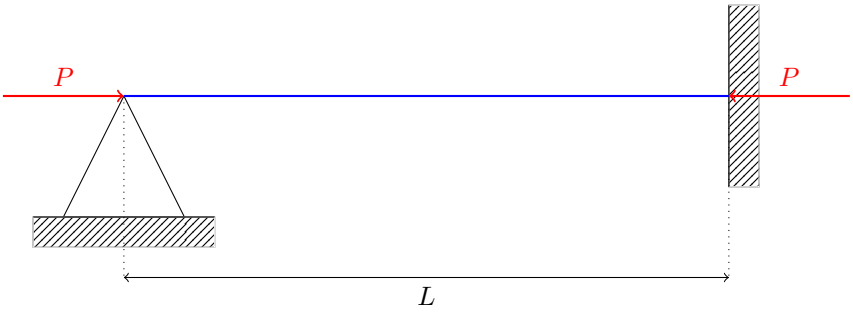

Figure 3.11 – The configuration of a pinned-fixed beam in its non-buckled state. One end point is pinned. Thus the torque (EIw_{xx}) and the deflection w are zero at this point. The other end point is fixed. Thus the deflection w and the slope of the deflection w_x are zero at this point. A non-buckled straight state of the beam is shown in blue. The distance between both ends of the beams is L.

The boundary conditions for the pinned-fixed beam are (see table 3.1):

$$w(0) = 0 \tag{3.50}$$
$$w_{xx}(0) = 0 \tag{3.51}$$
$$w(L) = 0 \tag{3.52}$$
$$w_x(L) = 0 \tag{3.53}$$

By substituting these constraints in the general solution for our differential equation, we get the constraints on the different constants A through D.

$$B \qquad\qquad D \qquad = 0 \tag{3.54}$$
$$B \qquad\qquad\qquad = 0 \tag{3.55}$$
$$A\sin(kL) + B\cos(kL) \qquad +CL + D \qquad = 0 \tag{3.56}$$
$$kA\cos(kL) - kB\sin(kLl) \qquad +C \qquad = 0 \tag{3.57}$$

The first two of these constraints again yield that $B = D = 0$. Then we can use the last constraint to find that $C = -kA\cos(kL)$. If we substitute this in the last remaining constraint, we acquire:

$$A(\sin(kL) - kL\cos(kL)) = 0 \tag{3.58}$$

Again there are two possible things that can happen. We must have that either $A = 0$ or $\sin(kL) - kL\cos(kL) = 0$. To ensure non-trivial solution we need that $A \neq 0$, so for the buckled beam we are left with the later constraint. Rewriting this condition yields the condition that needs to be satisfied to allow for buckled beam configurations:

$$kL = \tan(kL) \tag{3.59}$$

We find the first non-negative solution to this condition via the computer. This yields that $kL \approx 4.5$. Hence we find that $P = EI\left(\frac{\pi}{mL}\right)^2$ with $m = 0.69$. So this means we can map this kind of beam to the previously examined pinned-pinned beam by using an effective length $L_{eff} = mL$ with $m = 0.69$. When this constraint is fulfilled the solution for the pinned-fixed beam is

$$w(x) = A(\sin(kx) - kx\cos(kL)) \tag{3.60}$$

This solution is plotted in figure 3.12. In this figure we clearly see that the solution looks like the solution for a pinned-pinned beam. The effective length that we have introduced before remarks the fact that the deflection just is a fraction more of the wavelength of the beam.

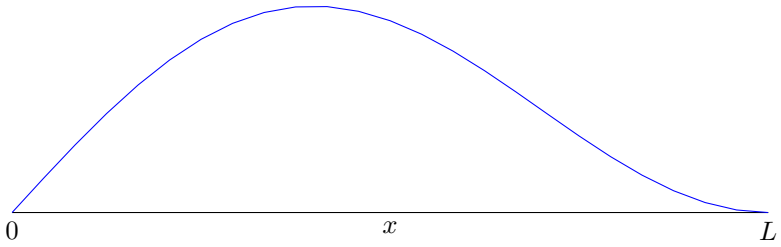

Figure 3.12 – The solution for the pinned-fixed beam configuration is plotted. We have used equation (3.60) with $A = 2$, $k = 4.49340945790906$ and $L = 1$.

A fixed-fixed beam

If we now also change the other end of the beam from pinned to fixed, we get a fixed-fixed beam (see figure 3.13). This means that the boundary conditions will require the solution to satisfy

$$w(0) = 0 \tag{3.61}$$
$$w_x(0) = 0 \tag{3.62}$$
$$w(L) = 0 \tag{3.63}$$
$$w_x(L) = 0 \tag{3.64}$$
$$\tag{3.65}$$

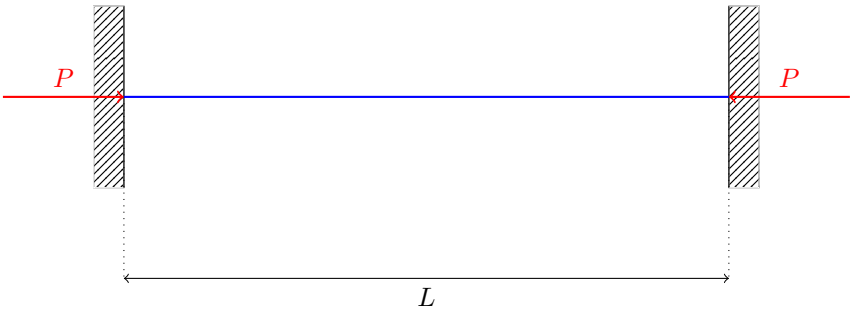

Figure 3.13 – The configuration of a fixed-fixed beam in its non-buckled state. Both end points of the beam are fixed. Thus the deflection w and the slope w_x must be zero. A non-buckled straight state of the beam is shown in blue. The distance between both ends of the beams is L.

Substituting these into the general solution of the beam we now get the following constraints on the constants:

$$\begin{aligned} B &+ D &= 0 \quad (3.66)\\ kA &+ C &= 0 \quad (3.67)\\ A\sin(kL) + B\cos(kL) &+ CL + D &= 0 \quad (3.68)\\ kA\cos(kL) - kB\sin(kL) &+ C &= 0 \quad (3.69) \end{aligned}$$

The first of these imply that $D = -B$ and the second constraint implies that $C = -Ak$. We can now use these relations to rewrite the remaining boundary conditions to the following constraints:

$$\begin{aligned} A(\sin(kL) - kL) + B(\cos(kL) - 1) &= 0 \quad (3.70)\\ Ak(\cos(kL) - 1) - Bk\sin(kL) &= 0 \quad (3.71) \end{aligned}$$

From the last of these conditions, we can find the relationship $B = A\frac{\cos(kL)-1}{\sin(kL}$. Now we can again use this relationship and rewrite the remaining constraint:

$$A\left(\sin(kL) - kL + \frac{(\cos(kL) - 1)^2}{\sin(kL)}\right) = 0 \quad (3.72)$$

This either means that $A = 0$ and the beam is not bended or that the term in the parenthesis is zero, so the beam can acquire non-zero deflections (and be buckled). If we do some rewriting of this equation we find that the following constraint must be satisfied to allow a buckled beam:

$$kL\sin(kL) = 2(1 - \cos(kL)) \quad (3.73)$$

This is equation is again numerically solvable. If we do this, we find that our condition for buckling in the fixed-fixed beam configuration is $kL \approx 6.2831853$. This looks very much like 2π and indeed $kL = 2\pi$ is a solution for this equation. It is also possible to proof that this indeed is the first positive solution to this

equation by inspecting the derivatives. This time the effective length hence will be $m = \frac{1}{2}$.

But since this solution for kL is a multiple of π we need to be careful. To make sure we don't mess up, we start again from the constraint in equations (3.70) and (3.71). This time we plug in our gained knowledge about $kL = 2\pi$. This gives us the new boundary conditions:

$$-A2\pi = 0 \tag{3.74}$$

$$0 = 0 \tag{3.75}$$

So the second boundary condition (i.e. $w'(L) = 0$) is thus automatically satisfied, but the former needs an additional condition: we need to fix $A = 0$, so there are no sine or linear terms in the deflection in this beam configuration. We now have found the deflection for the fixed-fixed beam and we end up with the solution below. This solution is plotted in figure 3.14

$$w(x) = B(\cos(kx) - 1) \tag{3.76}$$

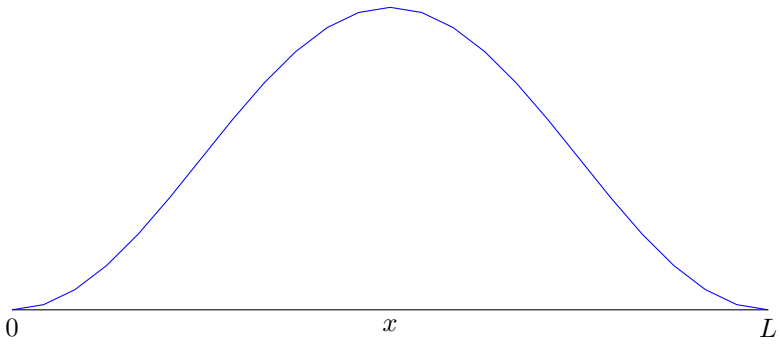

Figure 3.14 – The solution for the fixed-fixedbeam configuration is plotted. We have used equation (3.76) with $B = -2$, $kL = 2\pi$ and $L = 6$ (to ensure we have the buckled beam configuration).

3.1.6 Beam between two, freely rotary nodes

We now turn our attention to a more unusual configuration of an elastic beam. We inspect a single beam that is put between two circular, freely rotary, nodes of radius r. This is not a situation that is seen often in reality. It is however important, since this is configuration is the building block of the model of the elastic patterned sheets. In this section we study the behaviour of this configuration when we press the nodes together.

In its initial position the beam is attached in such way to the beams that is straight. During compression, the beam will bend and the nodes will rotate. The angle over which the nodes rotate is denoted with θ. This is also the so-called attachment angle of the beams (see figure 3.15). Moreover, we define the distance between the middle points of the nodes as D and the real lenght of the

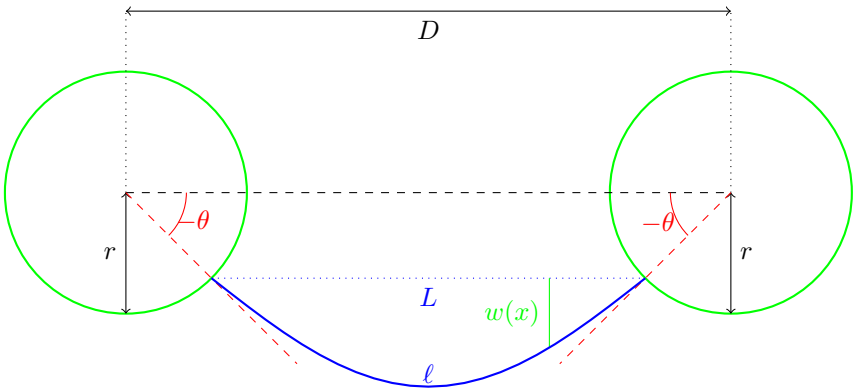

Figure 3.15 – Sketch of a buckled beam between two nodes. Here D is the length between the centra of the nodes, L is the distance between the left and right attachment positions of the beam, ℓ is the real lenght of the beam, r is the radius of the node, θ is the incoming (and outgoing) angle of the beam and $w(x)$ is the deflection of the beam at a certain point x on the beam.

beam as ℓ. Furthermore the distance between the attachment angles is called L. This length thus depends on D and the attachment angle θ in the following way

$$L = D - 2r\cos(\theta) \tag{3.77}$$

Since the nodes are free to rotate, the resulting torques on the nodes must be zero in the equilibrium positions of the system. Since the nodes have a finite radius $r \neq 0$, the boundary conditions associated with this property aren't as easy as for a pinned-pinned beam. The non-zero radius is the cause of an additional contribution to the torque on the node on top of the torque that the beam exerts directly (see figure 3.16). Hence we find the following constraints:

$$Pr\sin(\theta) + EIw_{xx}(0) = 0 \tag{3.78}$$
$$Pr\sin(\theta) - EIw_{xx}(L) = 0 \tag{3.79}$$

In the elastic patterned sheets, we see that the beams are sort of glued to the nodes. That means that they are attached orthogonal to the surface of the nodes. Hence we also have a constraint on the angle at the end points of the beam. Thus the constraints on the first derivatives at these points are

$$w_x(0) = \theta \tag{3.80}$$
$$w_x(L) = -\theta \tag{3.81}$$

Finally we know that the deflections at the end points are zero. Otherwise the beams wouldn't be attached to the nodes in the first place. Hence the following boundary conditions also need to be satisfied

$$w(0) = 0 \tag{3.82}$$
$$w(L) = 0 \tag{3.83}$$

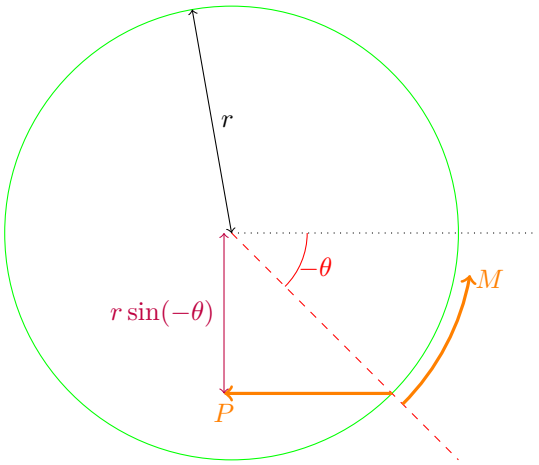

Figure 3.16 – The torque on the node. This torque consittutes of the torque of the beam (M) and the torque produced by the load P.

This means we have six boundary conditions and not only four. But the general solution to the governing ordinary differential equation has only four constants. So at first we forget about the first two boundary conditions (i.e. the torque balance on the nodes). Then we will make sure that the obtained solution also obeys the torque balance boundary conditions.

We use maple to get the solution to $w_{xxxx} + k^2 w_{xx} = 0$ with the boundary conditions $w(0) = w(L) = 0, w_x(0) = \theta, w_x(L) = -\theta$ (with $k \equiv \frac{P}{EI}$). We obtain

$$w(x) = \frac{\theta}{k}\frac{1}{\cos(kL) - 1}((\cos(kL) - 1)\sin(kx) - \sin(kL)\cos(kx) + \sin(kL)) \tag{3.84}$$

Now that we have found the solution, we still need to check to make sure that the torques on the nodes are in balance. Hence we need the second derivatives in the end points. Simple calculations show

$$EIw_{xx}(0) = -P\frac{\theta}{k}\frac{\sin(kL)}{\cos(kL) - 1} \tag{3.85}$$

$$EIw_{xx}(L) = P\frac{\theta}{k}\frac{\sin(kL)}{\cos(kL) - 1} \tag{3.86}$$

We substitute this information in equation (3.78) to find the condition for the torque balance. It turns out this condition is exactly the same for both nodes. This isn't that surprising since the whole system is symmetric. The condition is the following

$$P\left(\frac{\theta}{k}\frac{\sin(kL)}{\cos(kL) - 1} - r\sin(\theta)\right) = 0 \tag{3.87}$$

Clearly this constraint is obeyed when $P = 0$. That corresponds with an unloaded system. Most of the time the system is however loaded and $P \neq 0$. Then we need to have

$$\frac{\sin(kL)}{\cos(kL) - 1} = \frac{k}{\theta} r \sin(\theta) \tag{3.88}$$

This condition is similar to the condition for the pinned-pinned beam that lead to the buckling load (see equation (3.30)). More precisely, this constraint reduces to the condition for the pinned-pinned beam when the radius $r \to 0$ (i.e. $\sin(kL) = 0$). Hence the beam between the nodes can only be bended when this condition is obeyed.

With this constraint, it is possible to write the obtained solution for this problem in another form. To do this, we substitute this in equation (3.84). We obtain

$$w(x) = \frac{\theta}{k} \sin(kx) - r \sin(\theta) \cos(kx) + r \sin(\theta) \tag{3.89}$$

From this expression it is clear that we restore the normal pinned-pinned solution when the radius of the nodes becomes zero (i.e. $r \to 0$). This is the same equation as we obtained in equation (3.29). The only difference is that we used the amplitude in that expression and we now have used the angle θ. Since $A = \frac{\theta}{k}$ the two are similar.

Equation (3.89) gives us information about the deflections of the beam. However we need three variables that change during the compression: the load P, the distance between the nodes D and the attachment angle θ. Since these cannot be chosen independently, we need another constraint on the beam.

We are working with a beam model that models beams as inextensible. This means that the (real) length ℓ of the beam stays the same as the initial length L_0 during the whole compression. Hence we need to have $\ell = L_0$. To calculate the real length ℓ from the beams deflections we need equation (3.34) again. We use the approximate relation immediately since the deflection w is a mixture of sine and cosine terms. This makes the resulting integral impossible to solve exactly. So we need to have

$$L_0 = \int_0^L \sqrt{1 + w_x^2(x)}\ dx \approx \int_0^L (1 + \frac{1}{2} w_x(x))\ dx \tag{3.90}$$

Now we substitute the information about the deflection w (equation (3.89)) into the right hand side. Hence we find

$$L_0 - L = \int_0^L \frac{1}{2} w_x(x)\ dx \tag{3.91}$$

$$= \int_0^L \frac{1}{2} (\theta \cos(kx) + kr \sin(\theta) \sin(kx))^2\ dx \tag{3.92}$$

$$= \int_0^L \frac{1}{2} \big(\theta^2 \cos^2(kx) + k^2 r^2 \sin^2(\theta) \sin^2(kx) + 2\theta kr \sin(\theta) \sin(kx) \cos(kx)\big)\ dx \tag{3.93}$$

$$= \frac{1}{2} \int_0^L \left(\frac{1}{2}(\theta^2 + k^2 r^2 sin^2(\theta)) + \frac{1}{2}(\theta^2 - k^2 r^2 \sin^2(\theta)) \cos(2kx) + \theta kr \sin(\theta) \sin(2kx)\right)\ dx \tag{3.94}$$

$$= \frac{1}{4} \left((\theta^2 + k^2 r^2 \sin^2(\theta))L + \frac{1}{2k}(\theta^2 - k^2 r^2 \sin^2(\theta)) \sin(2kL) - \theta r \sin(\theta) \cos(2kL) + 2\theta r \sin(\theta)\right) \tag{3.95}$$

This expression is however not very clear to interpret. Luckily we can use the previous constraint that ensures the torque balance (equation (3.88)). This conditions tells us that $r \sin(\theta) = \frac{\theta}{k} \frac{\sin(kL)}{\cos(kL)-1}$. For notational simplicity we define $F \equiv \frac{\sin(kL)}{\cos(kL)-1}$. Thus we have $r \sin(\theta) = \frac{\theta}{k} F$. Substituting this into equation (3.95) gives us:

$$L_0 - L = \frac{1}{4k}\big(k(\theta^2 + \theta^2 F^2)L + (\theta^2 - \theta^2 F^2) \sin(kL) \cos(kL) + 2\theta^2 F \sin^2(kL)\big) \tag{3.96}$$

$$= \frac{\theta^2}{4k}\big(k(1 + F^2)L + (1 - F^2) \sin(kL) \cos(kL) + 2F \sin^2(kL)\big) \tag{3.97}$$

When we carefully inspect the last two terms of this expression we see the following:

$$(1 - F^2) \sin(kL) \cos(kL) + 2F \sin^2(kL) \tag{3.98}$$

$$= \frac{\sin(kL)}{\cos(kL) - 1} \left(\frac{\cos^2(kL) - 2\cos(kL) + 1 - \sin^2(kL)}{\cos(kL) - 1} + 2\sin^2(kL)\right) \tag{3.99}$$

$$= \frac{\sin(kL)}{\cos(kL) - 1} \big(2\cos^2(kL) + 2\sin^2(kL)\big) \tag{3.100}$$

$$= 2\frac{\sin(kL)}{\cos(kL) - 1} \tag{3.101}$$

$$= 2F \tag{3.102}$$

Moreover, when we inspect the first term, $1 + F^2$, we find

$$1 + F^2 = \frac{\cos^2(kL) - 2\cos(kL) + 1 + \sin^2(kL)}{(\cos(kL) - 1)^2} \tag{3.103}$$

$$= 2\frac{1 - \cos(kL)}{(cos(kL) - 1)^2} \tag{3.104}$$

$$= -2\frac{1}{\cos(kL) - 1} \tag{3.105}$$

Hence the constraint on the length of the beam becomes

$$L_0 - L = \frac{\theta^2}{2k}\frac{1}{\cos(kL) - 1}(-kL + \sin(kL)) \tag{3.106}$$

From this expression it is not immediately clear that it reduces to the pinned-pinned beam case when $r \to 0$. To see this, we must recall that $kL = \pi$ when a pinned-pinned beam is buckled. Hence $\sin(kL) = 0$ and $\cos(kL) - 1 = -2$. Hence the equation reduce to equation (3.45):

$$\frac{L_0 - L}{L} = \frac{\theta^2}{4} \tag{3.107}$$

Equation (3.106) seems at first sight not of any help, since it is again an expression that is depending on the three variables, P, D and θ (recall that $D = L - 2r\cos(\theta)$). However at this point we have not one but two different equations that depend on those variables. Hence it is in theory possible to find the two others, given one of the variables.

In particular we now have a way to find the deflections of this system for a given compression $\frac{D_0 - D}{D_0}$ of the whole system. For that given D, we can find values for P and θ that solve both the following equations

$$L_0 - L = \frac{\theta^2}{2k}\frac{1}{\cos(kL) - 1}(-kL + \sin(kL)) \tag{3.108}$$

$$\frac{k}{\theta}r\sin(\theta) = \frac{\sin(kL)}{\cos(kL) - 1} \tag{3.109}$$

Since $L = D - 2r\cos(\theta)$ (see equation (3.77)), these expression can be made more explicitly depending on the variable D. To do this, we define D_0 as the initial distance between the node (i.e. before the compression starts). Hence we obtain:

$$D_0 - D = 2r(1 - \cos(\theta)) + \frac{\theta^2}{2k}\frac{-k(D - 2r) + \sin(kD - 2kr\cos(\theta))}{\cos(kD - 2kr\cos(\theta)) - 1} \tag{3.110}$$

$$\frac{k}{\theta}r\sin(\theta) = \frac{\sin(kD - 2kr\cos(\theta))}{\cos(kD - 2kr\cos(\theta)) - 1} \tag{3.111}$$

When we then have obtained the values for P and θ we have all the information that we need to find the deflection of the beam. That is,

$$w(x) = \frac{\theta}{k}\sin(kx) - r\sin(\theta)\cos(kx) + r\sin(\theta) \tag{3.112}$$

These above equations describe the whole system of an inextensible elastic beam between two circular, freely rotary nodes. They are however not easy to solve. To solve them, we need to resort to a computer. Since there was no time left to do these computer calculations, the results (including the theoretical force strain curve) for this set-up are not yet acquired and thus cannot be presented here in this thesis.

3.2 Inextensible model for large deflections

In this section we study a beam model that models the beams as inextensible. In contrary to the model in the previous section, the model in this section allows large deflections w. We start this section with an introduction and the derivation of the beam model. With this model we then study the pinned-pinned beam again. We focuss on the force strain relation for this configuration (and will not present the actual deflections of the beam).

3.2.1 Introduction to the model

As we did in the previous section for the Euler Bernoulli model (section 3.1.1), we inspect the same beam that is loaded from both sides with a force P. This time however we will not use the coordinate x and the deflection $w(x)$, but another system. We will use the coordinate s, which is the point, measured over the beam itself. Moreover, we will use the angle $\theta(s)$, which will be the angle between a tangent line to the point s and a line parallel to the x-axis (see Figure 3.17). The main difference with the model in section 3.1.1 is that we won't use an approximation for the deflections w in this section. The model of this section allows for large deflections and non-linear behaviour of the beams deflection, in contrary to the previous model in section 3.1.1.

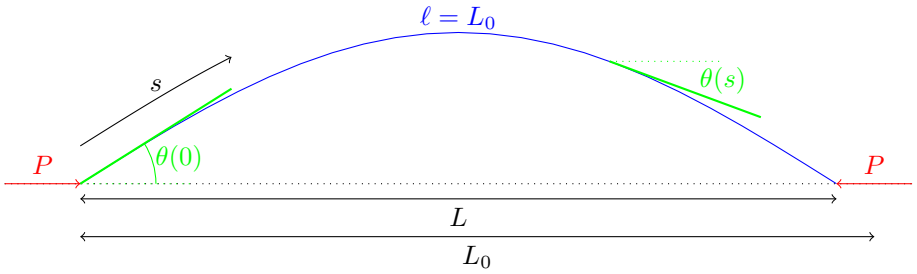

Figure 3.17 – The new setup of the beam with θ and the coordinate s, on the beam. $\theta(s)$ is the angle that the beam makes (with a line parallel to the surface) at a position s measured over the beam.

3.2.2 Energy in the model

Since we have not changed the essential attributes of the beam, the energy of the beam will be the same as it was in the previous section. This means we once again assume that there is no stretching (i.e. $\varepsilon = 0$) and no twisting (i.e. $\kappa_x = 0$). By doing so we end up with the the following Lagrangian which looks very much like the one we had previously in equation (3.3). We have neglected all the kinetic energy, since we are most interested in the equilibrium deflections of the beam.

$$\mathcal{L} = \int -\frac{1}{2} EI_{yy}\kappa_y^2 ds + P\Delta L \tag{3.113}$$

This time around the curvature κ_y is simple, for $\kappa_y = \frac{d\theta}{ds}$ (note that this is without approximation this time). The strain ΔL can also be found in a way similar to what we have done before. This time around, we only need to express dx in terms of ds and θ. This is quite easy and we find that $dx = \cos(\theta)ds$. Thus we acquire

$$\Delta L = \int (ds - dx) = \int (1 - \cos(\theta))ds \tag{3.114}$$

If we use these both equation and make one Lagrangian again, we now find without any assumption or approximation about the deflection the following Lagrangian:

$$\mathcal{L} = \int \left(-\frac{1}{2} EI_{yy}(\theta_s)^2 + P(1 - \cos(\theta)) \right) ds \tag{3.115}$$

(with $\theta_s \equiv \frac{\partial}{\partial s}\theta$ in this expression.)

At this point we can use our Euler Lagrange variation method again to find the differential equation we were looking for. Doing so yields

$$EI\theta_{ss} + P\sin(\theta) = 0 \tag{3.116}$$

Or, if we set $k^2 \equiv \frac{P}{EI}$:

$$\theta_{ss} + k^2 \sin(\theta) = 0 \tag{3.117}$$

3.2.3 Boundary conditions and solution

Finding the general solution to this newly acquired beam model isn't that simple. Luckily there is a trick that we can exploit to find some expression for the solutions. What we do, is multiply the equation by $\theta_s = \frac{d\theta}{ds}$ and then integrate the whole equation. Hence we get:

$$\frac{1}{2}(\theta_s)^2 - k^2 \cos(\theta) = C \tag{3.118}$$

In this equation we have a constant C, that is depending on the boundary conditions of the beam. This time however these boundary conditions are a bit harder, but not much than before, since we have in principle that $\theta = w'$. So this means we suffice with a small modification of the previous boundary conditions in table 3.1. We hence acquire table 3.2.

As can be seen in this table, some of the boundaries now only have one boundary condition. This is since these boundaries have a condition on the deflection w at the respective point and θ will only say something about the angles (and the derivatives of it).

3.2.4 A pinned-pinned beam

As we did for the inextensible model for beams with small deflections in section 3.1.4 we first investigate the same pinned-pinned beam setup with our model

Table 3.2 – Summary of the most frequently occuring boundary conditions at the end s of a beam. If a beam is pinned at one end it is free to rotate and hence the torque of the beam must be zero (i.e. $\theta'(s) = 0$). If a beam is fixed at an end point, its starting angle is fixed. When a beam is free at an end point, this means it is free to rotate and its shear forces must be zero. In the table M is the torque and Q is the shear force at the point s.

Name	θ	θ_s $(= \frac{M}{EI})$	θ_{ss} $(= \frac{Q}{EI})$	θ'''
pinned		$\theta_s(s) = 0$		
fixed	$\theta(s) = 0$			
free		$\theta_s(s) = 0$	$\theta_{ss}(s) = 0$	

for large deflections. The boundary conditions for a pinned-pinned beam that we have found in table 3.2 can now be used. However it is convenient to add the boundary conditions $\theta(0) = \alpha$ and $\theta(\ell) = -\alpha$. We can think of these boundary conditions as the incoming and outgoing angles of the beam at its end points. These angles are dependent on the state of the beam (i.e. buckled or non-buckled) and will of course change with increasing loads.

If we now use two boundary conditions at the same end point (either $\theta(0) = \alpha$ and $\theta_s(0) = 0$ or $\theta(\ell) = -\alpha$ and $\theta_s(\ell) = 0$), we find the constant that we encountered in equation (3.118). If we do this we find that $C = -k^2\cos(\alpha)$. So by substituting this into equation (3.118) we acquire the problem for our pinned-pinned case.

$$\frac{1}{2}(\theta_s)^2 - k^2\cos(\theta) = -k^2\cos(\alpha) \tag{3.119}$$

Finding a Force Angle relation

Now we can - for a moment - write $\theta_s = \frac{d\theta}{ds}$ and use this to rewrite the equation above. If we do this we find a relationship between ds and $d\theta$:

$$ds = \frac{1}{k\sqrt{2(\cos(\theta) - \cos(\alpha))}}\, d\theta \tag{3.120}$$

We can exploit this relationship we got here by integrating over it. Since we now that $\int_0^\ell ds = \ell$ the left part of it is clear. The right part of it must be an integral over θ. By inspecting the boundary conditions we find that this is integrating over $\theta = \alpha$ to $\theta = -\alpha$. Hence we acquire:

$$\ell = \int_0^\ell ds = \int_\alpha^{-\alpha} \frac{1}{k\sqrt{2(\cos(\theta) - \cos(\alpha))}}\, d\theta \tag{3.121}$$

But in this form we can do little with the right hand sides integral we got. To use it effectively, we need a change of variables to find a nicer integral that we actually can calculate. The change of variables that we will use is the following:

$$\sin\left(\frac{\alpha}{2}\right)\sin(\phi) = \sin\left(\frac{\theta}{2}\right) \tag{3.122}$$

$$d\theta = \frac{2\sin\left(\frac{\alpha}{2}\right)\cos(\phi)}{\sqrt{1-\sin^2\left(\frac{\alpha}{2}\right)\sin^2(\phi)}}\,d\phi \tag{3.123}$$

But before we can use this change of variables we also need to rewrite the original equation by using some trigonometric identities to find:

$$\begin{aligned}
\cos(\theta)-\cos(\alpha) &= -2\sin(\frac{\theta-\alpha}{2})\sin(\frac{\theta+\alpha}{2}) && (3.124)\\
&= -2\left(\sin\frac{\theta}{2}\cos\frac{\alpha}{2}-\sin\frac{\alpha}{2}\cos\frac{\theta}{2}\right)\left(\sin\frac{\theta}{2}\cos\frac{\alpha}{2}+\sin\frac{\alpha}{2}\cos\frac{\theta}{2}\right) && (3.125)\\
&= -2\left(\sin^2\frac{\theta}{2}\cos^2\frac{\alpha}{2}-\sin^2\frac{\alpha}{2}\cos^2\frac{\theta}{2}\right) && (3.126)\\
&= -2\left(\sin^2\frac{\theta}{2}-\sin^2\frac{\alpha}{2}\right) && (3.127)\\
&= 2\sin^2\frac{\alpha}{2}\left(1-\frac{\sin^2\frac{\theta}{2}}{\sin^2\frac{\alpha}{2}}\right) && (3.128)
\end{aligned}$$

So if we combine this identity and the change of variables we find the following integral for our pinned-pinned beam:

$$\ell = \int_{-\alpha}^{\alpha}\frac{d\theta}{2k\sin\left(\frac{\alpha}{2}\right)\left(1-\frac{\sin^2\left(\frac{\theta}{2}\right)}{\sin^2\left(\frac{\alpha}{2}\right)}\right)} = \int_{-\frac{\pi}{2}}^{\frac{\pi}{2}}\frac{1}{k}\frac{d\phi}{\sqrt{1-\sin^2\left(\frac{\alpha}{2}\right)\sin^2(\phi)}} \tag{3.129}$$

This last integral that we acquired is the complete elliptic integral of the first kind. It is denoted with the symbol K and is defined as follows:

$$K(m) \equiv \int_0^{\frac{\pi}{2}}\frac{dx}{\sqrt{1-m\sin^2(x)}} \tag{3.130}$$

So if we write this elliptic integral for the integral we wanted to calculate we find an expression. Since the elliptic integrals are well studied (see Wolfram), we can look up the Taylor approximation for small m:

$$K(m) \approx \frac{\pi}{2}\left(1+\frac{1}{4}\frac{m}{1-m}-\frac{1}{8}\frac{m^2}{1-m}\right)+\mathcal{O}(m^3) \tag{3.131}$$

If we use this information about these kind of integrals we find for our integral:

$$\ell = \frac{2}{k}K(\sin^2\left(\frac{\alpha}{2}\right)) \approx \frac{1}{k}\pi\left(1+\frac{1}{4}\frac{\sin^2\left(\frac{\alpha}{2}\right)}{1-\sin^2\left(\frac{\alpha}{2}\right)}\right)+\mathcal{O}(sin^4(\alpha/2)) \tag{3.132}$$

Although this relationship seem to be not much of a help for us, it is. If we remember that $k = \sqrt{\frac{P}{EI}}$ we have essentially found a relationship between the load P and the attachment angle α. This relationship is:

$$P = EI\frac{\pi^2}{\ell^2}\frac{\left(K(\sin^2\left(\frac{\alpha}{2}\right))\right)^2}{\left(\frac{\pi}{2}\right)^2} \approx EI\frac{\pi^2}{\ell^2}\left(1 + \frac{1}{4}\frac{\sin^2\left(\frac{\alpha}{2}\right)}{1-\sin^2\left(\frac{\alpha}{2}\right)}\right)^2 \approx EI\frac{\pi^2}{\ell^2}\left(1 + \frac{1}{8}\alpha^2\right) \tag{3.133}$$

In this equation we find the term $EI\frac{\pi^2}{\ell^2}$ which looks familiar. Since we are inspecting an inextensible beam we have that the arc length ℓ of the beam is identical to the initial length L_0. So this term is precisely the same as the Euler load $P_e \equiv EI\frac{\pi^2}{L_0^2}$. So we can also denote this relation in the following way:

$$\frac{P}{P_e} = \frac{\left(K(\sin^2\left(\frac{\alpha}{2}\right))\right)^2}{\left(\frac{\pi}{2}\right)^2} \approx 1 + \frac{1}{8}\alpha^2 \tag{3.134}$$

So at this point we have found the force angle relationship for a pinned-pinned beam with the inextensible beam model for large deflections (this relationship is plotted in figure 3.18). However, force strain relations are much more useful since they are easier to measure in experiments. So we need to find a way to acquire this kind of relationship, as we did in the previous model for small deflections (see equation (3.32)).

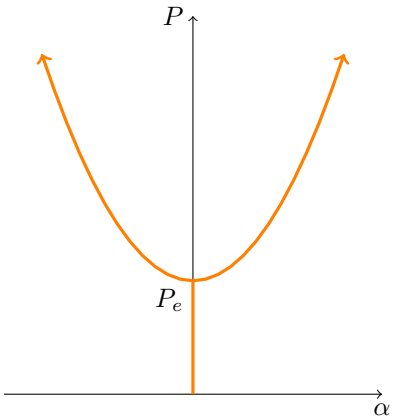

Figure 3.18 – Plot of the force angle relationship for the pinned-pinned beam configuration in the inextensible beam model as derived in equation (3.134).

Strain Angle and Force Strain relations

To do just this, we may go back to the definition of the strain $\Delta L = L_0 - L$. Since the beam is assumed to be inextensible we have that $L_0 = \ell$. Moreover the length L can be calculated with the integral $\int_0^\ell \cos(\theta(s))ds$. So the strain ΔL can be found by calculating the following integral:

$$\Delta L = \ell - \int_0^{\ell} \cos(\theta(s))\ ds \tag{3.135}$$

This integral looks as horrible as the last one and luckily it is in fact *as* horrible so we can use the same techniques as before to calculate it. We first start by using the relation between ds and $d\theta$ (equation (3.120)) and applying the trigonometric identity in equation (3.128). This yields:

$$\Delta L = \ell - \int_{-\alpha}^{\alpha} \frac{1}{\sqrt{2}k} \frac{\cos(\theta)}{\sqrt{\cos(\theta) - \cos(\alpha)}} d\theta = \ell - \int_{-\alpha}^{\alpha} \frac{d\theta}{2k} \frac{2\big(1 - \sin^2\big(\frac{\theta}{2}\big)\big) - 1}{\sqrt{\sin^2\big(\frac{\alpha}{2}\big)\left(1 - \frac{\sin^2\big(\frac{\theta}{2}\big)}{\sin^2\big(\frac{\alpha}{2}\big)}\right)}} \tag{3.136}$$

Now that we have acquired this form for the strain ΔL we must apply the same change of variables as before (equations (3.122) and (3.123)). If we do this we get the following expression:

$$\Delta L = \ell - \int_{-\frac{\pi}{2}}^{\frac{\pi}{2}} \frac{2}{k} \sqrt{1 - \sin^2\Big(\frac{\alpha}{2}\Big) \sin^2(\phi)}\ d\phi + \int_{-\frac{\pi}{2}}^{\frac{\pi}{2}} \frac{1}{k} \frac{1}{\sqrt{1 - \sin^2\big(\frac{\alpha}{2}\big) \sin^2(\phi)}}\ d\phi \tag{3.137}$$

One of these integrals is an integral we already know: the complete elliptic integral of the first kind (K). The other integral is also an elliptic integral. It is the complete integral of the second kind. This integral is denoted by E and is defined as:

$$E(m) \equiv \int_0^{\frac{\pi}{2}} \sqrt{1 - m \sin^2(x)}\ dx \tag{3.138}$$

If we write the integral as these complete elliptic integrals and again use the Euler load $P_e = EI\frac{\pi^2}{\ell^2}$ we get a relation for the relative strain $\frac{\Delta L}{L_0} = \frac{\Delta L}{\ell}$:

$$\frac{\Delta L}{L_0} = 1 - \sqrt{\frac{P_e}{P}} \frac{2E(\sin^2\big(\frac{\alpha}{2}\big)) - K(\sin^2\big(\frac{\alpha}{2}\big))}{\frac{\pi}{2}} \tag{3.139}$$

We now have essentially a relation between the strain and the forces and angles. But since this strain both depends on the angle α and the force P this is not useful in this form. What we want to do is use equation (3.134) and plug it into this equation, so we find a clean relationship between the strain ΔL and the angle α. If we do this we find:

$$\frac{\Delta L}{L_0} = 1 - \frac{2E(\sin^2\big(\frac{\alpha}{2}\big)) - K(\sin^2\big(\frac{\alpha}{2}\big))}{K(\sin^2\big(\frac{\alpha}{2}\big))} = 2\left(1 - \frac{E(\sin^2\big(\frac{\alpha}{2}\big))}{K(\sin^2\big(\frac{\alpha}{2}\big))}\right) \tag{3.140}$$

If we use the approximations for these complete elliptic integrals for small angles α we get the relationship for the beam when it just is buckled (since then the angle α of the beam will be small). The approximations are:

$$K(m) \approx \frac{\pi}{2}\left(1 + \frac{1}{4}\frac{m}{1-m} - \frac{1}{8}\frac{m^2}{1-m}\right) + \mathcal{O}(m^3) \tag{3.141}$$

$$E(m) \approx \frac{\pi}{2}\left(1 - \frac{1}{4}m - \frac{3}{64}m^2\right) + \mathcal{O}(m^3) \tag{3.142}$$

So when we use these approximations on the previous equation, equation (3.140), and the Taylor expansion for the sine around zero, we get the following relationship for the post-buckling configuration of the pinned-pinned beam:

$$\frac{\Delta L}{L_0} = \frac{\alpha^2}{4} + \mathcal{O}(\alpha^4) \tag{3.143}$$

So we can now combine this equation (3.143) with the force angle relation in equation (3.134). This yields the following force strain relation for the pinned-pinned beam when the beam is just in its buckled state:

$$\frac{P}{P_e} \approx 1 + \frac{1}{2}\frac{\Delta L}{L_0} + \mathcal{O}(\alpha^4) \tag{3.144}$$

This force-strain relationship is plotted in figure 3.31 along with the force strain curve of the Euler Bernoulli beam equation for inextensible beams with small deflections to stress the difference between both models (see equation (3.134)).

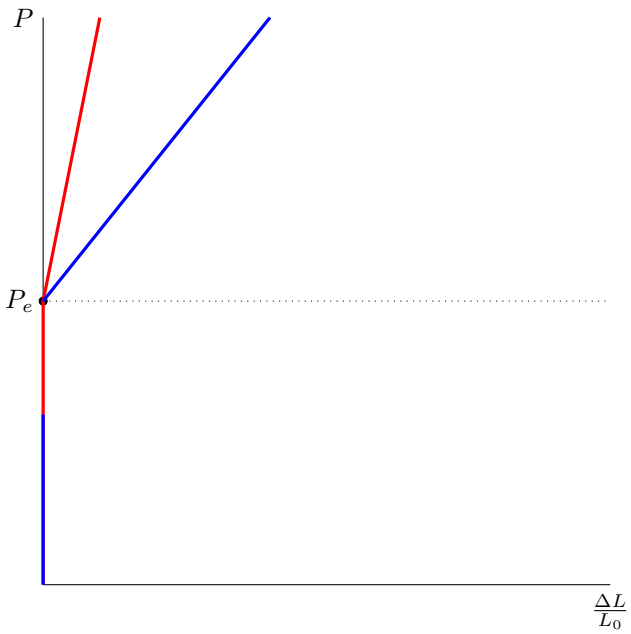

Figure 3.19 – The force strain relationship for an (inextensible) beam before and after buckling for both the model for small deflections (red) and for large deflections (blue). The slope of the after buckling part is 2 when using the approximation for small deflections and $\frac{1}{2}$ when not using this approximation (i.e. the model for large deflections).

3.3 Extensible beam model for small deflections

In the previous sections we have studied beam models that modeled the elastic beams as inextensible. In this section we present a model that takes the extensibility of the beams into account, but assumes that the deflections of the beam are small. We start this section with the derivation of the model. After we have obtained the governing equations for this model, we use them to study the pinned-pinned beam again. We focus on both the force strain relation as the actual configuration of the pinned-pinned beam. Moreover, we also study the configuration with an extensible elastic beam between two circular, freely rotary nodes at the end of this section.

3.3.1 Introduction to the model

In this section we will inspect a beam model which does not assume that the beams are inextensible. Instead this model lets the beams be extensible, which complicates the model. However the standard set-up remains the same as before. We will inspect a beam as in figure 3.20 that is loaded from both sides with a force P. Note that in this extensible model we have the real length ℓ of the beam, which is not necessarily the same as the initial lenght L_0 of the beam. In this section we will again assume that the slope of the deflections w_x stays small,

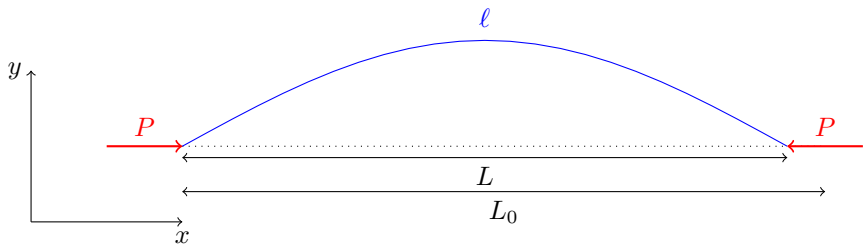

Figure 3.20 – General set-up for the beam. The load P is applied in the x-direction, while the deflection, $w(x)$ is in the z-direction. The blue line represent the beam (bended in this case). ℓ is the real length of the beam.

as we did in section 3.1 for the (inextensible) Euler Bernoulli beam model.

For the extensible model we use a different coordinate. In the previous models we have used both the coordinates x and s, which are the current positions of a point on the beam. For this model however we will use the coordinate $\hat{x}$. This coordinate is the position a particular point had along the initial beam (see figure 3.21). This means that $\hat{x} \in [0, L_0]$ for all beam configurations.

Moreover we need to take the displacements in the x-direction into account in this extensible beam model. These displacements are denoted by $u(\hat{x})$. The displacements in the y-directions are called $w(\hat{x})$ (See figure 3.22 for an illustration of these displacements u and w).

3.3.2 Energy in the model

As before, in this set up we have both the elastic energy (equation (3.1)) and the work that is done by the load P that we apply on the beam, $W = P\Delta L$. Since we have changed our coordinates and have used the deflection in the x-direction, the strain this time will simply be $\Delta L = -(u(L_0) - u(0))$, with $\hat{x} = 0$ and $\hat{x} = L_0$ being the end points of the beam.

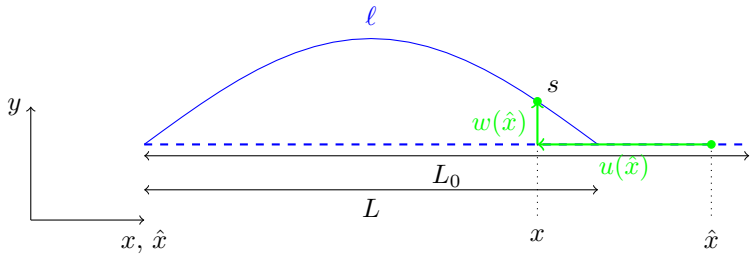

Figure 3.21 – The current set-up for the extensible beam model. In this sketch the initial beam configuration (dashed, blue) and the current configuration (blue) are shown. Moreover a point of the beam is chosen and both the deflections in the x-direction, $u(\hat{x})$, and the deflection in the y-direction, $w(\hat{x})$, of that point are drawn. Furthermore the newly coordinates $\hat{x}$ and the previous coordinates x and s for this point are shown.

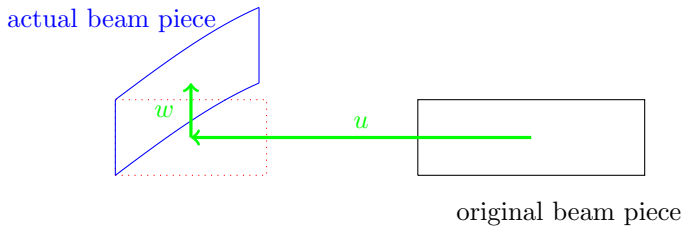

Figure 3.22 – The two kind of deflections for an infinitesimal piece of the beam. The black part is the original beam and the blue part is the beam in its current configuration.

Now that we are taking the extensibility of a beam into account, the elastic energy will also change. In the inextensible cases we have assumed that $\varepsilon = 0$. Since this ε is associated with the stretching mode of the beam, this is not true for an extensible beam. ϵ turns out to be (see page 5 of Marguerre [1947] and Kondoh and Atluri [1985]):

$$\varepsilon = \sqrt{(1 + u_{\hat{x}})^2 + w_{\hat{x}}^2} - 1 \approx u_{\hat{x}} + \frac{w_{\hat{x}}^2}{2} \tag{3.145}$$

In this equation $u_{\hat{x}} \equiv \frac{\partial}{\partial \hat{x}} u$ and $w_{\hat{x}} \equiv \frac{\partial}{\partial \hat{x}} w$.

The curvature κ_y of the beam will remain what it was: $\kappa_y = (w_{\hat{x}\hat{x}})^2$.

So if we combine both the ε and the κ_y we can express the elastic energy of equation (3.1) in the beam as follows:

$$E_{el} = \int_0^{L_0} \left(\frac{1}{2} EA \left(u_{\hat{x}} + \frac{w_{\hat{x}}^2}{2} \right)^2 + \frac{1}{2} EI w_{\hat{x}\hat{x}}^2 \right) d\hat{x} \tag{3.146}$$

The other thing that is working on the beam, is the load P we have applied on both ends of the beam. By use of the fundamental theorem of calculus we can express the strain ΔL as an integral:

$$-\Delta L = u(L_0) - u(0) = \int_0^{L_0} u_{\hat{x}} d\hat{x} \tag{3.147}$$

So now we can find the Lagrangian for these kind of extensible beams again by using the above equations. This gives us:

$$\mathcal{L} = \int_0^{L_0} \left(\frac{1}{2} EA \left(u_{\hat{x}} + \frac{w_{\hat{x}}^2}{2} \right)^2 + \frac{1}{2} EI w_{\hat{x}\hat{x}}^2 + P u_{\hat{x}} \right) d\hat{x} \tag{3.148}$$

Now that we have found our Lagrangian again, we will use the Euler Lagrange optimization again. First we define Π as the integrand of this Lagrangian. That means:

$$\Pi = \frac{1}{2}EA\left(u_{\hat{x}} + \frac{w_{\hat{x}}^2}{2}\right)^2 + \frac{1}{2}EIw_{\hat{x}\hat{x}}^2 + Pu_{\hat{x}} \tag{3.149}$$

From the general formulation for the Euler Lagrange variation method it follows that an energy optimum must satisfy:

$$\begin{cases} 0 = \dfrac{\partial \Pi}{\partial u} - \dfrac{\partial}{\partial \hat{x}}\dfrac{\partial \Pi}{\partial u_{\hat{x}}} + \dfrac{\partial^2}{\partial \hat{x}^2}\dfrac{\partial \Pi}{\partial u_{\hat{x}\hat{x}}} & \text{(3.150a)} \\ 0 = \dfrac{\partial \Pi}{\partial w} - \dfrac{\partial}{\partial \hat{x}}\dfrac{\partial \Pi}{\partial w_{\hat{x}}} + \dfrac{\partial^2}{\partial \hat{x}^2}\dfrac{\partial \Pi}{\partial w_{\hat{x}\hat{x}}} & \text{(3.150b)} \end{cases}$$

We can use the previously defined Π to find the conditions for the energy extrema. If we do so we find conditions for the equilibriums for the extensible beams. In the following derivatives we will again assume that E, A and I are the same all over the beam we are inspecting (i.e. E, A and I are constants and do not depend on the position $\hat{x}$).

$$\begin{cases} 0 = EA\dfrac{\partial}{\partial \hat{x}}\left(u_{\hat{x}} + \dfrac{w_{\hat{x}}^2}{2}\right) & \text{(3.151a)} \\ 0 = EA\dfrac{\partial}{\partial \hat{x}}\left(u_{\hat{x}} + \dfrac{w_{\hat{x}}^2}{2}\right)w_{\hat{x}} + EAw_{\hat{x}\hat{x}}\left(u_{\hat{x}} + \dfrac{w_{\hat{x}}^2}{2}\right) - EIw_{\hat{x}\hat{x}\hat{x}\hat{x}} & \text{(3.151b)} \end{cases}$$

If we use the first equation of these two and substitute it into the second, we see that one term vanishes. Moreover, we find that $\left(u_{\hat{x}} + \frac{w_{\hat{x}}^2}{2}\right)$ should be constant. We will investigate the value of this constant later on. The resulting coupled differential equations will hence look like:

$$\begin{cases} 0 = \dfrac{\partial}{\partial \hat{x}}\left(u_{\hat{x}} + \dfrac{w_{\hat{x}}^2}{2}\right) & \text{(3.152a)} \\ 0 = EA\left(u_{\hat{x}} + \dfrac{w_{\hat{x}}^2}{2}\right)w_{\hat{x}\hat{x}} - EIw_{\hat{x}\hat{x}\hat{x}\hat{x}} & \text{(3.152b)} \end{cases}$$

We have found from the first of these equations that $u_{\hat{x}} + \frac{w_{\hat{x}}^2}{2} = C$ in which C is a constant. We did not however know yet what this constant is. Luckily there is a way for us to find this constant. We need to use another thing from the elasticity. As it happens from the elasticity it is known that the normal force N that a beam exerts can be calculated via the expression (see Barber [2010]):

$$N = -EA\frac{1}{L_0}\int_0^{L_0} \varepsilon \, d\hat{x} \tag{3.153}$$

If deflections are small, this normal force will more or less be the same as the load P we apply on the beam, so we could replace it with P (see Figure 3.23). For now, however, we wil continue to use the normal force N.

We have observed before that $\varepsilon \approx u_{\hat{x}} + \frac{1}{2}w_{\hat{x}}^2$. If we now use equation (3.152a) and combine this with the equation for the normal force, equation (3.153), we get the additional condition for the constant C that we encoutered:

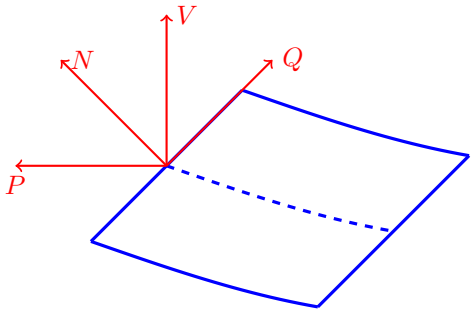

Figure 3.23 – A small piece of the beam with all the forces that it produces. N is the normal force, which is along the centroid of the beam. Q is the shear force that is perpendicular to the normal force N. P is the horizontal force that the beam exerts. This is the force that counters the load that we apply on the beam. V is the normal force, which is perpendicular to the horizontal force P. When the deflections stay small, the centroid of the beam is almost straight. If that happens, then the horizontal force P and the normal force N are the same. So we can assume that $N = P$ when the deflections are small (i.e. when w is small).

$$-\frac{N}{EA} = \frac{u(L_0) - u(0) + \frac{1}{2}\int_0^{L_0} w_{\hat{x}}(\hat{x})^2 d\hat{x}}{L_0} = C \tag{3.154}$$

So this equation tells us that $C = u_{\hat{x}} + \frac{1}{2}w_{\hat{x}}^2 = -\frac{N}{EA}$. So now that we have found this constant C, we can rewrite our system of differential equations (3.152) to find the extensible beam model:

$$\begin{cases} u(\hat{x}) = u(0) - \dfrac{N}{EA}\hat{x} - \dfrac{1}{2}\displaystyle\int_0^{\hat{x}} w_{\hat{x}}(x)^2 dx & \text{(3.155a)} \\ EIw_{\hat{x}\hat{x}\hat{x}\hat{x}} + Nw_{\hat{x}\hat{x}} = 0 & \text{(3.155b)} \end{cases}$$

3.3.3 A pinned-pinned beam

Now that we have found the extensible beam model we will turn our attention again at the most simple beam configuration: a pinned-pinned beam (see figure 3.24). The boundary conditions that we found for the inextensible case in section 3.1.4 are easily adapted to the new situation, since only the coordinates need to be changed. However, in the extensible model we also have the horizontal deflections $u(\hat{x})$ and we need one boundary condition for this deflection. The most used condition is $u(0) = 0$, which means that the position of the left

end point of the beam is kept fixed. Hence the boundary conditions are:

$$w(0) = 0 \tag{3.156}$$
$$w(L_0) = 0 \tag{3.157}$$
$$w_{\hat{x}\hat{x}}(0) = 0 \tag{3.158}$$
$$w_{\hat{x}\hat{x}}(L_0) = 0 \tag{3.159}$$
$$u(0) = 0 \tag{3.160}$$
$$\tag{3.161}$$

We now assume that $N \approx P$. This is valid for small deflections as we explained in the previous section (see figure 3.23). Hence the beam model of equation (3.155b) now becomes

$$\begin{cases} u(\hat{x}) = u(0) - \dfrac{P}{EA}\hat{x} - \dfrac{1}{2}\displaystyle\int_0^{\hat{x}} w_{\hat{x}}(x)^2 dx & \text{(3.162a)} \\ EIw_{\hat{x}\hat{x}\hat{x}\hat{x}} + Pw_{\hat{x}\hat{x}} = 0 & \text{(3.162b)} \end{cases}$$

We start with the second expression, $EIw_{\hat{x}\hat{x}\hat{x}\hat{x}} + Pw_{\hat{x}\hat{x}} = 0$. Since both the differential equation and the boundary conditions for this problem have the same form as the pinned-pinned beam problem in the inextensible case (see section 3.1.4), the solution also has the same form.

Hence we know the solution for w:

$$\begin{cases} w = 0 & \text{if } P \neq EI\left(\frac{n\pi}{L_0}\right)^2 \\ w = D\sin(kx) & \text{if } P = EI\left(\frac{n\pi}{L_0}\right)^2 \end{cases} \tag{3.163}$$

In this $k \equiv \sqrt{\frac{P}{EI}}$ and $n \in \mathbb{N}$. Moreover, D is the amplitude of the resulting sine deflection w. For a particular configuration, this D is constant. See figure 3.25 for a graphical illustration of the current information.

We can however find the value for D. To do this, we must use equation (3.162a). One of the boundary conditions is $u(0) = 0$. If we substitute this in equation (3.162a) we find

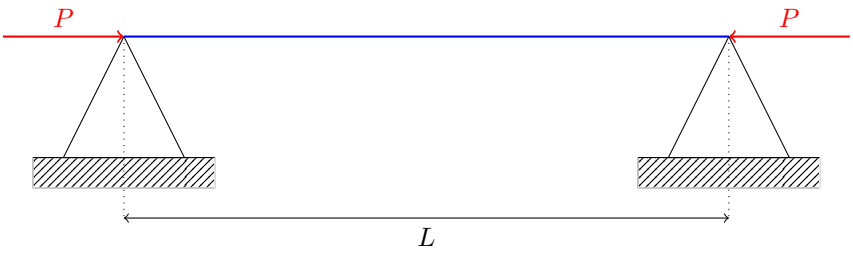

Figure 3.24 – The configuration of a pinned-pinned beam in its non-buckled state. Both end points of the beam are pinned. Thus the torque ($EIw_{\hat{x}\hat{x}}$) and the deflection w are zero at these points. A non-buckled straight state of the beam is shown in blue. The distance between both ends of the beams is L.

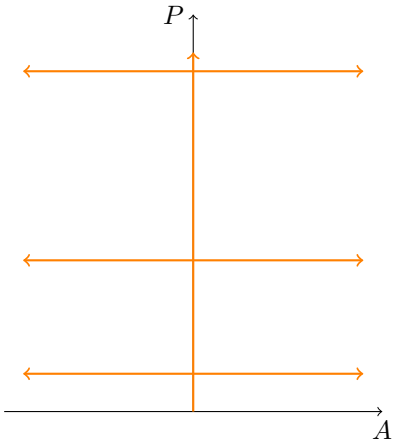

Figure 3.25 – Graphical illustration of the possible values of the constant D in equation (3.163) as function of a varying load P. It is shown that from above considerations D could take on any value at some of the values for P, but for most values of the load P the constant D should be zero.

$$u(\hat{x}) = -\frac{P}{EA}\hat{x} - \frac{1}{2}\int_0^{\hat{x}} w_{\hat{x}}^2(x)dx \tag{3.164}$$

The most interesting property that follows from this expression is the strain ΔL. We have seen before that $\Delta L = -u(L_0)$ (see equation (3.147)). Hence we can find the strain ΔL through

$$\Delta L = \frac{P}{EA}L_0 + \frac{1}{2}\int_0^{L_0} w_{\hat{x}}^2(x)dx \tag{3.165}$$

When the beam is not yet buckled, we have found that $w = 0$. Hence we know the strain:

$$\Delta L = \frac{P}{EA}L_0 \tag{3.166}$$

Or equivalently

$$P = EA\frac{\Delta L}{L_0} \tag{3.167}$$

which is in correspondence with the Elastica as seen in equation (3.153).

When the beam however is buckled, we have found that $w = D\sin(k\hat{x})$. Hence the strain becomes

$$\begin{cases} \Delta L &= \frac{P_c}{EA}L_0 + \frac{1}{2}k^2D^2\int_0^{L_0}\cos^2(kx)dx \\ &= \frac{P_c}{EA}L_0 + \frac{k^2D^2}{4}L_0 \end{cases} \tag{3.168}$$

in which we have used the fact that $\sin(2kL_0) = 0$, since $kL_0 = \pi$ when the beam is buckled.

This relates the strain ΔL and the amplitude D of the sine deflection w. It is more convenient to find the amplitude A as a function of the strain ΔL, since we can measure this value directly. We obtain

$$kD = \pm 2\sqrt{\frac{\Delta L}{L_0} - \frac{P_c}{EA}} \tag{3.169}$$

To make this relation more clear, we use the following change of variables

$$\frac{\Delta L}{L_0} = \delta + u \tag{3.170}$$

in which δ denotes the strain at which the beam start to buckle and u measures the additional strain. That is,

$$\delta \equiv \frac{P_e}{EA} \tag{3.171}$$

Hence equation (3.169) transforms into

$$kD = \pm 2\sqrt{u} \tag{3.172}$$

Thus we now have described the deflection w completely:

$$\begin{cases} w = 0 & \text{if } P \neq EI\left(\frac{n\pi}{L_0}\right)^2 \\ w = \pm\frac{2}{k}\sqrt{u}\sin(kx) & \text{if } P = EI\left(\frac{n\pi}{L_0}\right)^2 \end{cases} \tag{3.173}$$

With these expression at hand, we now can calculate both the applied load P and the amplitude D when we know the strain $\frac{\Delta L}{L_0}$ of the beam. To summarize, we have:

$$\begin{cases} P = EA\frac{\Delta L}{L_0} & \text{if } \frac{\Delta L}{L_0} \leq \delta \\ P = P_c & \text{if } \frac{\Delta L}{L_0} \geq \delta \end{cases} \tag{3.174}$$

and

$$\begin{cases} kD = 0 & \text{if } u \leq 0 \\ kD = \pm 2\sqrt{u} & \text{if } u \geq 0 \end{cases} \tag{3.175}$$

with $P_c = EI\left(\frac{\pi}{L_0}\right)^2$, $\delta = \frac{P_c}{EA}$ and $u = \frac{\Delta L}{L_0} - \delta$.

Both results are graphically illustrated in figure 3.26. From this it is clear that in this model the load P cannot exceed the critical Euler load P_e. Experiments however do not support this and hence we must conclude that this model is not a good model for the beams.

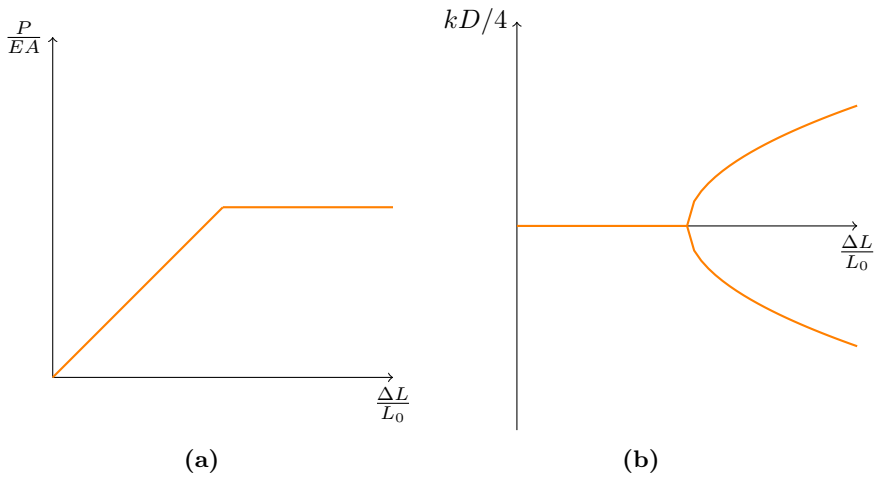

Figure 3.26 – Plots of the strain force relation (a) and the strain amplitude relation (b) for a pinned-pinned extensible beam. In this figures we have plotted equations (3.174) and (3.175)

3.3.4 Beam between two, freely rotary nodes

In section 3.1.6 we studied the unusual system of an elastic beam between two circular, freely rotary nodes with an inextensible beam model. In this section we investigate the same system, but with the extensible beam model of equation (3.155b).

As before, we have two circular nodes of radius r. An elastic beam is placed between them, initially in such a way that the beam is straight. During compression, the beam will bend and the nodes will rotate. The angle over which the nodes rotate is denoted with θ (the so-called attachment angle). The distance between the middle points of the nodes is D, the real length of the beam is ℓ and the distance between the attachment points of the beam is L (see figure 3.27). As before we thus have

$$L = D - 2r\cos(\theta) \tag{3.176}$$

Since this system is the same as in section 3.1.6, the boundary conditions are the same. So we have two boundary conditions that ensure that the deflection w at the end points are zero, two boundary conditions that make sure the beam is attached in the right way to the nodes and finally two boundary conditions that guarantee torque balance on the nodes. The only difference is that the end points are now located at $\hat{x} = 0$ and $\hat{x} = L_0$ (and not $x = 0$ and $x = L$). Hence

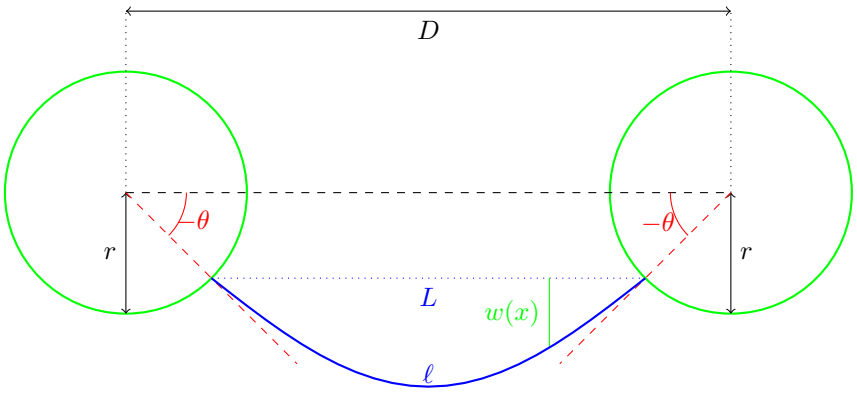

Figure 3.27 – Sketch of a buckled beam between two nodes. Here D is the length between the centra of the nodes, L is the distance between the left and right attachment positions of the beam, ℓ is the real lenght of the beam, r is the radius of the node, θ is the incoming (and outgoing) angle of the beam and $w(x)$ is the deflection of the beam at a certain point x on the beam.

for this problem we have the following constraints

$$w(0) = 0 \tag{3.177}$$
$$w(L_0) = 0 \tag{3.178}$$
$$w_{\hat{x}}(0) = \theta \tag{3.179}$$
$$w_{\hat{x}}(L_0) = \theta \tag{3.180}$$
$$Pr\sin(\theta) + EIw_{\hat{x}\hat{x}}(0) = 0 \tag{3.181}$$
$$Pr\sin(\theta) - EIw_{\hat{x}\hat{x}}(L_0) = 0 \tag{3.182}$$
$$\tag{3.183}$$

The only difference with the inextensible case is the change of the second end point coordinate of the beam (i.e. $\hat{x} = L_0$ instead of $x = L$). Since the general differential equation is also the same, we end up with the same solution (with L_0 instead of L). Thus by inspecting equations(3.89) and (3.88) we find the deflection w for this extensible elastic beam between two nodes:

$$w(\hat{x}) = \frac{\theta}{k}\sin(k\hat{x}) - r\sin(\theta)\cos(k\hat{x}) + r\sin(\theta) \tag{3.184}$$

with the additional condition that the following constraint is obeyed

$$\frac{\sin(kL_0)}{\cos(kL_0) - 1} = \frac{k}{\theta} r\sin(\theta) \tag{3.185}$$

At this point we encounter a problem. Most experiments we do are strain-controlled. That is, we know the amount of compression of the whole system (i.e. $\frac{D_0 - D}{D_0}$), but these expressions are independent of D. Moreover, when we know the load P, we can find the attachment angle θ from equation (3.185) and then find the deflections via equation (3.184). But this is all independent of the value of D at this moment. Hence we need to find another constraint.

We cannot use the same strategy as before (see equation (3.90)), since the beam is extensible in this model. Luckily we have another constraint in our model:

$$u(\hat{x}) = u(0) - \frac{N}{EA}\hat{x} - \frac{1}{2}\int_0^{\hat{x}} w_{\hat{x}}^2(x)\ dx \tag{3.186}$$

The distance L of the beam at the current position is related to $u(\hat{x}$ via $L - L_0 = u(L_0) - u(0)$ (see equation (3.147)). Hence with the above expression we have

$$\Delta L = L_0 - L = \frac{P}{EA}L_0 + \frac{1}{2}\int_0^{L_0} w_{\hat{x}}^2(x)\ dx \tag{3.187}$$

(in which we again have used the approximation $N \approx P$, which is true for small deflections)

With the same reasoning as in equations (3.91) through (3.95) we now obtain

$$L_0 - L = \frac{P}{EA}L_0 - \frac{\theta^2}{2}\frac{1}{\cos(kL_0) - 1}L_0 + \frac{\theta^2}{2k}\frac{\sin(kL_0)}{\cos(kL_0) - 1} \tag{3.188}$$

This expression reduces to equation (3.169), when the radius $r \to 0$. We can see this when we recall that $kL_0 = \pi$ when the radius $r = 0$, since that is the buckling condition for a pinned-pinned beam.

At this point we have a complete description of the system. From equations (3.188) and (3.185) we can find both the load P and the attachment angle θ for a given value of L. After these are found we can use equation (3.184) to find the deflections w for the beam.

We must however not forget that L is still depending on θ. Hence to make things more explicitly we replace L with $L = D - 2r\cos(\theta)$. Hence the expressions become:

$$D_0 - D = 2r(1 - \cos(\theta) + \frac{P}{EA}(D_0 - 2r) - \frac{\theta^2}{2k}\frac{-kD_0 + 2rk + \sin(kD_0 - 2kr)}{\cos(kD_0 - 2kr)} \tag{3.189}$$

$$\frac{k}{\theta}r\sin(\theta) = \frac{\sin(kD_0 - 2kr)}{\cos(kD_0 - 2kr) - 1} \tag{3.190}$$

$$w(\hat{x}) = \frac{\theta}{k}\sin(k\hat{x}) - r\sin(\theta)\cos(k\hat{x}) + r\sin(\theta) \tag{3.191}$$

The above expression describe in principle the system of a beam between two nodes. It is however not clear how to solve these analytically. It is better to resort to a computer for these calculations. By lack of time, these computer calculations are unfortunately not done for now.

3.4 Extensible beam model for large deflections

In the previous section 3.3 we discussed a beam model that takes the extensibility of the elastic beams into account. One of the assumptions we made was however that the deflections w of the beam stay small. In this chapter we extend the extensible beam model to allow for huge deflections as we did in section 3.2 for the Euler Bernoulli inextensible beam model.

We start with the derivation of the beam model via the Euler Lagrangian variational principle. After we have found the governing equations for this model, we use it to study the pinned-pinned beam configuration once more. We focus on the force strain relations in this study of the pinned-pinned beam (and we will not present results on the actual deflections of the beam).

3.4.1 Introduction to model

We inspect the same beam setup as we did in section 3.3 (see figure 3.28). Hence we inspect a beam with initial length L_0 that is loaded from both sides with a force P. In this chapter we remain using the coordinate $\hat{x}$ (i.e. the position a particular point had along the initial beam configuration) as introduced in section 3.3. However, in this section not the deflections $w(\hat{x})$ and $u(\hat{x})$ but rather the angle $\theta(\hat{x})$ (i.e. the angle between the tangent line and the x-axis, see section 3.2.1) describes the form of the beam.

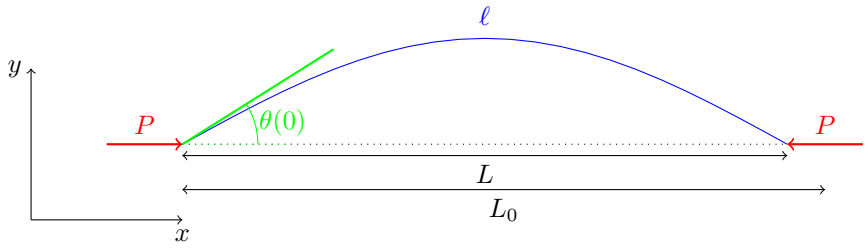

Figure 3.28 – General set-up for the beam. The load P is applied in the x-direction, while the deflection, $w(x)$ is in the z-direction. The blue line represent the beam (bended in this case). ℓ is the real length of the beam.

3.4.2 Energy in the model

As before in section 3.3 in this set up we have both elastic energy of the beam and the work by the load P contributing to the total energy of the elastic beam. We have $\kappa_y = \theta_{\hat{x}}$ as in section 3.2. Moreover $-\Delta L = u(L_0) - u(0) = \int_0^{L_0} u_{\hat{x}}\, d\hat{x}$ (see equation (3.147)). Hence the total Lagrangian for the equilibrium positions of the beam is

$$\mathcal{L} = \int_0^{L_0} \left(\frac{1}{2} EA\varepsilon^2 + \frac{1}{2} EI\theta_{\hat{x}}^2 + Pu_{\hat{x}} \right) d\hat{x} \tag{3.192}$$

In this expression the deflection u is used. In the introduction we however said that we use the tangent slope θ. So we need to express the deflection u in terms of θ. To do this we first inspect what's going on in an infinitesimal piece of the beam when it endures deflections.

Deflections in an infinitesimal piece of the beam

Following Kondoh and Atluri [1985], Christodoulou and Kounadis [1986] and Magnusson et al. [2001], we now consider an infinitesimal piece of an elastic beam of initial length $d\hat{x}$ (see figure 3.29). This beam piece is deformed into another configuration through displacements in the x-direction (i.e. u) and in the y-direction (i.e. w).

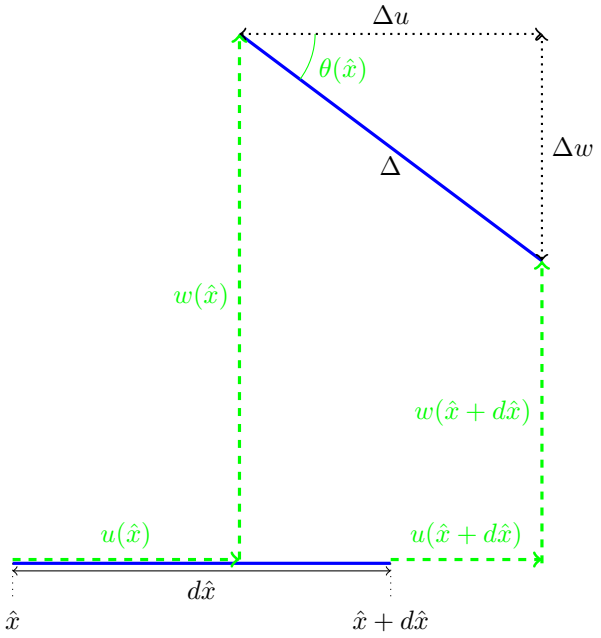

Figure 3.29 – The displacement of an infinitesimal beam piece with an original length of $d\hat{x}$. In blue are both the original (straight) and the new (displaced) beam configurations of the beam. In green the displacements in the x and y directions are shown for both the beginning and the end of the beam piece (respectively with u for the horizontal displacement and w for the vertical displacements). Δu is the difference in x-position of both ends of the beams in the displaced configuration and Δw is the difference in the y-position. Δ denotes the length of the new configuration of the beam. Finally $\theta(\hat{x})$ is the slope of the beam at $\hat{x}$.

The difference between the vertical positions on the deformed beam piece of the start and end of this beam piece is defined as Δw and the difference in the horizontal positions as Δu. Note that this is the difference in the positions rather than the difference in the deflections. This means that we need to take the initial difference of $d\hat{x}$ in the positions into account. From figure 3.29 it is then apparent that

$$\Delta w = w(\hat{x}) - w(\hat{x} + d\hat{x}) \tag{3.193}$$

and

$$\Delta u = u(\hat{x}) - u(\hat{x} + d\hat{x}) + d\hat{x} \tag{3.194}$$

We now define the new distance of the beam as Δ. Hence from the Pythagorean theorem follows

$$\Delta = \sqrt{(\Delta w)^2 + (\Delta u)^2} = \sqrt{\left(w(\hat{x}) - w(\hat{x} + d\hat{x})\right)^2 + \left(u(\hat{x}) - u(\hat{x} + d\hat{x}) + d\hat{x}\right)^2} \tag{3.195}$$

Now we introduce again the angle $\theta(\hat{x})$ as the angle between a line tangent to the deflection at position $\hat{x}$ and a line parallel to the x-axis (as shown in figure 3.29). Hence by geometric considerations we acquire

$$\sin(\theta(\hat{x})) = \frac{\Delta w}{\Delta} \tag{3.196}$$

$$= \frac{w(\hat{x}) - w(\hat{x} + d\hat{x})}{\sqrt{\left(w(\hat{x}) - w(\hat{x} + d\hat{x})\right)^2 + \left(u(\hat{x}) - u(\hat{x} + d\hat{x}) + d\hat{x}\right)^2}} \tag{3.197}$$

$$= \frac{\frac{w(\hat{x}) - w(\hat{x} + d\hat{x})}{d\hat{x}}}{\sqrt{\left(\frac{w(\hat{x}) - w(\hat{x} + d\hat{x})}{d\hat{x}}\right)^2 + \left(\frac{u(\hat{x}) - u(\hat{x} + d\hat{x})}{d\hat{x}} + 1\right)^2}} \tag{3.198}$$

and

$$\cos(\theta(\hat{x})) = \frac{\Delta u}{\Delta} \tag{3.199}$$

$$= \frac{u(\hat{x}) - u(\hat{x} + d\hat{x}) + d\hat{x}}{\sqrt{\left(w(\hat{x}) - w(\hat{x} + d\hat{x})\right)^2 + \left(u(\hat{x}) - u(\hat{x} + d\hat{x}) + d\hat{x}\right)^2}} \tag{3.200}$$

$$= \frac{\frac{u(\hat{x}) - u(\hat{x} + d\hat{x})}{d\hat{x}} + 1}{\sqrt{\left(\frac{w(\hat{x}) - w(\hat{x} + d\hat{x})}{d\hat{x}}\right)^2 + \left(\frac{u(\hat{x}) - u(\hat{x} + d\hat{x})}{d\hat{x}} + 1\right)^2}} \tag{3.201}$$

These expressions are valid for all initial lengths $d\hat{x}$. Thus we can inspect the limit behaviour when $d\hat{x} \to 0$. We have per definition (of the derivative) that

$$\lim_{d\hat{x} \to 0} \frac{u(\hat{x}) - u(\hat{x} + d\hat{x})}{d\hat{x}} = \frac{\partial u}{\partial d\hat{x}} = u_{\hat{x}} \tag{3.202}$$

and

$$\lim_{d\hat{x} \to 0} \frac{w(\hat{x}) - w(\hat{x} + d\hat{x})}{d\hat{x}} = \frac{\partial w}{\partial d\hat{x}} = w_{\hat{x}} \tag{3.203}$$

Hence in the limit case when $d\hat{x} \to 0$ the equations (3.198) and (3.201) become the following

$$\sin(\theta(\hat{x})) = \frac{w_{\hat{x}}}{\sqrt{(1+u_{\hat{x}})^2 + (w_{\hat{x}})^2}} \tag{3.204}$$

$$\cos(\theta(\hat{x})) = \frac{(1+u_{\hat{x}})}{\sqrt{(1+u_{\hat{x}})^2 + (w_{\hat{x}})^2}} \tag{3.205}$$

At this point we recall the expression for ε of equation (3.145)[2]

$$\varepsilon = \sqrt{(1+u_{\hat{x}})^2 + (w_{\hat{x}})^2} - 1 \tag{3.206}$$

Since $\varepsilon + 1$ is the same as the denominator of equations (3.204) and (3.205), we can substitute this stretching term in these equation. Hence we acquire

$$\sin(\theta(\hat{x})) = \frac{w_{\hat{x}}}{\varepsilon + 1} \tag{3.207}$$

$$\cos(\theta(\hat{x})) = \frac{(1+u_{\hat{x}})}{\varepsilon + 1} \tag{3.208}$$

So now we have relationships between the displacements (u and w) and the tangent slope θ. In the Lagrangian in equation (3.192) we have the displacements that we must replace with θ. So it is more useful to rewrite the results of equations (3.207) and (3.208). Thus we obtain

$$w_{\hat{x}} = (\varepsilon + 1)\sin(\theta(\hat{x})) \tag{3.209}$$

$$u_{\hat{x}} = (\varepsilon + 1)\cos(\theta(\hat{x})) - 1 \tag{3.210}$$

The Lagrangian and the beam model

We now substitute equation (3.210) in the general Lagrangian of equation (3.192). Hence we obtain the Lagrangian for this problem in terms of only the stretching ε and the angle θ. We obtain:

$$\mathcal{L} = \int_0^{L_0} \left(\frac{1}{2} EA\varepsilon^2 + \frac{1}{2} EI(\theta_{\hat{x}})^2 + Pu_{\hat{x}} \right) d\hat{x} \tag{3.211}$$

$$= \int_0^{L_0} \left(\frac{1}{2} EA\varepsilon^2 + \frac{1}{2} EI(\theta_{\hat{x}})^2 + P((\varepsilon + 1)\cos(\theta(\hat{x})) - 1) \right) d\hat{x} \tag{3.212}$$

As we did in for the previous beam models we can now use the Euler Lagrange variation method to find the differential equations for the equilibrium positions of the beam in this model. Hence we obtain

$$\begin{cases} 0 = EA\varepsilon + P\cos(\theta(\hat{x})) & \text{(3.213a)} \\ 0 = EI\theta_{\hat{x}\hat{x}} + P(\varepsilon + 1)\sin(\theta(\hat{x})) & \text{(3.213b)} \end{cases}$$

[2]We also have found an explanation for this expression: since ε measures the strain in the beam, it is the difference between the initial length and the new length of an infinitesimal piece of the beam. Hence $\varepsilon = \Delta - 1$

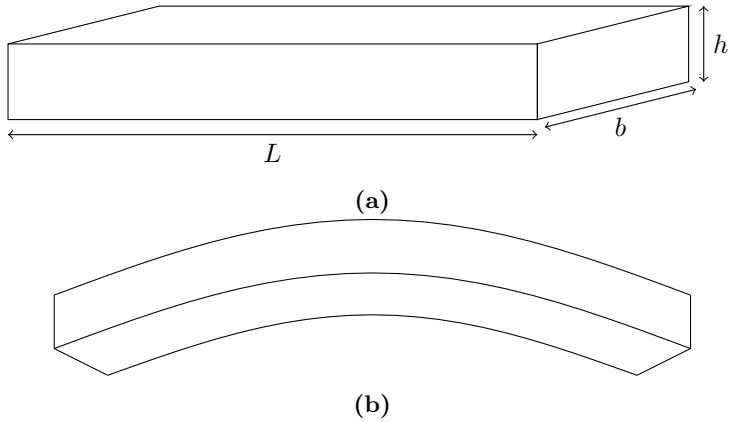

Figure 3.30 – 3D sketch of an elastic rod both in a straight (a) and a bended (b) position.

We now use the first of these equations (equation (3.213a)) to find an relationship between ε and θ. Hence we acquire the following expression

$$\varepsilon = \frac{-P}{EA}\cos(\theta(\hat{x})) \tag{3.214}$$

It is now possible to substitute this relation into the set of equations (3.213). More precisely it is possible to substitute this relationship into equation (3.213b). We thus obtain the differential equation for the extensible beam model that allows huge deflection. This differential equation is:

$$0 = EI\theta_{\hat{x}\hat{x}} + P\left(\frac{-P}{EA}\cos(\theta(\hat{x})) + 1\right)\sin(\theta(\hat{x})) \tag{3.215}$$

$$0 = EI\theta_{\hat{x}\hat{x}} + P\sin(\theta(\hat{x})) - \frac{P^2}{EA}\cos(\theta(\hat{x}))\sin(\theta(\hat{x})) \tag{3.216}$$

When the last term of this differential equation is dropped, this relation reduces to the inextensible beam model for huge deflections (i.e. equation (3.116)). This occurs when $\varepsilon \to 0$ (or equivalently when EA becomes huge), precisely when we want the stretching of the beam to disappear (and the beams to become inextensible). This is also clear when we set $\varepsilon = 0$ in equation (3.213b). Hence this extensible beam model is a small expansion to the normal, inextensible beam model.

Moreover, we now see when we should use this extensible model and when an inextensible beam model suffice for elastic beams. When we for instance inspect an elastic rod with which has length h in the direction in which it can buckle and a length b in the other direction (see figure 3.30), we know the beam's area and its second moment of inertia:

$$A = hb \tag{3.217}$$

$$I = \frac{h^3 b}{12} \tag{3.218}$$

Hence we have $A = \frac{12}{h^2} I$. If we substitute this into the differential equation (3.216), we acquire

$$EI\theta_{\hat{x}\hat{x}} + P\sin(\theta(\hat{x})) - \frac{P^2}{12EI} h^2 \cos(\theta(\hat{x}))\sin(\theta(\hat{x})) \tag{3.219}$$

Hence from this we see that the contribution of the last term becomes small when h is small. Since this last term is the only difference between the differential equation for the extensible beam model and the equation for the inextensible beam model (see equation (3.116) in section 3.2.2), we conclude that the stretching of the beams is more relevant in thicker beams. Hence the inextensible beam model and the results using it from section 3.2 are better for thin beams than for thick ones. Moreover, we see that the thicker the beams become the more the extensibility is necessary to acquire realistic predictions from the theory.

3.4.3 A pinned-pinned beam

In section 3.2.4 we inspected a pinned-pinned beam with an inextensible beam model that allows for large deflections (see equation (3.116)). In this section we will study the same beam configuration once more, but now with the extensible beam model of equation (3.216). We will generally follow the same line of thought as in section 3.2.4, but the resulting integrals are harder to solve this time.

To get started, we first multiply equation 3.216 by $\theta_{\hat{x}}$ and then integrate it. Hence we obtain:

$$\frac{EI}{2}(\theta_{\hat{x}})^2 - P\cos(\theta) + \frac{P^2}{2EA}\cos^2(\theta) = C \tag{3.220}$$

In this expression C is a constant. The value of this constant is determined by the boundary conditions of the beam configuration that we are inspected. In section 3.2.4 we already found the boundary conditions of this configuration. We have that $\theta_{\hat{x}}(0) = \theta_{\hat{x}}(L_0) = 0$ and $\theta(0) = \alpha = -\theta(L_0)$, with α being the slope at the beginning of the beam.

We now substitute the boundary conditions at the beginning of the beam into equation (3.220) to find the value of the constant C. Hence we find:

$$C = -P\cos(\alpha) + \frac{P^2}{2EA}\cos^2(\alpha) \tag{3.221}$$

With this value we have in principle the whole description of the pinned-pinned beam, when we substitute this into equation (3.220). We find the expression

$$\frac{EI}{2}\theta_{\hat{x}}^2 = P(\cos(\theta) - \cos(\alpha)) - \frac{P^2}{EA}\big(\cos^2(\theta) - \cos^2(\alpha)\big) \tag{3.222}$$

However this expression is not very helpful in its current form. We need to modify it in order to find real information about the pinned-pinned beam. Our goal is to find a relationship between the force and the strain. We use the same strategy as in section 3.2.4 and start by finding a relation between the force and the starting angle α. Then we derive an expression that relates this starting angle α and the strain. Finally we combine these two to obtain the force strain relation.

Finding a relation between the force P and the angle α

Our first step is rewriting equation (3.257) with trigonometric identities. More precisely we use $\cos(\lambda) = 1 - 2\sin^2(\frac{\lambda}{2})$. Hence we find the following identities:

$$\cos(\theta) - \cos(\alpha) = \big(1 - 2\sin^2(\theta/2)\big) - \big(1 - 2\sin^2(\alpha/2)\big) \tag{3.223}$$

$$= 2\big(\sin^2(\alpha/2) - \sin^2(\theta/2)\big) \tag{3.224}$$

$$\cos^2(\theta) - \cos^2(\alpha) = \big(1 - 2\sin^2(\theta/2)\big)^2 - \big(1 - 2\sin^2(\alpha/2)\big)^2 \tag{3.225}$$

$$= 4\big(\sin^2(\alpha/2) - \sin^2(\theta/2)\big) - 4\big(\sin^4(\alpha/2) - \sin^4(\theta/2)\big) \tag{3.226}$$

We substitute these in equation (3.257). Then we rewrite the resulting expression to find:

$$\theta_{\hat{x}}^2 = \frac{4P}{EI}\left((1 - \frac{P}{EA})\big(\sin^2(\alpha/2) - \sin^2(\theta/2)\big) + \frac{P}{EA}\big(\sin^4(\alpha/2) - \sin^4(\theta/2)\big)\right) \tag{3.227}$$

Now we can write $\theta_{\hat{x}}$ explicitly as $\frac{d\theta}{d\hat{x}}$. If we do this, we find a relationship between $d\theta$ and $d\hat{x}$:

$$d\hat{x} = \sqrt{\frac{EI}{4P}}\frac{d\theta}{\sqrt{(1 - \frac{P}{EA})\big(\sin^2(\alpha/2) - \sin^2(\theta/2)\big) + \frac{P}{EA}\big(\sin^4(\alpha/2) - \sin^4(\theta/2)\big)}} \tag{3.228}$$

We can exploit this relation by integrating over it. Since we have that $\int_0^{L_0} d\hat{x} = L_0$ the left part is clear. The right part must be an integral over θ. By inspecting the boundary conditions we find that we need to integrate from $\theta = \alpha$ to $\theta = -\alpha$. Hence we acquire:

$$L_0 = \int_{-\alpha}^{\alpha} \sqrt{\frac{EI}{4P}}\frac{d\theta}{\sqrt{(1 - \frac{P}{EA})\big(\sin^2(\alpha/2) - \sin^2(\theta/2)\big) + \frac{P}{EA}\big(\sin^4(\alpha/2) - \sin^4(\theta/2)\big)}} \tag{3.229}$$

This form is however not very easy to work with. To use it effectively we need a change of variables to find a better integral that we can work with. The change of variables that we will use is the following:

$$\sin\left(\frac{\alpha}{2}\right)\sin(\phi) = \sin\left(\frac{\theta}{2}\right) \tag{3.230}$$

$$d\theta = \frac{2\sin\big(\frac{\alpha}{2}\big)\cos(\phi)}{\sqrt{1 - \sin^2\big(\frac{\alpha}{2}\big)\sin^2(\phi)}}\, d\phi \tag{3.231}$$

Hence our integral of equation (3.229) transforms into

$$L_0 = \int_{-\frac{\pi}{2}}^{\frac{\pi}{2}} \sqrt{\frac{EI}{4P}} \frac{2c\cos(\phi)}{\sqrt{1-c^2\sin^2(\phi)}} \frac{d\phi}{\sqrt{(1-\frac{P}{EA})c^2(1-\sin^2(\phi)) + \frac{P}{EA}c^4(1-\sin^4(\phi))}} \tag{3.232}$$

In this expression we have written $\sin(\alpha/2) = c$ for notational simplicity. This expression is however still not easy to evaluate in its current form. We need more trigonometric identities. This time we will exploit the following:

$$\begin{aligned} 1-\sin^4(\phi) &= \sin^2(\phi) + \cos^2(\phi) - \sin^4(\phi) && (3.233)\\ &= \sin^2(\phi)(1-\sin^2(\phi)) + \cos^2(\phi) && (3.234)\\ &= \cos^2(\phi)\big(1+\sin^2(\phi)\big) && (3.235) \end{aligned}$$

When we substitute this in equation (3.232) we obtain

$$L_0 = \int_{-\frac{\pi}{2}}^{\frac{\pi}{2}} \sqrt{\frac{EI}{4P}} \frac{2c\cos(\phi)}{\sqrt{1-c^2\sin^2(\phi)}} \frac{d\phi}{\sqrt{(1-\frac{P}{EA})c^2\cos^2(\phi) + \frac{P}{EA}c^4\cos^2(\phi)(1+\sin^2(\phi))}} \tag{3.236}$$

Since this integral is symmetric around $\phi = 0$ we can suffice by only calculating the integral from 0 to $\frac{\pi}{2}$ and multiply the result by 2. Hence we find the following relation:

$$L_0 = 2\int_0^{\frac{\pi}{2}} \sqrt{\frac{EI}{P}} \frac{1}{\sqrt{1-c^2\sin^2(\phi)}} \frac{d\phi}{\sqrt{(1-\frac{P}{EA}) + \frac{P}{EA}(c^2 + c^2\sin^2(\phi))}} \tag{3.237}$$

This is however still not an integral that we can evaluate directly. So instead of trying to evaluate this integral, we will construct an integral that has the same behaviour as this integral for small starting angles α. In order to do this we use the Taylor expansions of both the fractions in the integrand. These Taylor approximations are:

$$\frac{1}{\sqrt{1-c^2\sin^2(\phi)}} \approx 1 + \frac{1}{2}c^2\sin^2(\phi) + \mathcal{O}(c^4) \tag{3.238}$$

and

$$\frac{1}{\sqrt{(1-\frac{P}{EA}) + \frac{P}{EA}(c^2 + c^2\sin^2(\phi))}} \approx \frac{1}{\sqrt{1-\frac{P}{EA}+\frac{P}{EA}c^2}}\left(1 - \frac{1}{2}\frac{\frac{P}{EA}c^2}{1-\frac{P}{EA}+\frac{P}{EA}c^2}\sin^2(\phi)\right) + \mathcal{O}(c^4) \tag{3.239}$$

So with these approximation we can actually determine the integral of equation (3.237) up to the order c^3 for small starting angles α. By substituting these Taylor approximation in equation (3.237) we obtain the following integral:

$$L_0 \approx \\ 2\sqrt{\frac{EI}{P}} \int_0^{\pi/2} \frac{1}{\sqrt{1-e+ec^2}} \left(1 + \frac{1}{2}c^2 \sin^2(\phi)\right) \left(1 - \frac{1}{2}\frac{ec^2}{1-e+ec^2} \sin^2(\phi)\right) d\phi \tag{3.240}$$

in which we have written $e \equiv \frac{P}{EA}$ for notational simplicity.

Now we expand the integrand. When we do this, we only need to take terms into account up to order c^2, since we have already used Taylor expansion up to this order. Hence the resulting relation up to this order becomes:

$$L_0 \tag{3.241}$$

$$\approx 2\sqrt{\frac{EI}{P}} \frac{1}{\sqrt{1-e+ec^2}} \int_0^{\pi/2} \left(1 + \frac{1}{2}c^2 \sin^2(\phi) - \frac{1}{2}\frac{ec^2}{1-e+ec^2} \sin^2(\phi)\right) d\phi \tag{3.242}$$

$$= 2\sqrt{\frac{EI}{P}} \frac{1}{\sqrt{1-\frac{P}{EA}+\frac{P}{EA}c^2}} \frac{\pi}{2} \left(1 + \frac{1}{4}c^2 - \frac{1}{4}\frac{\frac{P}{EA}c^2}{1-\frac{P}{EA}+\frac{P}{EA}c^2}\right) \tag{3.243}$$

in which we have written $e \equiv \frac{P}{EA}$ for notational simplicity.

This relation is however not clear and it is vague to which order of c this expression is correct. To solve this problem, we need to make yet two other Taylor approximations. Since we are only interested in the behaviour directly after buckling, we have a small incoming angle α and hence a small c, as we have stated before. Hence we can make the following Taylor expansions (for when c is small).

$$\frac{1}{\sqrt{1-\frac{P}{EA}+\frac{P}{EA}c^2}} \approx \frac{1}{\sqrt{1-\frac{P}{EA}}} \left(1 - \frac{1}{2}\frac{\frac{P}{EA}}{1-\frac{P}{EA}}c^2\right) + \mathcal{O}(c^4) \tag{3.244}$$

and

$$\frac{1}{1-\frac{P}{EA}+\frac{P}{EA}c^2} \approx \frac{1}{1-\frac{P}{EA}} \left(1 - \frac{\frac{P}{EA}}{1-\frac{P}{EA}}c^2\right) + \mathcal{O}(c^4) \tag{3.245}$$

Substituting these approximation into equation (3.241) yields an expression that is correct up to the order of c^4. It has however terms that are of order c^4, so we must forget about these terms. Hence we acquire the relation between the

force P and c:

$$L_0 \tag{3.246}$$

$$\approx \sqrt{\frac{EI}{P}} \frac{1}{\sqrt{1-e}} \left(1 - \frac{1}{2}\frac{e}{1-e}c^2\right) \pi \left(1 + \frac{1}{4}c^2 - \frac{1}{4}c^2 \frac{e}{1-e}\left(1 - \frac{e}{1-e}c^2\right)\right) + \mathcal{O}(c^4) \tag{3.247}$$

$$= \sqrt{\frac{\pi^2 EI}{P}} \frac{1}{\sqrt{1-\frac{P}{EA}}} \left(1 + \frac{1}{4}c^2 - \frac{1}{4}\frac{\frac{P}{EA}}{1-\frac{P}{EA}}c^2 - \frac{1}{2}\frac{\frac{P}{EA}}{1-\frac{P}{EA}}c^2\right) \tag{3.248}$$

$$= \sqrt{\frac{EI\pi^2}{P}} \frac{1}{\sqrt{1-\frac{P}{EA}}} \left(1 + \frac{1}{4}c^2 - \frac{3}{4}\frac{\frac{P}{EA}}{1-\frac{P}{EA}}\right) + \mathcal{O}(c^4) \tag{3.249}$$

in which we have written $e \equiv \frac{P}{EA}$ for notational simplicity.

But this expression is still not the desired relation between the force P and the incoming angle α. To acquire this relation we need to use yet another Taylor expansion. This time we use the Taylor approximation $c = \sin(\alpha/2) \approx \alpha/2$. Moreover, we rearrange some terms and use the Euler load $P_e = EI\frac{\pi^2}{L_0^2}$. Hence we obtain

$$\sqrt{\frac{P}{P_e}} \approx \frac{1}{\sqrt{1-e}} \left(1 + \frac{1}{16}\alpha^2 - \frac{3}{16}\frac{e}{1-e}\alpha^2\right) + \mathcal{O}(\alpha^4) \tag{3.250}$$

In which we have written $e \equiv \frac{P}{EA}$ for notational simplicity.

Then we square this expression. Thus we find up to order α^4:

$$\frac{P}{P_e} \approx \frac{1}{1-e} \left(1 + \frac{1}{8}\alpha^2 - \frac{3}{8}\frac{e}{1-e}\alpha^2\right) + \mathcal{O}(\alpha^4) \tag{3.251}$$

This relation is similar to the relation for the inextensible beam that we found in section 3.2.4 (see equation (3.134)). More precisely this equation reduces to the inextensible one, when $e = \frac{P}{EA} \to 0$, which is a good measure for how inextensible a beam is, as we have seen in section 3.4.2. So the extensible beam model doesn't change that much to the force angle relation for a pinned-pinned beam.

Moreover it is not a problem that we divide by zero when $e = 1$, since e will never be 1. If $e = 1$, this means that $P = EA$. But this can only arise when the beam is completely compressed, which cannot ever happen.

There is however another interesting thing to equation (3.251). When the beam still must buckle, we have $\alpha = 0$. The equation then reduces to

$$\frac{P}{P_e} \approx \frac{1}{1-e} \tag{3.252}$$

Now, when the beam is extensible (i.e. $e \neq 0$) we have that $P = P_c$ is not a solution anymore. In other words, when the beam is extensible the euler load P_e isn't the critical load at which the beam starts to buckle. The critical load is

the load P which satisfies this equation. This is in correspondance with other studies of the extensible beam model (see for instance Magnusson et al. [2001]). We will denote this critical load as P_c.

A relation between the angle α and the strain

We have found a relation between the starting angle α and the force P. However, it is more convenient to have a force strain relation. In order to find this relation, we need an expression that relates the starting angle α and the strain ΔL as we did in the inextensible case in section 3.2.4.

In this extensible beam model, we have a good measure for how much a certain point of the beam has changed. This is measured with $u(\hat{x})$, with $\hat{x}$ the coordinate along the initial beam. This $u(\hat{x})$ measures how much a point is displaced to the right. Hence we have for the strain

$$\Delta L = -(u(L_0) - u(0)) \tag{3.253}$$

We then use the fundamental theorem of calculus and obtain

$$\Delta L = -\int_0^{L_0} u_{\hat{x}} d\hat{x} \tag{3.254}$$

In equation (3.210) we have found an expression for $u_{\hat{x}}$ in terms of ε and θ and in equation (3.214) we found an expression for ε in terms of θ. We now combine these two equations and substitute them into (3.254). Hence we obtain

$$\Delta L = -\int_0^{L_0} ((\varepsilon + 1)\cos(\theta) - 1) d\hat{x} \tag{3.255}$$

$$= \int_0^{L_0} \left(1 - \cos(\theta) + \frac{P}{EA}\cos^2(\theta)\right) d\hat{x} \tag{3.256}$$

$$= L_0 - \int_0^{L_0} \cos(\theta) d\hat{x} + \frac{P}{EA}\int_0^{L_0} \cos^2(\theta) d\hat{x} \tag{3.257}$$

We now have an expression with θ as the main variable. However, the integral is over $d\hat{x}$. Luckily, we have found a relation between $d\hat{x}$ and $d\theta$ in equation (3.228). We substitute this relation in equation (3.257) to find

$$\Delta L = L_0 - \int_{-\alpha}^{\alpha} \sqrt{\frac{EI}{4P}} \frac{\cos(\theta) - e\cos^2(\theta)}{\sqrt{(1-e)(c^2 - \sin^2(\theta/2)) + e(c^4 - \sin^4(\theta/2))}}\, d\theta \tag{3.258}$$

in which we have used $e \equiv \frac{P}{EA}$ and $c \equiv \sin(\alpha/2)$ for notational simplicity.

We need to rewrite this equation. Our first step in this is with the trigonometric

identity $\cos(\lambda) = 1 - 2\sin^2(\lambda/2)$. Hence we obtain

$$\frac{\Delta L}{L_0} = 1 - \frac{1}{L_0}\sqrt{\frac{EI}{4P}}\int_{-\alpha}^{\alpha} \frac{(1 - 2\sin^2(\theta/2)) - e(1 - 4\sin^2(\theta/2) + 4\sin^4(\theta/2))}{\sqrt{(1-e)(c^2 - \sin^2(\theta/2)) + e(c^4 - \sin^4(\theta/2))}} \tag{3.259}$$

$$= 1 - \frac{1}{L_0}\sqrt{\frac{EI}{4P}}\int_{-\alpha}^{\alpha} \frac{(1-e) + 2(2e-1)\sin^2(\theta/2) - 4e\sin^4(\theta/2)}{\sqrt{(1-e)(c^2 - \sin^2(\theta/2)) + e(c^4 - \sin^4(\theta/2))}} \tag{3.260}$$

This integral is as horrible as the one we found in the force angle relation. Hence we need to apply the same change of variables as we did before. That is, we use the change of variables of equations (3.230) and (3.231). Hence we obtain:

$$\frac{\Delta L}{L_0} = 1 - \frac{1}{L_0}\sqrt{\frac{EI}{P}}\int_{-\pi/2}^{\pi/2} \frac{(1-e) + 2(2e-1)c^2\sin^2(\phi) - 4ec^4\sin^4(\phi)}{\sqrt{(1-e) + ec^2(1+\sin^2(\phi))}\sqrt{1 - c^2\sin^2(\phi)}}\, d\phi \tag{3.261}$$

This is however still not an integral that we can evaluate directly. The most integral information of this integral is the behaviour of the relation just after buckling. Since the incoming angle α is very small just after buckling, so must be $c = \sin(\alpha/2)$. Hence we can use Taylor approximations to find an integral that we can actually calculate. To do this, we use the following Taylor expansions:

$$\frac{1}{\sqrt{(1-e) + ec^2(1+\sin^2(\phi))}} \approx \frac{1}{\sqrt{1-e}}\left(1 - \frac{1}{2}\frac{e}{1-e}c^2(1+\sin^2(\phi))\right) + \mathcal{O}(c^4) \tag{3.262}$$

$$\frac{1}{\sqrt{1 - c^2\sin^2(\phi)}} \approx 1 + \frac{1}{2}c^2\sin^2(\phi) \tag{3.263}$$

Hence the integrand of the integral of equation (3.261) will look like

$$\frac{1}{\sqrt{1-e}}\big((1-e) + 2(2e-1)c^2\sin^2(\phi) - 4ec^4\sin^4(\phi)\big)\cdot \left(1 + \frac{1}{2}c^2\sin^2(\phi)\right)\left(1 - \frac{1}{2}\frac{e}{1-e}c^2(1+\sin^2(\phi))\right) + \mathcal{O}(c^4) \tag{3.264}$$

When we expand this expression we find not only terms of order c^0 and c^2, but also of order c^4. We have however used Taylor approximation up to order c^3. Hence the terms of order c^4 are irrelevant, since this expression is not true for these orders. Hence we can forget about them. Thus we obtain for the integrand of equation (3.261)

$$\frac{1}{\sqrt{1-e}}\left((1 - e - \frac{e}{2}c^2) + (3e - \frac{3}{2})c^2\sin^2(\phi)\right) + \mathcal{O}(c^4) \tag{3.265}$$

Hence by substituting this expression into equation (3.261) we acquire an approximation for the integral. It is possible to calculate this integral. Hence we obtain

$$\frac{\Delta L}{L_0} \tag{3.266}$$

$$= 1 - \frac{1}{L_0}\sqrt{\frac{EI}{P}}\frac{1}{\sqrt{1-e}}\int_{-\pi/2}^{\pi/2}\left((1-e-\frac{e}{2}c^2) + (3e-\frac{3}{2})c^2\sin^2(\phi)\right)d\phi + \mathcal{O}(c^4) \tag{3.267}$$

$$= 1 - \frac{1}{L_0}\sqrt{\frac{EI}{P}}\frac{\pi}{\sqrt{1-e}}\left(1-e-\frac{1}{2}ec^2+\frac{3}{2}ec^2-\frac{3}{4}c^2\right) + \mathcal{O}(c^4) \tag{3.268}$$

$$= 1 - \sqrt{\frac{EI\pi^2}{PL_0^2}}\frac{1}{\sqrt{1-e}}\left((1-e)+(e-\frac{3}{4})c^2\right) + \mathcal{O}(c^4) \tag{3.269}$$

$$= 1 - \sqrt{\frac{P_e}{P}}\frac{1}{\sqrt{1-e}}\left((1-e)+(e-\frac{3}{4})c^2\right) + \mathcal{O}(c^4) \tag{3.270}$$

in which we have used the critical Euler load $P_e = EI\frac{\pi^2}{L_0^2}$.

There is a problem with the current form of this expression. We must get rid of the term $\sqrt{\frac{P_c}{P}}$. Luckily we have found a relation between this terms and the c in equation (3.250). When we take the inverse of this we have

$$\sqrt{\frac{P_c}{P}} = \sqrt{1-e}\left(1+\frac{1}{4}c^2-\frac{3}{4}\frac{e}{1-e}c^2\right)^{-1} \tag{3.271}$$

Hence by substituting this expression in equation (3.270) we obtain

$$\frac{\Delta L}{L_0} = 1 - \left((1-e)+(e-\frac{3}{4})c^2\right)\left(1+\frac{1}{4}c^2-\frac{3}{4}\frac{e}{1-e}c^2\right)^{-1} + \mathcal{O}(c^4) \tag{3.272}$$

Now we make yet another Taylor approximation around $c = 0$. Then we find the relation up to order c^2. We find

$$\frac{\Delta L}{L_0} \approx 1 - \left((1-e)+(e-\frac{3}{4})c^2\right)\left(1-\frac{1}{4}c^2+\frac{3}{4}\frac{e}{1-e}c^2\right) + \mathcal{O}(c^4) \tag{3.273}$$

$$= 1 - \left((1-e)+(e-\frac{3}{4})c^2 - \frac{1-e}{4}c^2 + \frac{3}{4}ec^2\right) + \mathcal{O}(c^4) \tag{3.274}$$

$$= e - 2ec^2 + c^2 \tag{3.275}$$

The last step we now take is another Taylor expansion. Since we are interested in the behaviour of the beam just after buckling, we have already assumed that α is small. Hence we can approximate $c = \sin(\alpha/2)$ with $c \approx \frac{\alpha}{2}$. Hence we obtain the relation between the strain and the starting angle α:

$$\frac{\Delta L}{L_0} = e - \frac{1}{2}e\alpha^2 + \frac{1}{4}\alpha^2 + \mathcal{O}(c^4) \tag{3.276}$$

This relation reduces to the inextensible case (see equation (3.143)) when $\varepsilon \to 0$ (i.e. when EA becomes very large), as we would like.

Moreover the expression makes sense, since the beam is now extensible. Hence when the beam is not buckled (i.e. when $\alpha = 0$) the beam can have a non-zero strain. This can be seen in the expression since there is now a e terms which does not depend on the incoming angle α at all. More precisely when $\alpha = 0$, we have

$$\frac{\Delta L}{L_0} = e = \frac{P}{EA} \tag{3.277}$$

Or equivalently,

$$P = EA\frac{\Delta L}{L_0} \tag{3.278}$$

which is in agreement with equation (3.153) for the pre buckled state of the elastic beams.

Force strain curve

Now that we have found both a relation between the force P and the angle α (equation (3.251)) and a relation between the incoming angle α and the strain $\frac{\Delta L}{L_0}$ (equation (3.276)), it is possible to derive the force strain curve for an extensible pinned-pinned beam by combining these two expressions.

First, we rewrite equation (3.276) and find α in terms of the strain. Hence we obtain:

$$\alpha^2 = 4\frac{\frac{\Delta L}{L_0} - e}{1 - 2e} \tag{3.279}$$

We then substitute this expression in equation (3.251). Hence we acquire

$$\frac{P}{P_e} = \frac{1}{(1-e)^2}\left((1-e) + \frac{1}{8}(1-4e)\alpha^2\right) \tag{3.280}$$

$$= \frac{1}{(1-e)^2}\left((1-e) + \frac{1}{2}(1-4e)\frac{\frac{\Delta L}{L_0} - e}{1-2e}\right) \tag{3.281}$$

$$= \frac{1}{(1-e)^2(1-2e)}\left((1 - \frac{7}{2}e + 4e^2) + (\frac{1}{2} - 2e)\frac{\Delta L}{L_0}\right) \tag{3.282}$$

As before, this expression reduces to the inextensible force strain relation (see equation (3.144)), when $e \to 0$. Moreover, when the beam is not yet buckled, we have $\frac{\Delta L}{L_0} = \frac{P}{EA} = e$. Hence then this equation reduces to

$$\frac{P}{P_e} = \frac{1}{1-e} \tag{3.283}$$

from which we can determine the critical load P_c by solving it for P as stated before.

The relation is however not very clear in its current form. For one thing it relates the current load P to the Euler load P_e, while it is more convenient to relate this to the critical load P_c, since this load can be determined from experiments by inspecting the acquired force strain curve. Moreover it is better to measure the strain only from the moment that the beam buckled. To acquire this, we use the following substitutions:

$$\frac{\Delta L}{L_0} = \delta + u \tag{3.284}$$

$$e = \delta + \Delta e \tag{3.285}$$

in which we have

$$\delta = \frac{P_c}{EA} \tag{3.286}$$

and

$$\Delta e = e - \delta \tag{3.287}$$

Since the beam is not buckled until the critical load is exceeded, δ is the strain at which the beam will begin to buckle. Hence u measures the extra strain, beyond the critical strain δ. We now substitute these in equation (3.282). Moreover, we observe that $\frac{P}{P_e} = \frac{\frac{P}{EA}}{\frac{P_e}{EA}} = \frac{e}{\hat{e}}$ (in which $\hat{e} \equiv \frac{P_e}{EA}$). Hence we obtain for the force strain relation:

$$\frac{\delta}{\hat{e}} + \frac{\Delta e}{\hat{e}} = \frac{(1-\delta)(1-2\delta) + \Delta e \frac{12\delta - 7}{2} + 4(\Delta e)^2 + \frac{1-4\delta-4\Delta e}{2} u}{(1-\delta)^2(1-2\delta)(1-\frac{1}{1-\delta}\Delta e)^2(1-\frac{2}{1-2\delta}\Delta e)} \tag{3.288}$$

Since P_c is the solution for $= \frac{\delta}{\hat{x}} = \frac{P_c}{P_E} = \frac{1}{1-\frac{P_c}{EA}} = \frac{1}{1-\delta}$, we now replace one of the $\frac{1}{1-\delta}$ terms by $\frac{\delta}{\hat{e}}$. Hence we obtain:

$$\frac{\delta}{\hat{e}} + \frac{\Delta e}{\hat{e}} = \frac{\delta}{\hat{e}} \frac{1}{(1-\frac{\Delta e}{1-\delta})^2(1-\frac{2\Delta e}{1-2\delta})} \left(1 + \frac{\Delta e \frac{12\delta-7}{2} + 4(\Delta e)^2 + \frac{1-4\delta-4\Delta e}{2} u}{(1-\delta)(1-2\delta)}\right) \tag{3.289}$$

Since we are most interested in the behaviour of the beam just after buckling, we know that the load P will be close to P_c. This means that Δe will be small. Hence we can find an approximation up to order (Δe) via Taylor expansion. We now use the following Taylor approximations:

$$\left(\frac{1}{1-\frac{\Delta e}{1-\delta}}\right)^2 \approx 1 + \frac{2}{1-\delta}\Delta e + \mathcal{O}((\Delta e)^2) \tag{3.290}$$

$$\frac{1}{1-\frac{2\Delta e}{1-2\delta}} \approx 1 + \frac{2}{1-2\delta}\Delta e + \mathcal{O}((\Delta e)^2) \tag{3.291}$$

With these Taylor approximations the expression in equation (3.289) can now also be approximated up to this order. Hence we find

$$\delta + \Delta e \tag{3.292}$$

$$= \left(\delta + 2\Delta e \frac{2\delta - 3\delta^2}{(1-\delta)(1-2\delta)}\right)\left(1 + \frac{\frac{\Delta e}{2}(12\delta - 7) + \frac{u}{2}(1 - 4\delta - 4\Delta e)}{(1-\delta)(1-2\delta)}\right) + \mathcal{O}((\Delta e)^2) \tag{3.293}$$

$$= \delta\left(1 + \frac{1-4\delta}{2(1-\delta)(1-2\delta)}u + \Delta e\left(\frac{12\delta - 7}{2(1-\delta)(1-2\delta)} + \frac{8 - 12\delta}{2(1-\delta)(1-2\delta)} + \frac{(4-6\delta)(1-4\delta) - 4}{2(1-\delta)^2(1-2\delta)^2}u\right)\right) + \mathcal{O}((\Delta e)^2) \tag{3.294}$$

And hence

$$\Delta e \tag{3.295}$$

$$= \frac{\delta}{2(1-\delta)(1-2\delta)}\left((1-4\delta)u + \Delta e\left(1 + 2\delta\frac{12\delta - 11}{(1-\delta)(1-2\delta)}u\right)\right) + \mathcal{O}((\Delta e)^2) \tag{3.296}$$

By rearranging these terms we end up with:

$$\Delta e = \tag{3.297}$$

$$\big(2(1-\delta)^2(1-2\delta)^2 - \delta(1-\delta)(1-2\delta) + 2\delta(11-12\delta)\big) = \delta(1-4\delta)u + \mathcal{O}((\Delta e)^2) \tag{3.298}$$

Hence we obtain for Δe:

$$\Delta e = \frac{\delta(1-4\delta)}{(2(1-\delta)^2(1-2\delta)^2 - \delta(1-\delta)(1-2\delta) + 2\delta(11-12\delta))u}u + \mathcal{O}((\Delta e)^2) \tag{3.299}$$

Since $\Delta e = e - \delta$, we now acquire the desired force strain relation after rearranging the terms. We find

$$P = P_c + \frac{P_c(1-4\delta)}{2(1-\delta)^2(1-2\delta)^2 - \delta(1-\delta)(1-2\delta) + 2\delta(11-12\delta)u}u + \mathcal{O}((\Delta e)^2) \tag{3.300}$$

Once again, we are most interested in the behaviour just after buckling. By definition we now that $u \approx 0$ when the beam has just buckled, since $u = 0$ at the moment the beam start to buckle. Hence we make a Taylor expansion around u and find:

$$P = P_c + \frac{P_c(1-4\delta)}{(2(1-\delta)^2(1-2\delta)^2 - \delta(1-\delta)(1-2\delta))}u \tag{3.301}$$

When the beams are inextensible we are in the limit when $\delta \to 0$. Then this equation reduces to the inextensible expression in equation (3.144) as should be. But we could also inspect the case when a beam *is* extensible, but not that much. That means that $\delta \approx 0$. Hence we must take only those terms into

account that are constant or linear in δ. Moreover, we can neglect terms that are bilinear in δ and u, since these are both small and their product is hence very small. Thus we end up with an approximate relation when a beam is a little extensible:

$$P = P_c + \frac{P_c}{2 - 13\delta} u \tag{3.302}$$

This relation is *not* in correspondence with the relation in Bazant and Cendolin [2009]. The minus sign in this term however can explain why some beams have a negative after-buckling slope.

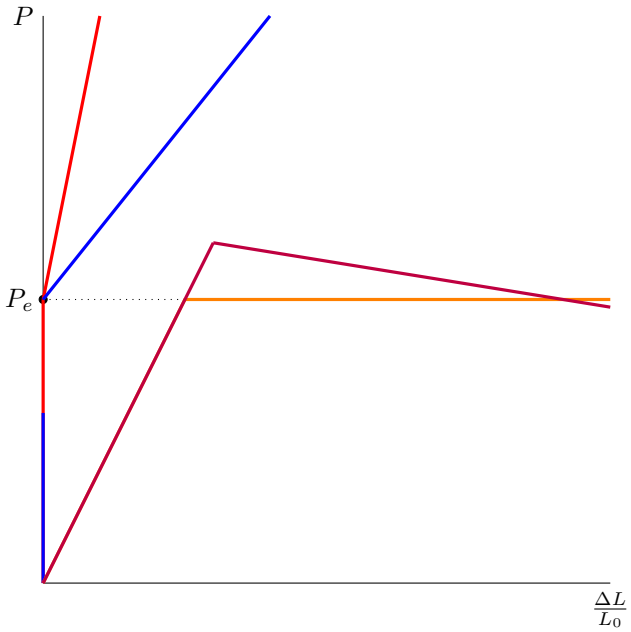

Figure 3.31 – The force strain relationship before and after buckling for inextensible beam models (red and blue), for the extensible beam model with small deflections (orange) and for beams that are a little extensible (purple).

Chapter 4

Simulations on Elastic Sheets

In the last chapter, chapter 3, we derived various mathematical models for elastic beams that are axially loaded with a force P. With these models at hand we also studied some possible configurations of the beam such as a pinned-pinned beam (see sections 3.1.4, 3.2.4, 3.3.3 and 3.4.3) and a beam on a node (see sections 3.1.6 and 3.3.4). In these sections we studied these configurations analytically. However, in this chapter we will stop doing everything analytically and we will study the more complex configurations of the beam with numerical simulations.

We start this chapter with some general remarks about the model used for the simulations. We explain what kind of beam model is used and why. Moreover we investigate the assumptions that we make and discuss whether or not these assumptions are realistic.

Our goal in this chapter is to find a good model for the elastic patterned sheets. We want to understand the behaviour of these elastic network with this model (see chapter 1). We will come to these simulations in section 4.3. Before we go to these elastic sheets however, we will first investigate a more simple configuration. In section 4.2 we will study a beam on a node by means of simulation.

4.1 Assumption in the simulations

In chapter 1 we saw that the elastic patterned sheets have interesting properties. For instance the force-strain curves of these networks have a peak which is yet not understood (see figure 4.1). We also introduced a way to model these elastic sheets with 'nodes' connecting the 'beams' between them (see chapter 1 and figure 4.2). In this chapter we will use numerical simulation of this model to study the behaviour of the elastic networks. We will mainly focus on the force strain relations, but we will also present some other relations.

Since the elastic networks are manufactured by molding, the nodes and beams are attached at a particular, fixed manner. This attachment of the beams to

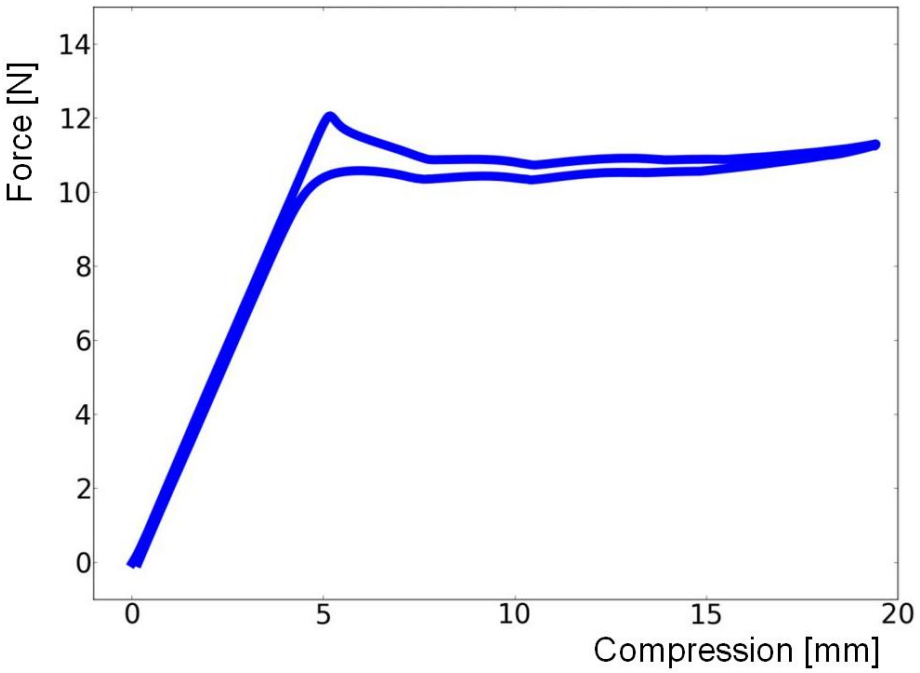

Figure 4.1 – Experimantally measured force strain curve for a monoholar elastic patterned sheet. The upper curve is the force strain curve when the network is compressed, while the lower one is the curve when the beam is stretched back to its original state (after the compressing). The most interesting part of this curve is the peak at about 5 mm compression. This peak suggests that we need less force to compress the beam further, which is an unusual property of the elastic networks.

the nodes cannot change during an experiment. Hence we must make sure that this cannot change in the simulations as well. We thus assume that the beams are always attached to the nodes such that it is attached perpendicular to the circles surface (see figure 4.3).

In the numerical model we assume that the beams (blue in figure 4.2) are elastic rods which can be described by a beam model of chapter 3. However, the nodes cannot be modified in the simulation. That is, they can rotate and move, but they maintain their shape. Hence the nodes don't compress or extend when we load them. Since the nodes are generally thicker than the beams this seems a fair assumption. But when we carefully inspect an experiment with the elastic sheets, we see that the nodes are in fact deforming a little during compression.

The beam model that is used for the 'beams' in the networks is an extensible beam model for small deflections (see section 3.3). As we stated before in section 3.1 this is not a very realistic model, since the deflections of the beams aren't really small. This model however is easier to implement in a numeric simulation than the models that allow large deflections of the beam. Moreover it can also give us a qualitative idea of what is going on in the elastic networks.

The beam model is however not the general one that we derived in section 3.3,

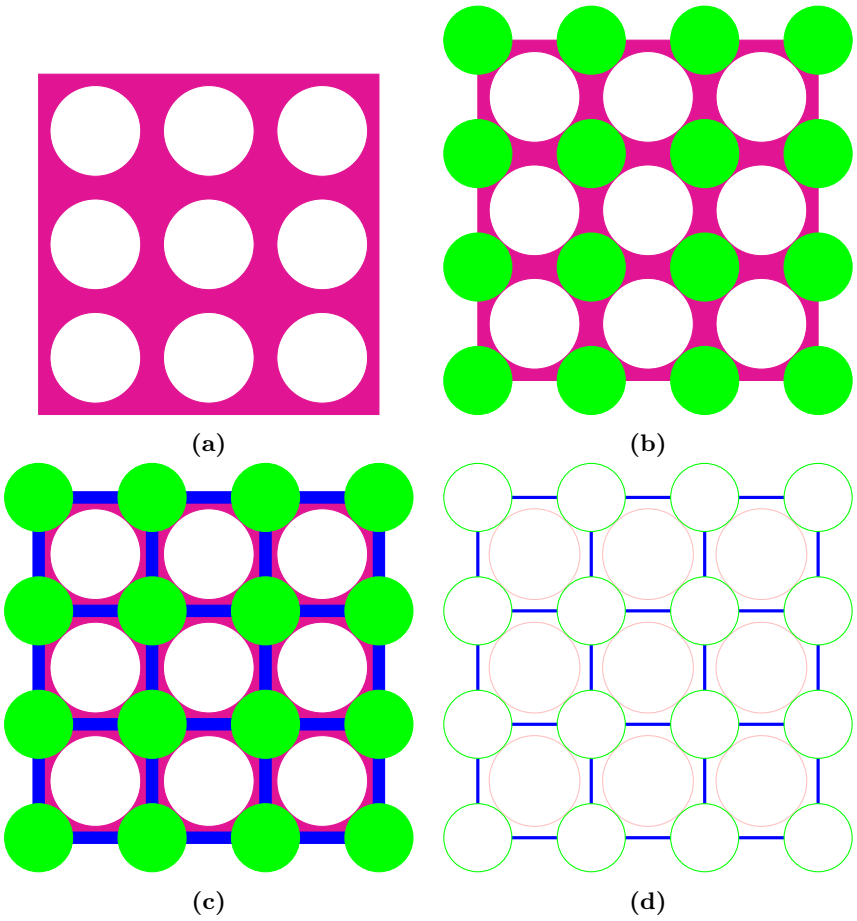

Figure 4.2 – Illustration of the model of a elastic patterned sheet (pink) as combination of nodes (green) and beams (blue). In figure (a) a piece of the elastic patterned sheet is shown. The white circles are the holes in the network. In figure (b) the nodes (green) are drawn. These are placed at the places that connect the beams. Then in figure (c) also the beams (blue) are shown. These are placed on the elastic sheet pink such that they connect the nodes. In figure (d) the resulting model is shown. In this last picture the elastic sheet in pink is erased. The original holes in the elastic patterned sheets are drawn as a reminder of the original elastic patterned sheet. In the simulations these circles are not shown anymore.

but it has some small modifications. In particular all the beams must satisfy the normal differential equation for beams,

$$EIw_{xxxx} + Pw_{xx} = 0 \tag{4.1}$$

Since the simulations we do are strain controlled (in contrary to force/load controlled), the force P is unknown and must be calculated trough the configuration of the beam. That is, we calculate P via (see equation (3.153))

$$P \approx N = -EA\frac{\Delta\ell}{L_0} \tag{4.2}$$

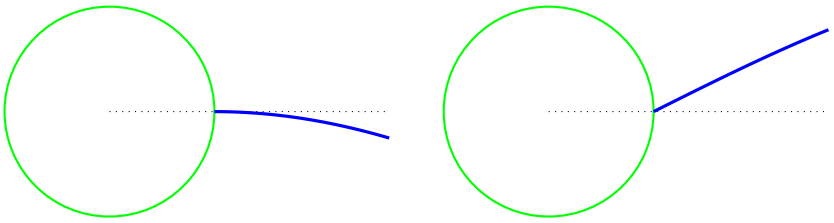

(a) Sketch of a right attachment **(b)** sketch of a wrong attachment

Figure 4.3 – Sketch of possible attachments of the beams (blue) to the nodes (green). In figure (a) a right attachment is shown, while in figure (b) a wrong attachment is sketched. In the simulation all attachments are required to be perpendicular to the surface of the circles as in figure (a)

in which $\Delta\ell = \ell - L_0$ is the change of (arc) length of the beam.

This expression is an approximation, since $P \approx N$ only when the deflections of the beam are small. However for a qualitative study of the simulation this is a good first approximation.

4.2 Simulations on a single beam

In this section we inspect a beam which is attached to two nodes (see figure 4.4). We already studied this configuration analytically in sections 3.1.6 and 3.3.4. This time we abandon the analytic approach and use simulations to study the behaviour of this beam set-up. Note that in the simulations the set up is turned 90 degrees. Thus the beam is now vertically aligned between the nodes, while it was horizontally aligned in the previous sections. Since this is merely a change of coordinates, this does not matter for the physics or mathematics of the problem.

In this sections we first discuss the numeric model for the simulations in depth in section 4.2.1. Then we inspect the result of various simulations with this model for the single beam in section 4.2.2.

4.2.1 Explanation of numeric simulation

The numerical simulation of the single beam between nodes (and also the elastic network) is done with the numerical computing environment MATLAB. The simulations in this section are done with either 'MATLAB R2012b' or 'MATLAB R2009b'. In this section we briefly discuss the schematics of the numerical scheme behind the simulations.

In short, the code first creates an initial configuration of beams and nodes. In this case this configuration is a beam which is attached to two nodes as in figure 4.4. After the initializing the program pushes the upper node down a certain, specified discrete distance. After that the simulation calculates the configuration of the beam and the remaining node a certain times, until the set-up is again in a equilibrium configuration (see figure 4.5 for a more in-depth

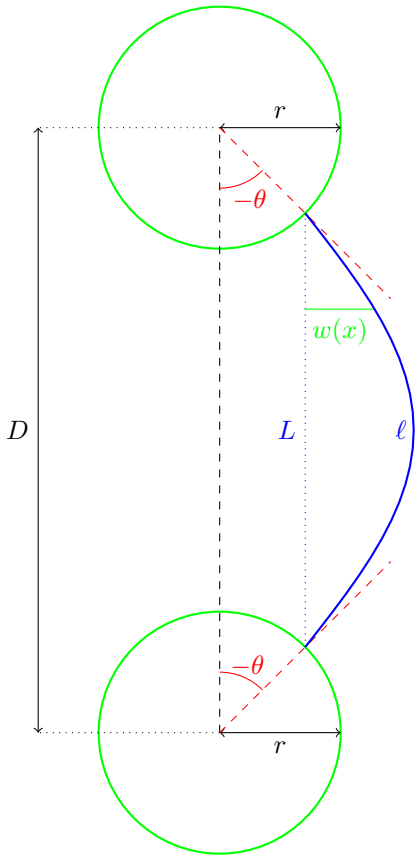

Figure 4.4 – Sketch of a buckled beam between two nodes in the simulation. Here D is the length between the centra of the nodes, L is the distance between the left and right attachment positions of the beam, ℓ is the real lenght of the beam, r is the radius of the node, θ is the incoming (and outgoing) angle of the beam and $w(x)$ is the deflection of the beam at a certain point x on the beam. Note that this is the same configuration as in figure 3.15 but rotated 90 degrees.

explanation of this updating scheme). We then repeat this process a few times, while monitoring systems configuration at each time step. Optionally, after the compression the beam can be stretched again to its original configuration.

To avoid that the beam stays in its unstable trivial equilibirium with a straight beam, we have build in a check on the load P. If this load becomes more than the critical Euler load P_e for the current beam, then the beam must buckle. To ensure this, we apply a (small) disturbance to the system. We turn the nodes over a large angle and let the system find its way to the equilibrium configuration from this new disturbed state.

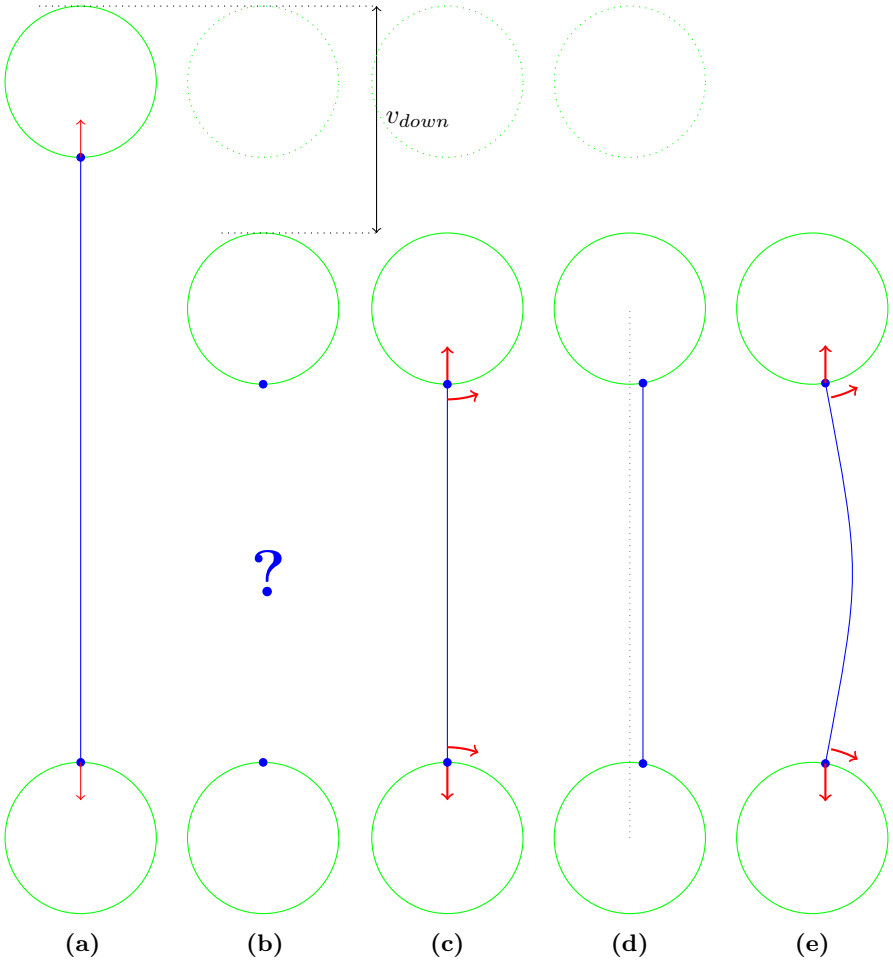

Figure 4.5 – A schematic illustration of the updating scheme used in the simulations with the nodes in green, the beam in blue, the attachment points of the beam as blue circles and the forces and torques in red. The first figure (a) describes the original position of the system at a certain time t. In this position the forces and the torques on the node are in balance. To obtain the new configuration at a following time $t+dt$ (in which dt denotes the time step we choose for our simulations), first the upper node is pushed down a certain value v_{down}. This is illustrated in figure (b). At this moment in the simulation we don't know what the shape of the beam is. The following step is to actually find this shape. This is done with the differential equation for the beam, $EIw_{xxxx} + Pw_{xx} = 0$ (with the incoming angles as the boundary conditions). The force P in this equation is calculated from the previous shape of the beam (i.e. in figure (a)). The shape of the beam then determines what forces and torques are applied to the nodes as is illustrated in figure (c). We then use these forces and torques to calculate how much the nodes rotate. Hence the attachment points on the nodes change and the beam is attached at these (rotated) points (d). This is however not a realistic configuration, since the resulting torques on the nodes aren't zero (i.e. the system is not in equilibrium). Hence we need to redo the steps (b) through (d) a certain times to find the actual state of the system at this time $t+dt$. This new system is shown in (e). This becomes the new starting point for a following time step.

Finding the equilibrium

The most difficult part in the simulation is to find the real equilibrium configuration of the system. We want to avoid situations where the beam is attached to the beam in a non-realistic way (for an example see figure 4.5d). As we explained in figure 4.5 we need to redo the calculations on the beam and the nodes a certain times to find this real configuration.

To illustrate the need for this, we now look at a simulation that ignores this refining. That is, we do an experiment in which steps (b) trough (d) from figure 4.5 are done only once at each time step. In first half of the simulation we compress the system (i.e. push the upper node down) and after that we stretch the system until the upper node is at its initial position again. A few states of the system are shown in figure 4.6. The resulting force-strain curve is plotted in figure 4.7.

Those figures exhibition some strange behaviour of this simulation. Foremost we clearly see that the configuration at the end of the simulation is not the same as the initial state of the system (compare figures 4.6a and 4.6f). This is stressed by the force-strain curve which does not end in the origin, but a lot below it. Moreover the after-buckling curve doesn't look different from the pre-buckling curve if we ignore the translation. However this should be different according to the theory that we discussed in chapter 3.

This strange behaviour occurs in this simulation because we neglect to let the system find its (real) equilibrium state. Hence at each time step the torque on the nodes was not in balance. This is shown in figure 4.8. In the most ideal case the resulting torques are zero. They are clearly non-zero in this simulation.

In the simulations in the rest of this chapter thus need to make sure that the resulting torques are zero (or as close to it as possible). There are two ways to achieve this. We could either iterate the updating scheme a fixed times at each time step or we could iterate this updating scheme until the resulting torques are below a certain threshold. Both methods have their own benefits and flaws as we shall see in the next section.

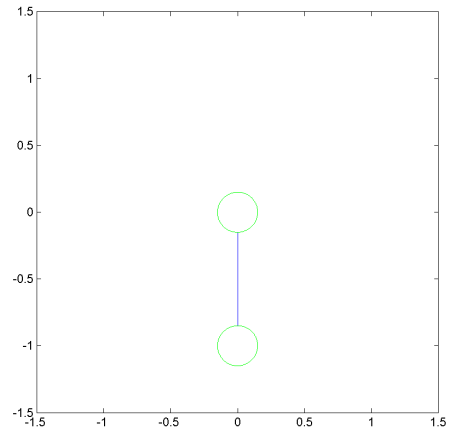

(a) timestep 50

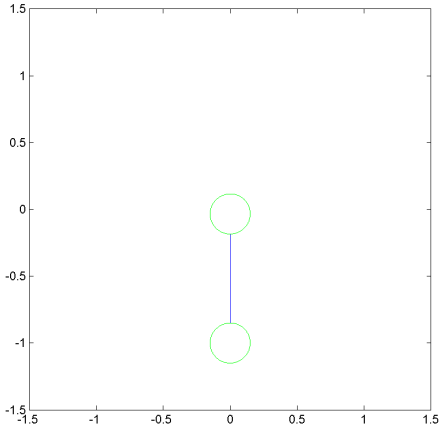

(b) timestep 2500

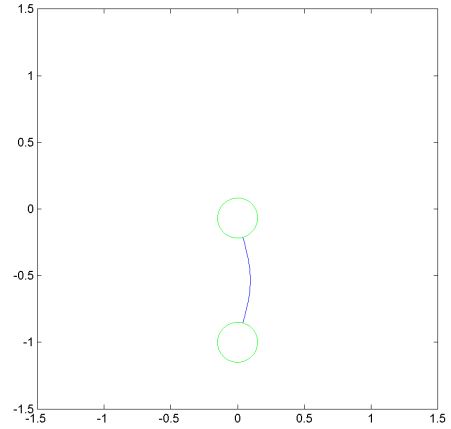

(c) timestep 5000

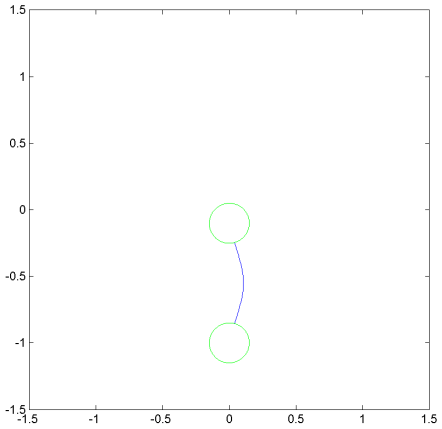

(d) timestep 7500

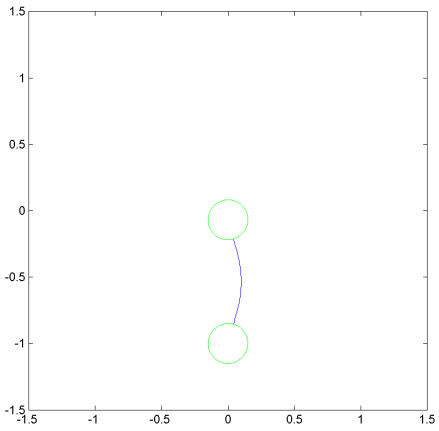

(e) timestep 10000

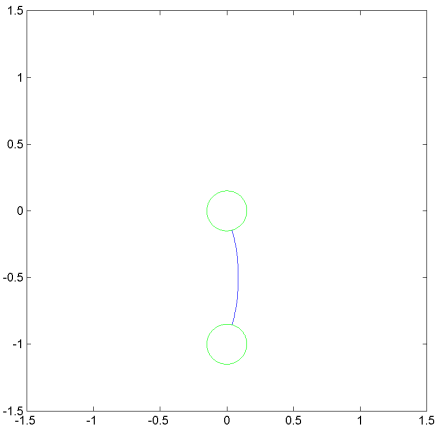

(f) timesetep 15000

Figure 4.6 – MATLAB figures of the configuration of the system at various increasing timesteps. The initial configuration is shown in (a), the configuration at the end of the simulation in (f). In this simulation we have used $E = 471000$, $h = 0.167$, $v_{down} = 1.5$, mass $= 1/32$ (of the nodes), rotational inertia $= 1$, transviscosity $= 150$, rotational viscosity $= 1$ and the radius of the nodes $= .15$.

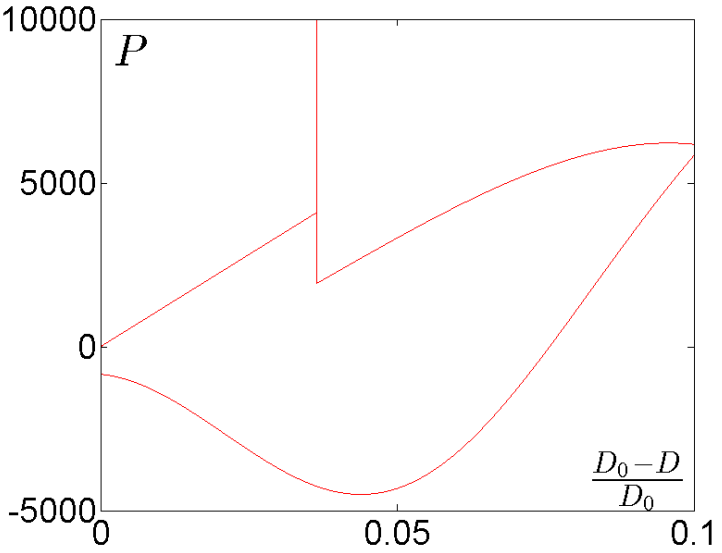

Figure 4.7 – Force versus strain plot made for a single beam when we update the beam and nodes only ones, made with MATLAB. The steep jump in this curve is the moment when the beam buckles (since we then rotate the nodes). The upper line is the curve when the system is compressed, the lower curve is when the beam is stretched. In this simulation we have used $E = 471000$, $h = 0.167$, $v_{down} = 1.5$, mass $= 1/32$ (of the nodes), rotational inertia $= 1$, transviscosity $= 150$, rotational viscosity $= 1$ and the radius of the nodes $= .15$.

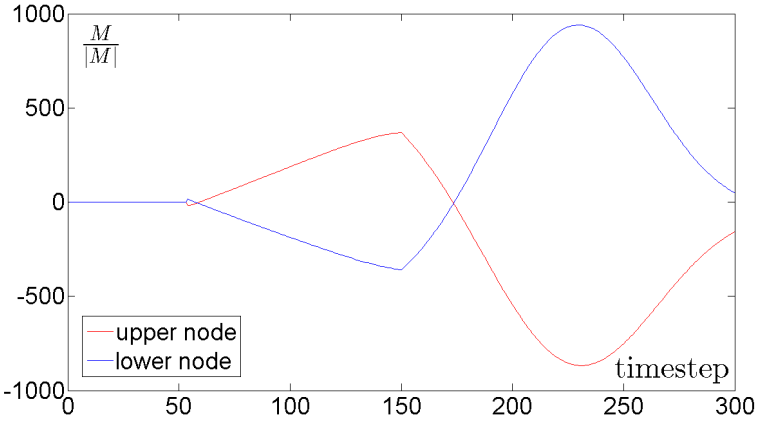

Figure 4.8 – The torques that are working on the nodes at each time step, made with MATLAB. In this figure we have plotted the resulting torques divided by the sum of the absolute values of the various contribution to the torque on the beam (see figure 3.16. From the moment the beam is buckled (around time step 50), the torques on the node are significantly different from zero. Hence from this figure we can conclude that the system is not in its equilibrium state.

4.2.2 Numeric study of a single beam

Since we saw in the previous section that the first, naive try with the simulation results in strange behaviour in the force strain curve, we need to be more careful with the force balance during the simulation. In this section we will first investigate two possible solution for this problem. First we try to run the calculations for the beams and the nodes a fixed amount of times at each time step. Then we try to incorporate a simple check that ensures that the resulting torques on the nodes are small. After we have tried these solution, we will use the simulation to study the behaviour of the beam between two circular, freely rotary nodes for different radii of the nodes.

More calculations per time step

In section 4.2.1 we found that a simple simulation with only one calculation of the configurations of the beams and the nodes won't yield us the equilibrium states of the system. We found that the underlying cause was the violation of the torque balance during the simulation (see figure 4.8).

The most simple approach to solve this problem is the following. Instead of calculation the configuration of the beams and the positions of the nodes just once at each time step, we could repeat these calculation a fixed amount of times. This gives the system time to 'find' its equilibrium position. To figure out how many calculation iterations are needed to get an acceptable torque balance we use the numerical simulation with various possible calculation steps at each time step. The acquired force strain curves are shown in figure 4.9. In figure 4.10 we also present the value of the resulting torques on the upper node.

As we see in figures 4.9 and 4.10 the more calculation iterations the simulation has, the better torque balances are acquired. However even at 1024 calculation iteration the resulting torques are still not neglectable small. It isn't realistic to use more calculations at each time step, since the simulation with 1024 calculations already needed about seven and a half hours to complete the simulation. We hence conclude that this method of optimization isn't the right one to choose.

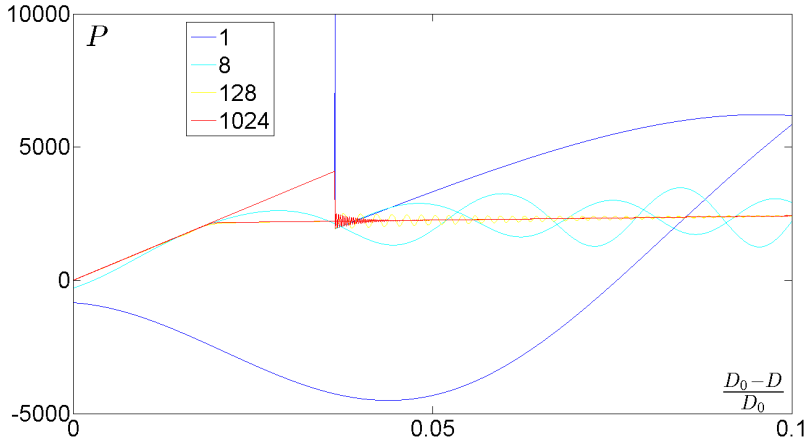

Figure 4.9 – Force strain curve of simulations of a single beam between two circular, freely rotary nodes for different calculation iterations at each time step. In this figure we see that the system is not in equilibrium for low calculation iteration values. Even when we do 1024 calculations for the beams and the nodes we still have a system that is not in equilibrium. In this simulation we have used $E = 471000$, $h = 0.167$, $v_{down} = 1.5$, mass $= 1/32$ (of the nodes), rotational inertia $= 1$, transviscosity $= 150$, rotational viscosity $= 1$ and the radius of the nodes $= .15$.

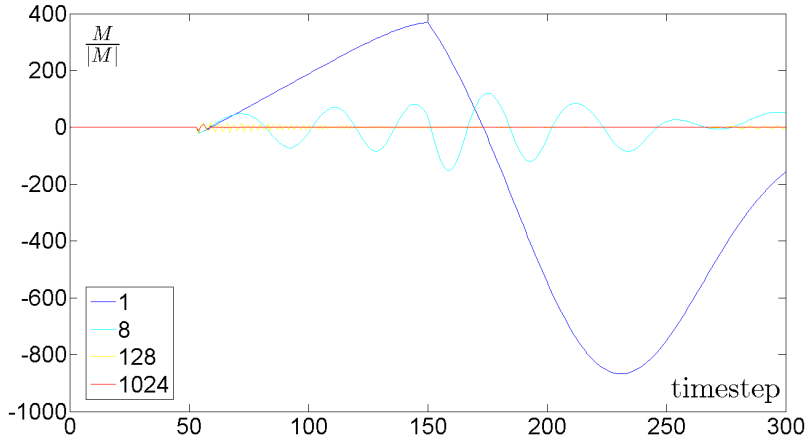

Figure 4.10 – The torques of the upper nodes during the simulation for simulation with different calculation iteration values for a simulation of a beam between two circular, freely rotary nodes. In this figure we clearly see that more calculations means a better simulation. However even at 1024 calculation iteration at each time step the torques on the nodes are still not in balance (see figure 4.11). In this simulation we have used $E = 471000$, $h = 0.167$, $v_{down} = 1.5$, mass $= 1/32$ (of the nodes), rotational inertia $= 1$, transviscosity $= 150$, rotational viscosity $= 1$ and the radius of the nodes $= .15$.

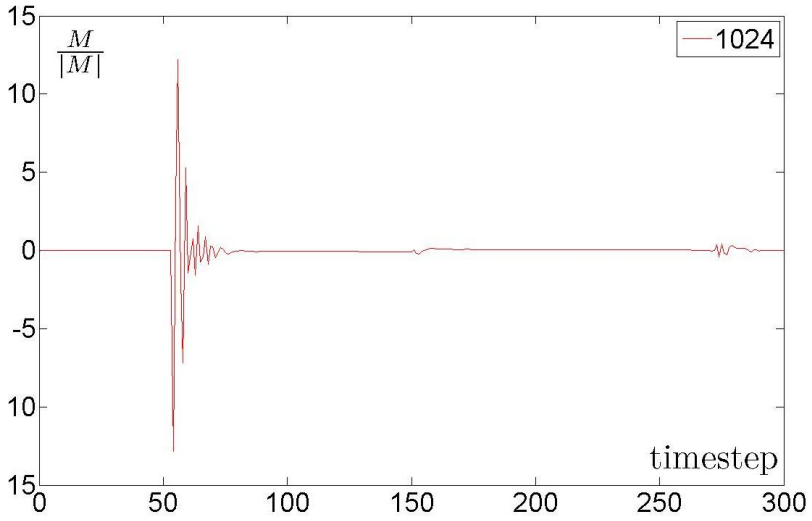

Figure 4.11 – The torques of the upper node during the simulation with 1024 calculations iterations at each time step. In this figure we see clearly that the torques on the upper node are not in balance. The torque is especially large around timestep 50, when the beam start to buckle.

Constraint on the torque balance

There is another method that we can use to ensure that the torques on the nodes are in balance. Instead of calculating the configuration of the beam and the rotation of the nodes a fixed amount of times at each time step, we now check after each calculation whether or not the torques on the node are in balance. To do this, we check the value of $\frac{\sum M}{\sum |M|}$ for each node. In this the sums are over all the torques that act on the node (see figure 3.16). If the system is in equilibrium, the torques on all nodes must be in balance. Hence the value $\frac{\sum M}{\sum |M|}$ must be zero.

So to ensure that the system is in its equilibrium position, we can check the value $\frac{\sum M}{\sum |M|}$. If the absolute value of this fraction is above a certain threshold (which we specify at the start of the simulation), we say that the system is not in equilibrium. When this is the case, we ask the simulation to recalculate the beams configuration and the rotation of the beams. This process of checking and recalculating is repeated until the torques are small enough. We have done this kind of simulation for different threshold values. The resulting force strain curves are shown in figure 4.12.

We see that the simulation isn't good, when the threshold is too high. So we need to choose a threshold that is low enough to find the real equilibrium states for the system. However, if we choose a threshold that is too low, the simulation takes too long. For instance the simulation with a threshold of 0.1 took about 40 minutes, while the simulation with a threshold value of 0.01 took approximately 80 minutes. Since the difference in the force strain curve isn't that great, we will keep using this threshold value in the simulations of the single beam.

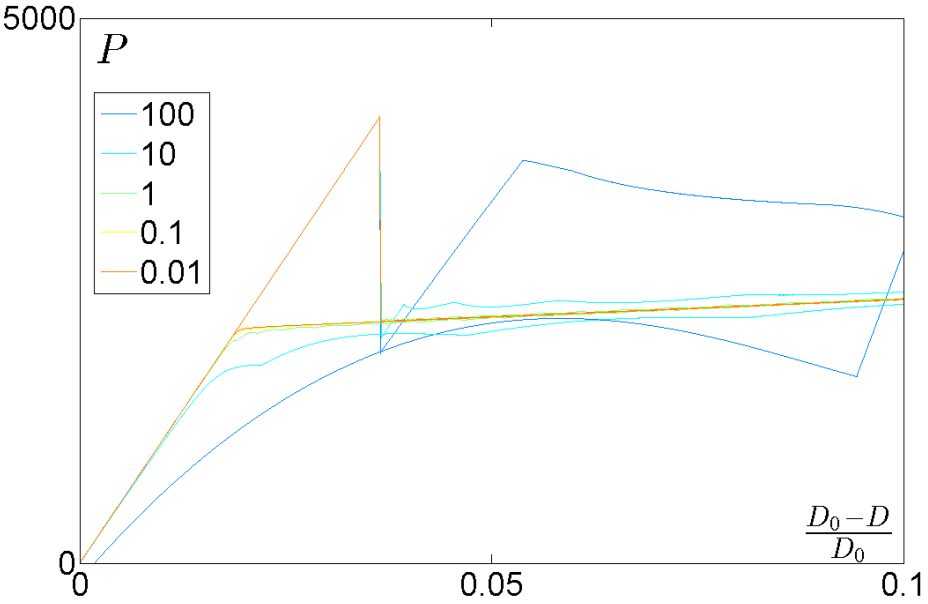

Figure 4.12 – Simulations of a single beam between two circular, freely rotary nodes for different calculation iterations at each time step. In this figure we clearly see that the checking for the torques is a good way to find the equilibrium states of the system. In this simulation we have used $E = 471000$, $h = 0.167$, $v_{down} = 1.5$, mass $= 1/32$ (of the nodes), rotational inertia $= 1$, transviscosity $= 150$, rotational viscosity $= 1$ and the radius of the nodes $= .15$.

Further, we conclude that it is far better to use this check of the torques on the nodes than it is to use a fixed amount of calculation iteration as we did before. This not only yields us more realistic simulations, but it is also a much faster way to simulate this system. There is however a draw-back of this method. It is possible that we need to do too much refining calculation before the torques are below the threshold. This can result in simulation that take too long and it is even possible that the threshold is never met, when the system is not damped well enough.

Different radii for the nodes

In the previous paragraphs we have concluded that the simulation works best when we check the resulting torques on each node at each time step. We will continue to use this procedure in the next simulations. In this paragraph we use the numerical simulation to investigate the behaviour of an elastic beam which is attached to two circular, freely rotary nodes of a certain radius r. We will vary this radius and let the beams become very small. In the limit when $r \to 0$ we expect to regain the normal pinned-pinned beam configuration and expect to see its behaviour (see section 3.1.6).

The resulting force strain curves of the simulation are shown in figure 4.13. We however don't see the standard bi-linear behaviour of a pinned-pinned beam

when the radius r is very small, since the force strain curve has a peak - even when the nodes have a very small radius of 0.001.

The curve for the relaxation does show us the desired bi-linear relation. This suggests that the peak is in fact not a real peak, but is a consequence of the numerical scheme we use. In the simulation the beam can be kept too long in the pre-buckled phase. When the beam is 'released' it immediately jumps to the right buckled state at the specific strain value. This would explain the jumps in all the graphs.

This is also endorsed by the relation between the strain and the amplitude of the beam (see figure 4.14). In this figure we see a jump at a certain strain value. However, when we do real experiments, these kind of jumps are not seen. Instead the amplitude then slowly increases when the beam is buckled. So we would inspect this amplitude strain relation to look more like the relaxation curve for it is looking.

Hence we need to conclude that the code used for the simulation has some flaws. It looks like the main problem lies in determine whenever a beam starts to buckle. The check that we have used for these simulation doesn't suffice.

In the current simulation we check whether or not the beam buckles with only the beams length. Maybe we need to treat the whole configuration (including

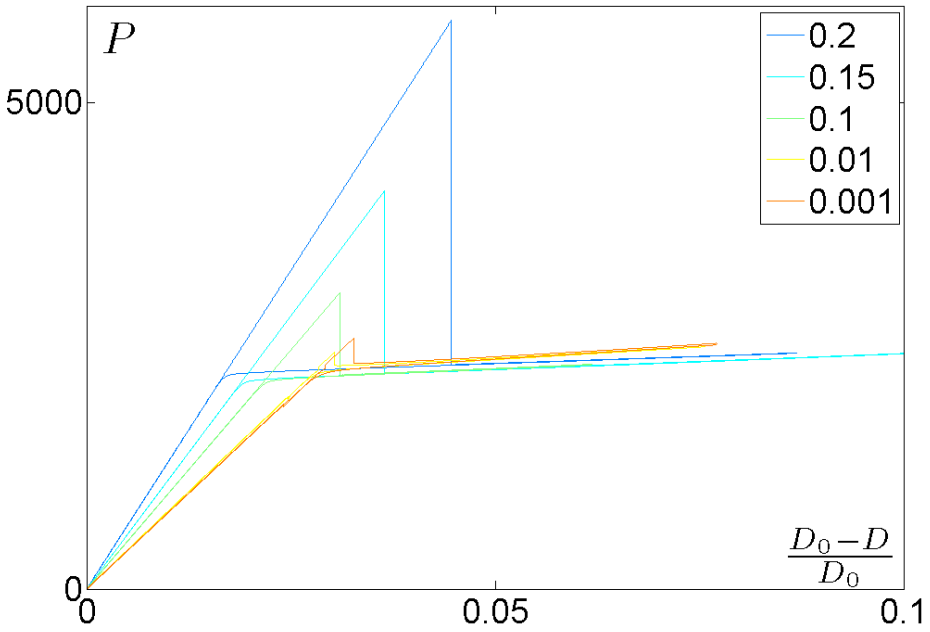

Figure 4.13 – Force strain curve for both the compression and the relaxation of a single beam between two circular, freely rotary beams with various radii. We see that the peaks in the graph don't disappear when the radius of the nodes becomes very small. In this simulation we have used $E = 471000$, $h = 0.167$, $v_{down} = 1.5$, mass = 1/32 (of the nodes), rotational inertia = 1, transviscosity = 150, rotational viscosity = 1. The threshold value for the check on the torques was 0.01 for the simulations.

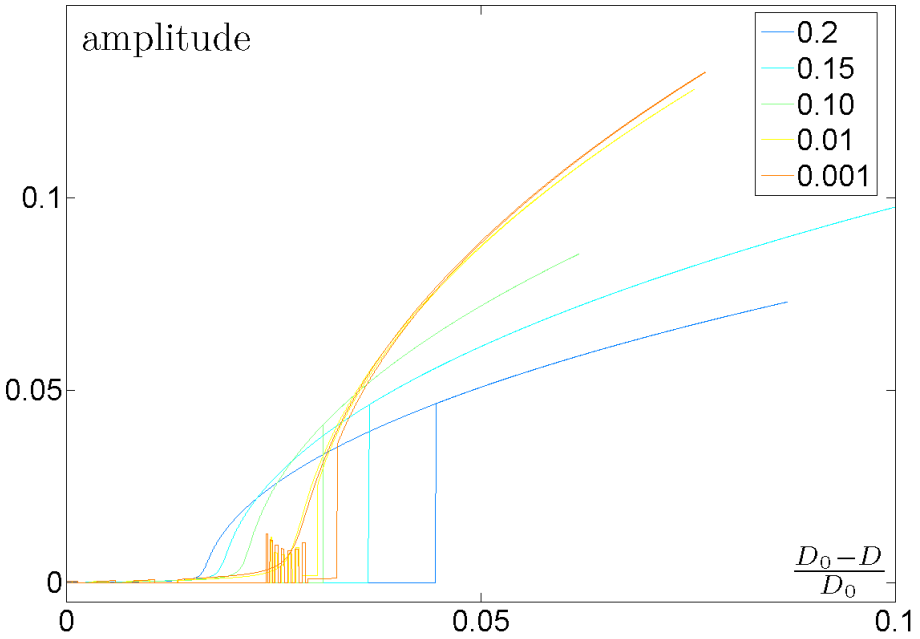

Figure 4.14 – Amplitude of the beams configuration versus the strain for a single beam between two circular, freely rotary beams with various radii. These are for both compression (the lines with the jumps) and relaxation of the system. We have no real explanation for the strange behaviour of the simulation with radius 0.001. In this simulation we have used $E = 471000$, $h = 0.167$, $v_{down} = 1.5$, mass $= 1/32$ (of the nodes), rotational inertia $= 1$, transviscosity $= 150$, rotational viscosity $= 1$. The threshold value for the check on the torques was 0.01 for the simulations.

the nodes) as one great system with pinned-pinned boundaries that buckles. Hence we would have a greater length, which would result in a lower critical load in the simulation. This could perhaps yield better simulations, without the peaks.

To check wether these peaks show the real relation, we have done another simulation. This time we won't perturbate the system only when the buckling load is exceeded, but every 10 time steps. As before, the system will be allowed to find its equilibrium position at each time step. Since we pertubate the system regularly, the simulation should not find unstable equilibrium positions, but will only find the real positions. Hence the peak should disappear in this simulation.

The resulting force strain curve and amplitude strain curves of this simulation are shown in figure 4.18. It is clear that most of the peak has disappeared in this new simulation. There is however still a part visible of the peak. This could mean that a straight beam is the stable position for this system, but it could be a problem of the simulation as well. The perturbations of the system are quite large (7 degree angles) and hence it is not clear if the right configurations are found. To determine this, we need other simulations with smaller perturbations.

There is however a benefit of these curves. From these simulation, we see that

there is a peak in the force strain curve (see figure 4.13) when the beam stays (too) long in its non-buckled state. Thinking back of the force strain curve for the monoholar elastic patterned sheets (figure 4.1), this could be what is causing the peaks. The vertical beams may want to buckle, but they are fixed in their straight configuration by the horizontal beams which apply a torque on them.

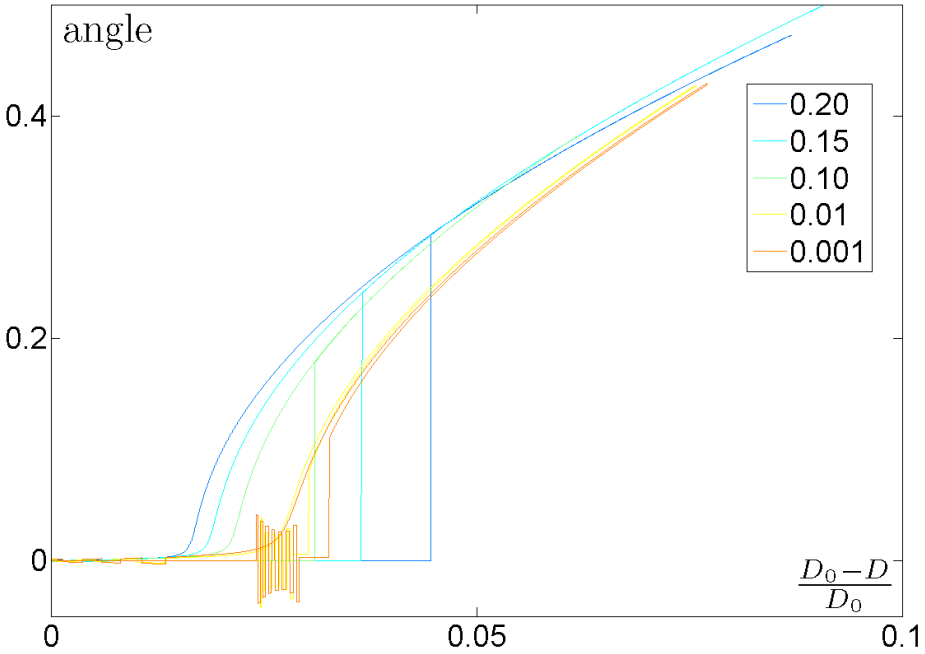

Figure 4.15 – Relation between the angle of the upper node and the strain of the whole system for a single beam between two circular, freely rotary nodes with various radii. These are for both compression (the lines with the jumps) and relaxation of the system. We have no real explanation for the strange behaviour of the simulation with radius 0.001. In this simulation we have used $E = 471000$, $h = 0.167$, $v_{down} = 1.5$, mass $= 1/32$ (of the nodes), rotational inertia $= 1$, transviscosity $= 150$, rotational viscosity $= 1$. The threshold value for the check on the torques was 0.01 for the simulations.

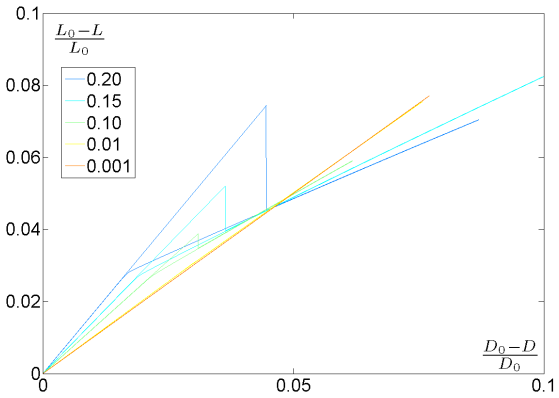

Figure 4.16 – The relation between the relative strain of the whole system ($\frac{D_0-D}{D_0}$) and the relative strain of the beam ($\frac{L_0-L}{L_0}$) of a system with a beam that is kept between two circular, freely rotary nodes with various radii. These curves are both for compression (the lines with the jump) and relaxation. We see that the beams strain first is linear with the systems strain. At a certain point, when the beam buckles, the attachment points move along the boundary of the circular nodes. As a result the beam stretches a bit. It looks like this process is again linear in the systems strain. In this simulation we have used $E = 471000$, $h = 0.167$, $v_{down} = 1.5$, mass $= 1/32$ (of the nodes), rotational inertia $= 1$, transviscosity $= 150$, rotational viscosity $= 1$. The threshold value for the check on the torques was 0.01 for the simulations.

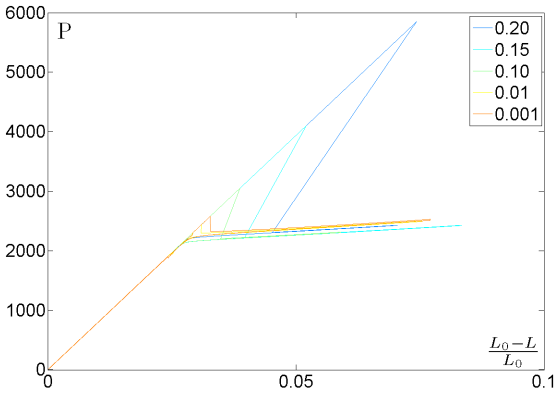

Figure 4.17 – This figure shows the force strain curves for a single beam between two circular, freely rotary nodes with various radii. In this figure the strain is actually the strain of the beam (and not of the whole system as in figure 4.13). This curves are shown for both compression (the upper curves with a jump) and relaxation of the system. We see clearly the usual, bi-linear behaviour of a pinned-pinned beam in the relaxation curves. In the compression curves we see that the beams stays too long in its non-buckled state. Then at a certain point the beam buckles. Since the attachment angles are then moving along the boundary of the nodes, the strain $\frac{L_0-L}{L_0}$ is then reduces (see figure 4.16). Hence the strain decreases at these moments. In this simulation we have used $E = 471000$, $h = 0.167$, $v_{down} = 1.5$, mass $= 1/32$ (of the nodes), rotational inertia $= 1$, transviscosity $= 150$, rotational viscosity $= 1$. The threshold value for the check on the torques was 0.01 for the simulations.

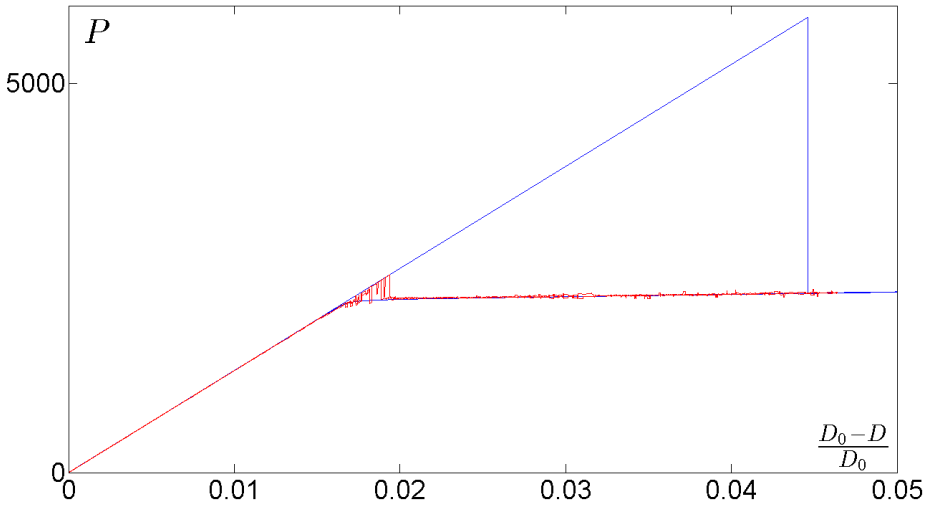

(a)

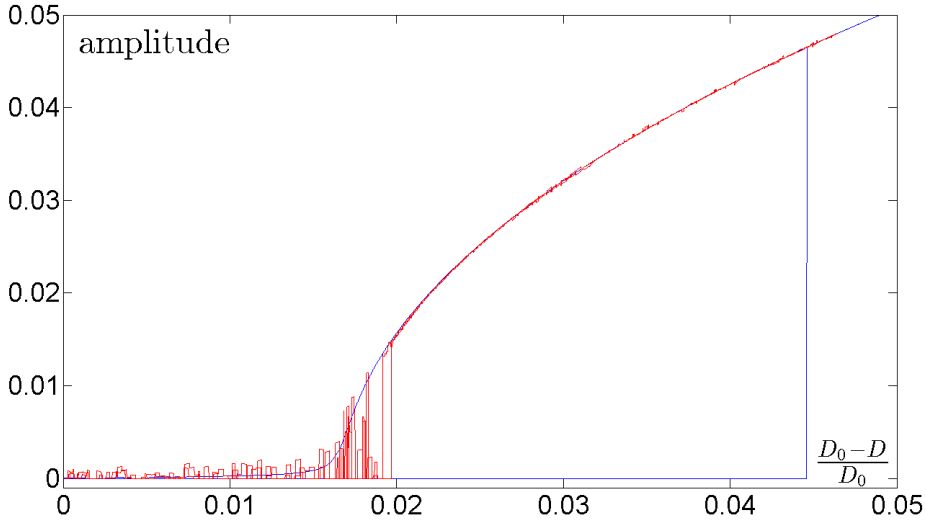

(b)

Figure 4.18 – Relation between the force and strain (a) and the distance and strain (b) for a single beam between two circular, freely rotary nodes with radius 0.2. The blue line is the simulation with only one perturbation, when the euler load is exceeded, while the red curve show the simulation when we perturbate the system each 10 time steps (over an angle of 7 degrees). It is clear that the particular peak in the force strain curve almost completely disappears in the new simulation. Since the simulation suggests that the system constantly changed between a straight and a bended beam, this pertubation over 7 degrees may be too large for the system to find the real stable equilibrium state.

4.3 Simulations on elastic patterned sheets

In this section we will inspect a model for the elastic patterned sheets (see chapter 1). We will use the model with the elastic beams between movable, freely rotary nodes, as explained in figure 4.2. First we explain some of the details of using this model in a numerical simulation and we discuss the differences with the single beam simulation in section 4.2. Then we will use the numerical simulation to ingestive the monoholar and biholar elastic patterned sheets in section 4.3.2.

4.3.1 Explanation of numeric simulation

The model for the elastic patterned sheets isn't much different from the model for the single beam between two circular, freely rotary nodes. Therefore the global numerical scheme for both models is the same. First the initial configuration (in this case the elastic patterned sheet) is constructed in the simulation. Then the upper nodes are again pushed down a certain, specific discrete distance. After that the simulation calculates the configurations of all the beams and then uses that information to find the positions and orientations of all the nodes in the system. As before, this process is repeated a few times to find the equilibrium configuration of the system. The simulation then continues to push the upper nodes down while the system is monitored at each of these time steps. Optionally, after the compression the elastic sheet can be stretched again to its initial configuration.

The most notable difference however between the model for the elastic patterned sheets and model for the single beam is that there are many more nodes and beams in this case. This not only means that the simulation needs more calculation time, but the nodes this time can also spatially move. So there is not only a torque balancing problem in the elastic patterned sheet, but also a force balance problem. Therefore we need to check for both the resulting torques and the resulting forces on all nodes.

4.3.2 Simulations on the elastic patterned sheets

In experiments we see a big difference between monoholar networks and biholar networks. For instance, monoholar networks have peaks in their force strain curves, while the biholar networks don't exhibit such kind of behaviour. They have a more flat curve as shown in figure 4.19.

A numerical simulation of these kind of networks should be able to recreate this kind of behaviour. To test this we run a simulation for a monoholar network and various biholar networks. As stated before, the biholar networks are made in the same way as the monoholar networks, but the beam between the nodes have an initial curvature. This initial curvature is of the form $A\sin(\pi x)$ (in which x denotes the relative place on the beam). A network is hence more biholar, when the amplitude A of this sine becomes larger. This corresponds with a greater difference between the radii of the holes in the real networks. When $A = 0$, there is no initial curvature and we have a normal monoholar network.

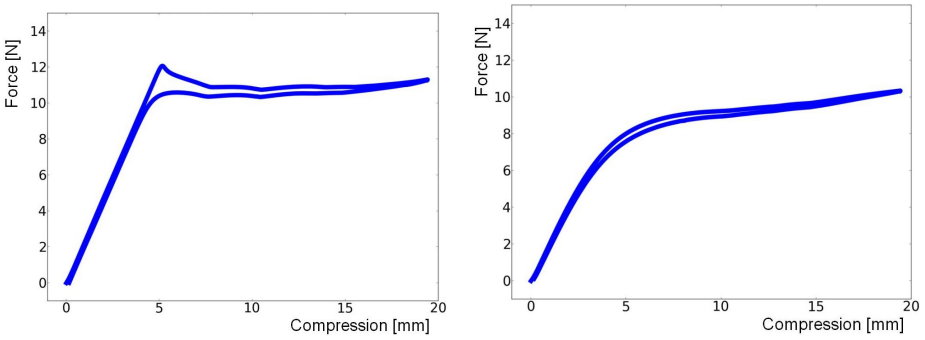

(a) **(b)**

Figure 4.19 – Experimentally obtained force strain curves for a monoholar (a) and a biholar (b) elastic patterned sheet. These curves show both the initial compression as well as the relaxation of the networks.

The resulting force strain curves of the simulations are shown in figure 4.20. We clearly see the desired peak in this curve for the monoholar networks. Moreover, the biholar networks don't exhibit this peak, which is also in correspondence with the experimental observations. Hence the used model with beams and nodes looks like a good model to use for simulations with the elastic patterned sheets.

Furthermore we learn from this simulation that the amplitude A of the initial curvature isn't that important. The curves generally have the same structure and exhibit the same behaviour. Moreover all the curves show roughly the same response when the strain is either small or large. Hence this supports the idea that the monoholar networks feature an instability which is resolved when the networks become biholar.

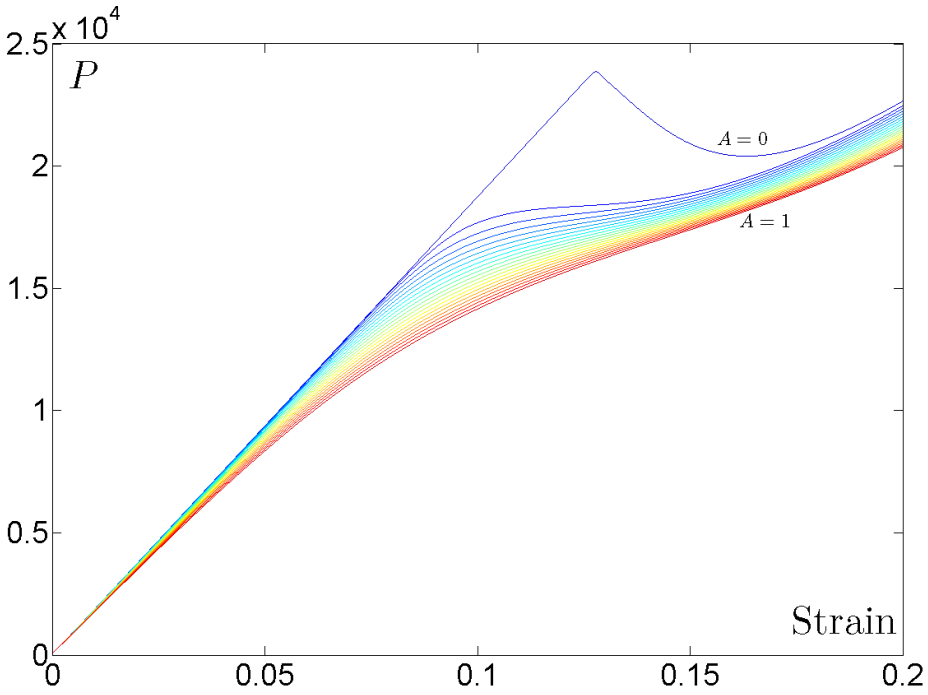

Figure 4.20 – Force strain curves for elastic patterned sheets with different initial curvature $A\sin(\pi x)$.The upper line (blue) shows the force strain curve when there is no initial curvature (i.e. $A = 0$). Hence this is the simulation for a monoholar sheet. The other curves shown curves for initial amplitudes A (increasing in steps of 0.05), which corresponds with biholar networks. In the monoholar case, we clearly see the peak in the curve, which we also see in experiments (see figure 4.19). As soon as the networks are biholar this peak however disappears, which is also in correspondance with the experiments. The behaviour at the start and at the end of the simulation is however roughly the same between the various simulations. In this simulations we have used a square lattice with $N^2 = 25$ nodes with radius 0.29, mass 0.0313, rotational inertia 1, rotational viscosity 1 and trans viscosity 150. The Young's modulus is 471000, the width of the beams was 0.167 and the length 0.42. The threshold for the force and torque balance was 0.5.

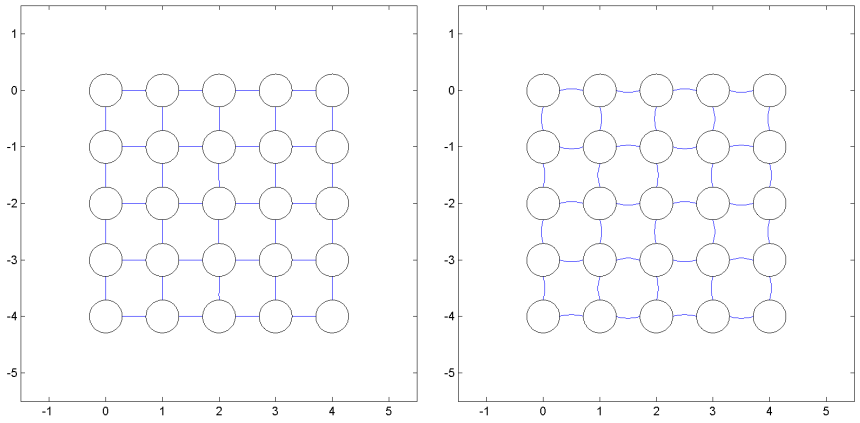

(a) Monoholar - timestep 100

(b) Biholar - timestep 100

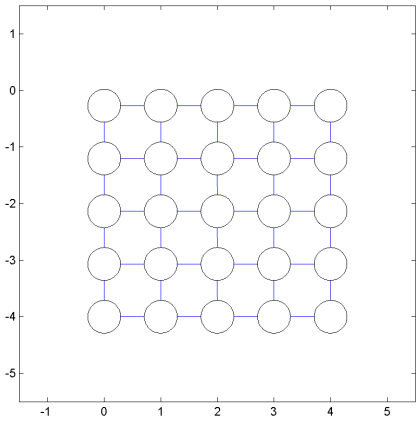

(c) Monoholar - timestep 10000

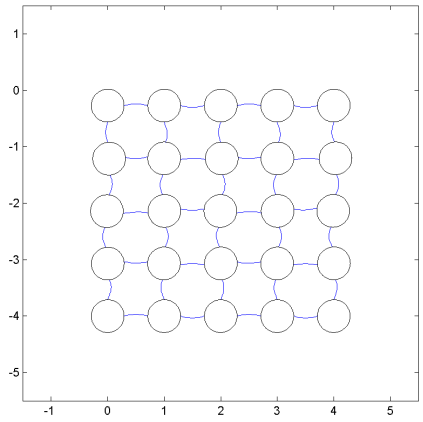

(d) Biholar - timestep 10000

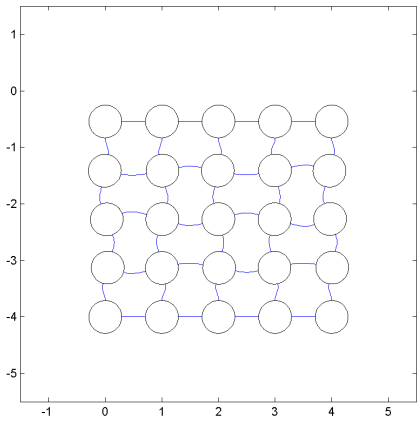

(e) Monoholar - timestep 20000

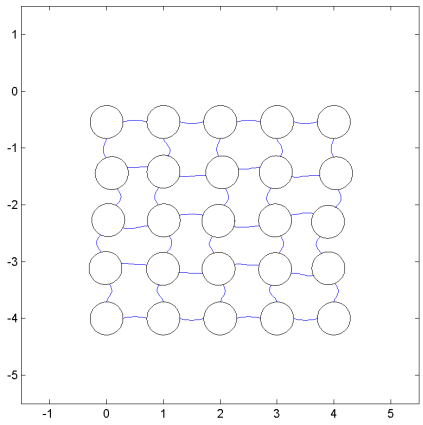

(f) Biholar - timestep 20000

Figure 4.21 – MATLAB figures of the configuration of both a monoholar (a),(c),(e) and a biholar (b), (d),(f) elastic patterned sheet simulation for various timesteps.

Chapter 5

Conclusion + Outlook

In this bachelor thesis, we found four different models for slender elastic rods that are axially loaded (see figure 5.1). These models differ in their assumptions on the elastic beams. For instance, some of them model the elastic beams as inextensible (i.e. their arc length is always the same). A summary of the assumptions of the four beam models found in this thesis can be found in table 5.1

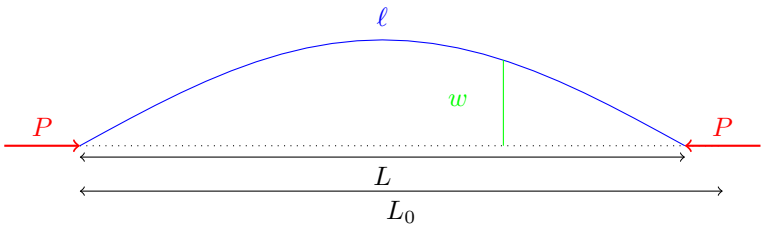

Figure 5.1 – General set-up for an elastic beam that is axially loaded with a load P. The load P is applied in the x-direction, while the deflection, $w(x)$ is in the y-direction. The blue line represent the beam (bended in this case). L_0 is the initial length of the beam, L is the current span in the x-direction of the beam and ℓ is the arc length of the beam.

We thus found four beam models that were increasingly realistic, but also increasingly difficult to use. The four models are related to each other. The

Table 5.1 – In this table, the assumptions of the various beam models are shown. 'no' means the model does not take said property of the beam into account, while a 'yes' means it does. The last column states for which kind of deflections the model is good.

beam model	stretching	bending	twisting	deflections
Section 3.1	no	yes	no	only small
Section 3.2	no	yes	no	all
Section 3.3	yes	yes	no	only small
Section 3.4	yes	yes	no	all

Table 5.2 – In this table the four beam models of this thesis are shown. The extensible model reduces to the inextensible model when $EA \to \infty$.

deflections	extensible	inextensible
small	$EIw_{\hat{x}\hat{x}\hat{x}\hat{x}} + Pw_{\hat{x}\hat{x}} = 0$ $\Delta L = \frac{P}{EA} L_0 + \frac{1}{2}\int_0^{L_0} w_{\hat{x}}(r)^2 \, dr$	$EIw_{xxxx} + Pw_{xx} = 0$ $\Delta L = \frac{1}{2}\int_0^{L} w_{x}(r)^2 \, dr$
large	$EI\theta_{\hat{x}\hat{x}} + P\sin(\theta) - \frac{P^2}{EA}\sin(\theta)\cos(\theta)$ $\Delta L = \int_0^{L_0} \left(1 - \cos(\theta) + \frac{P}{EA}\cos^2(\theta)\right) d\hat{x}$	$EI\theta_{ss} + P\sin(\theta) = 0$ $\Delta L = \int_0^{L_0} (1 - \cos(\theta)) \, ds$

models that take the stretching of the beam into account can be reduced to the the models that are neglecting it, when $EA \to \infty$. Hence the lower the Young's modulus E, the more important the stretching of the beam is. Moreover, we found that the stretching is also more important in thicker beams (when the other attributes of the beam stay constant).

In this thesis we used all of these four beam models to study the force strain curve for a pinned-pinned beam. A summary of the results is shown in figure 5.2. We clearly see the difference between the critical load in the various models and the post-buckling behaviour. The extensible model for large deflections is the only model that can explain the negative slope that is observed in experiments with elastic beams.

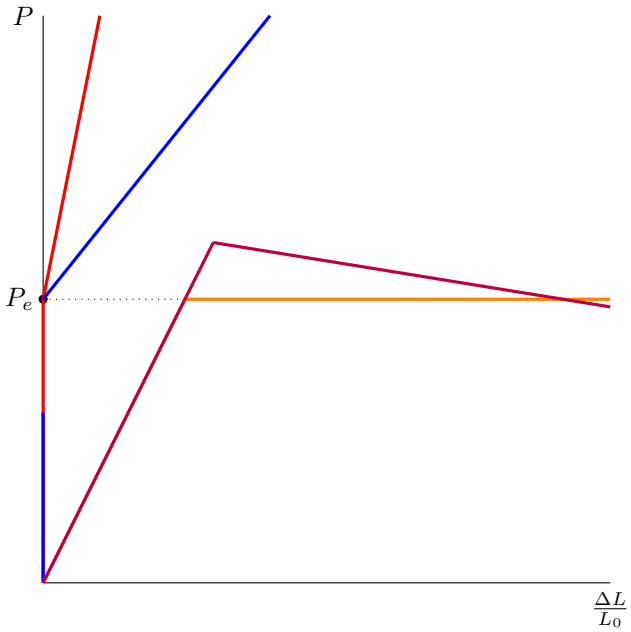

Figure 5.2 – Summary of the force strain relationship before and after buckling for a pinned-pinned beam. The inextensible models are shown in red and blue (red is for only small deflections). The extensible beam model for only small deflections is shown in orange, while the extensible model that allows for large deflections is purple. The purple line is the only line that has a negative post-buckling slope, since this can only occur in that model.

The beam models that we acquired all neglect the twisting of the beam. Follow-up research should point out when this twisting of the beam is important and when it can be neglected as we did in this thesis. Moreover we found a qualitative distinction between the inextensible and the extensible models, but it might be necessary to quantify this distinction, so we know when the simple (inextensible) models are not precise enough and when they suffice.

Furthermore in this thesis we focused on single beams that were initially straight. We only briefly mentioned the possibility of initial curvature. Since we also want to model the biholar elastic patterned sheet, this initial curvature is important. Hence it is necessary to find ways to take this initial curvature into account in the models presented in this thesis.

Elastic patterned sheets

In this thesis we also studied the behaviour of the elastic patterned sheets, both monoholar and biholar. The simulations in chapter 4 resembled the experimentally obtained force strain curves qualitatively. We also observed that the peak in this curve disappears when the elastic sheets becomes biholar. From this we concluded that the idea of modeling the elastic patterned sheets with the beams and nodes is a good approach.

Moreover, the study of an elastic beam between two circular, freely rotary nodes showed us a peak in the force strain curve when the elastic beam was kept too long in its (unstable) straight position. This can be precisely what's happening in the elastic patterned sheets. The vertical beams are kept in their unstable, straight position by the horizontal ones. While the vertical beams may want to buckle, the horizontal beams prevent this by applying a torque on them.

Follow-up research should focus on this idea. So not only should this research continue with the analytical study of the beam between two circular, freely rotary nodes, it should also incorporate more configurations with more beams and nodes (e.g. the Roorda frame). If these configurations also show this peak, this might suggest that this is the cause of the peak in the monoholar networks.

Furthermore the model that we used in this thesis lacks much detail. For instance the nodes are modeled as undeformable, while they are deformable in reality. Moreover, experiments show a positive Poisson's ratio before the elastic patterned sheets bend, but the simulations don't show this. New research could find a way to take these effects into account.

Chapter 6

Acknowledgments

I'd like to thank my thesis supervisors prof. dr. M. van Hecke and dr. V. Rottschäfer for their help and guidance during my research. Especially, I'd also like to thank dr. C. Coulais, who's enthusiasm and support were of a great help during the past months. Moreover, I'd like to thank Ernst Jan Vegter, Johan Lugthart and Bastiaan Florijn, who also worked on the elastic patterned sheets and contributed to the insights in this bachelor thesis.

Bibliography

Basile Audoly. *Thin Structures - MEC 563*.

J.R. Barber. *Elasticity*. Solid mechanics and its applications, v. 172. Springer Netherlands, 2010. ISBN 9789048138098. URL http://books.google.nl/books?id=lHWvv3kZeBIC.

Z. Bazant and L. Cendolin. *Stability of Structures*. World Scientific, 2009.

Katia Bertoldi, Pedro M. Reis, Stephen Willshaw, and Tom Mullin. Negative Poisson's Ratio Behavior Induced by an Elastic Instability. *ADVANCED MATERIALS*, 22(3):361+, JAN 19 2010. ISSN 0935-9648. doi: {10.1002/adma.200901956}.

M. Bourne. Radius of curvature. URL http://www.intmath.com/applications-differentiation/8-radius-curvature.php.

W.F. Chen and T. Atsuta. *Theory of Beam-Columns, Volume 1: In-Plane Behavior and Design*. J Ross Publishing Series. J. Ross Pub., 2007. ISBN 9781932159769. URL http://books.google.nl/books?id=szfS9ZurW3cC.

AA Christodoulou and AN Kounadis. Elastica buckling analysis of a simple frame. *Acta Mechanica*, 61(1-4):153–163, AUG 1986. ISSN 0001-5970. doi: {10.1007/BF01176370}.

DW Coffin and F Bloom. Elastica solution for the hygrothermal buckling of a beam. *INTERNATIONAL JOURNAL OF NON-LINEAR MECHANICS*, 34(5):935–947, SEP 1999. ISSN 0020-7462. doi: {10.1016/S0020-7462(98)00067-5}.

Samir A. Emam. *A Theoretical and Experimental Study of Nonlinear Dynamics of Buckled Beams*. 2002. URL http://scholar.lib.vt.edu/theses/available/etd-01092003-111357/unrestricted/final.pdf.

Joel Feldman. Equality of Mixed Partials. URL http://www.math.ubc.ca/~feldman/m200/mixed.pdf.

Alexander Humer. Elliptic integral solution of the extensible elastica with a variable length under a concentrated force. *ACTA MECHANICA*, 222(3-4):209–223, DEC 2011. ISSN 0001-5970. doi: {10.1007/s00707-011-0520-0}.

R.M. Jones. *Buckling of bars, plates, and shells*. Bull Ridge Publishing, 2006. ISBN 9780978722302. URL http://books.google.nl/books?id=UzVBr8b_jS8C.

Ken Kamrin and L. Mahadevan. Soft catenaries. *Journal of Fluid Mechanics*, 691:165–177, 0 2012. ISSN 1469-7645. doi: 10.1017/jfm.2011.466. URL `http://journals.cambridge.org/article_S0022112011004666`.

K Kondoh and SN Atluri. Influence of local buckling on global instability - simplified, large deformation, post-buckling analyses of plane trusses. *Computers & Structures*, 21(4):613–627, 1985. ISSN 0045-7949. doi: {10.1016/0045-7949(85)90140-3}.

R Lakes. Foam structures with a negative poissons ratio. *science*, 235(4792): 1038–1040, FEB 27 1987. ISSN 0036-8075. doi: {10.1126/science.235.4792.1038}.

L. D. (Lev Davidovich) Landau, E. M. (Evgenii Mikhailovich) Lifshitz, A. M. (Arnol'd Markovich) Kosevich, and L. P. (Lev Petrovich) Pitaevskii? *Theory of elasticity / by L.D. Landau and E.M. Lifshitz ; translated from the Russian by J.B. Sykes and W.H. Reid.* Oxford ; Boston : Butterworth-Heinemann, 3rd english ed., revised and enlarged by e.m. lifshitz, a.m. kosevich, and l.p. pitaevskii edition, 1995. ISBN 075062633X. Translation of: Teori?i?a uprugosti.

L.D. Landau and L.D Lifshitz. *Theory of Elasticity, 3rd Edition.* ISBN 075062633.

A Magnusson, M Ristinmaa, and C Ljung. Behaviour of the extensible elastica solution. *INTERNATIONAL JOURNAL OF SOLIDS AND STRUCTURES*, 38(46-47):8441–8457, NOV 2001. ISSN 0020-7683. doi: {10.1016/S0020-7683(01)00089-0}.

Karl Marguerre. *On the application of the energy method to stability problems.* National Advisory Committee for Aeronautics, 1947. URL `http://archive.org/details/onapplicationofe00unit`.

T. Mullin, S. Deschanel, K. Bertoldi, and M. C. Boyce. Pattern transformation triggered by deformation. *PHYSICAL REVIEW LETTERS*, 99(8), AUG 24 2007. ISSN 0031-9007. doi: {10.1103/PhysRevLett.99.084301}.

T. Sochi. Using Euler-Lagrange Variational Principle to Obtain Flow Relations for Generalized Newtonian Fluids. *ArXiv e-prints*, January 2013.

Wolfram. The best-known properties and formulas for incomplete elliptic integrals. URL `http://functions.wolfram.com/EllipticIntegrals/EllipticE2/introductions/IncompleteEllipticIntegrals/05/`.

Chapter 7

List of Notations

A	The cross-sectional area of the beam
ΔL	Strain, $\Delta L = L_0 - L$
$\Delta \ell$	Change of length of the beam $\Delta \ell = \ell - L_0$
E	Young's modulus
E_{el}	The elastic energy of an elastic beam
ϵ	The second rank strain tensor
ϵ_{ij}	Strain in the j-direction that is working on the i-face
$\epsilon_{ij,kl}$	Second derivative of ϵ_{ij} with respect to kl, i.e. $\epsilon_{ij,kl} \equiv \frac{\partial^2 \epsilon_{ij}}{\partial k \partial l}$
ε	The stretching inside an elastic beam
I_{ij}	The second (geometric) moment of inertia in the ij-direction
J	The torsion constant
k	Introduced constant with $k \equiv \frac{P}{EI}$
κ_y, κ_z	The bending inside an elastic beam (i.e. curvature of the beam)
κ_x	The twisting inside an elastic beam
L_0	The initial length of the elastic beam inspected
L	The span in the x-direction of the elastic beam's current position
ℓ	The arc length of the elastic beam in its current configuration
N	The normal force
P	The force (load) that acts on the end points of the elastic beam
P_c	The critical load at which a beam starts to buckled
P_e	The Euler load for a single beam $P_e = EI \frac{\pi^2}{L_{eff}^2}$ with L_{eff} the beam's effective length
Q	The shear force
σ	The second rank stress tensor
σ_{ij}	Stress in the j-direction that is working on the i-face
$\sigma_{ij,kl}$	Second derivative of σ_{ij}, i.e. $\sigma_{ij,kl} \equiv \frac{\partial^2 \sigma_{ij}}{\partial k \partial l}$
$\theta(s)$	Angle at position s of the beam (w.r.t. the x-axis)
$u(x)$	The deflections of a point on the beam in the horizontal, x-direction
$w(x,t)$	The deflection of the beam at position x and time t
$\hat{x}$	Coordinate along the initial configuration of the beam
$z_0(x)$	The original beam configuration (i.e. the initial bending of the beam)
Ω_0	The cross-sectional area of the beam